Geochemistry and leaching behaviour of potentially toxic elements in coastal legacy landfill sites across North West England and North Wales

By

James MacDonald

A thesis submitted in partial fulfilment of the requirements of Liverpool John Moores University for the degree of Master of Philosophy

November 2024

Declaration

I declare that no portion of the work referred to in the thesis has been submitted in support of an application for another degree or qualification of this or any other university or other institute of learning.

Contents

List of figures

List of tables

Acronyms Table

Full text	Abbreviated text
Potentially toxic elements	PTEs
Municipal solid waste	MSW
Site of special scientific interest	SSSI
Shoreline management policy	SMP
Department for environment, food and rural affairs	Defra
Scanning electron microscopy	SEM
Inductively coupled plasma-mass spectrometry	ICP-MS
Inductively coupled plasma-optical emissions spectroscopy	ICP-OES
British standard leaching test	BS EN 12457-2 2002
Nitric acid	HNO_3
Hydrochloric acid	HCl
Oxygen reduction potential	ORP
Electrical conductivity	EC
Artificial rainwater	ARW
Artificial seawater	ASW
Part per million	ppm
Part per billion	ppb
Chromium	Cr
Nickel	Ni
Copper	Cu
Zinc	Zn
Lead	Pb
Vanadium	V
Mercury	Hg
Cadmium	Cd
Arsenic	As
Chlorine	Cl
Iron	Fe
Beryllium	Be
Calcium	Ca

Magnesium	Mg
Titanium	Ti
Oxygen	O
Silica	Si
Aluminium	Al
Potassium	K
Manganese	Mn
Selenium	Se
Thallium	Tl
Cobalt	Co
Antimony	Sb

Acknowledgements

I would like to thank my primary supervisor Dr. Patrick Byrne and my secondary supervisor Dr Kostas Kiriakoulakis for their valuable feedback and guidance during the entirety of my MPhil project. Their approach to mentoring fostered an environment where my ideas were challenged in a constructive way, helping to think critically in a way which will be carried into other projects moving forward.

To my family and friends for their encouragement and belief, which have been a continued source throughout.

To my cat, Ozzy, for sitting on my keyboard countless times and deleting thousands of words worth of work…

And finally, to the academic staff and technicians at the School of Biological and Environmental Sciences at Liverpool John Moores University, who provided valuable insight at multiple stages of my MPhil project.

Highlights

- The increasing impacts of climate change evidenced by a greater frequency and severity of extreme weather events, elevated rates of coastal erosion, and the increased likelihood of coastal flooding pose a risk of releasing potentially hazardous elements into the coastal zone.
- Numerous metal concentrations across both colliery and steel slag-based waste exceed established sediment guideline values.
- The release of metals would result in considerable environmental and ecological damage.
- The release of elements in oxidised conditions was most prevalent in deionised water leachant, with numerous leached elements exceeding WHO drinking water quality guideline values.
- Environmentally representative ARW and ASW displayed minimal leaching in contrast to the deionised water leachant.
- Improvements to the British standard leaching method (BS EN 12457-2-2002) is recommended, as to be more representative of real-world conditions.

Abstract

Historic industry dating back to the Industrial Revolution from the 19th century onwards is responsible for the presence of PTE (potentially toxic element) concentrations within the coastal environment, of which colliery and steel industries were a considerable contributor. The increasing impacts of climate change on the coastal environment, as evidenced by a continuous global increase in sea level, elevated rates of coastal erosion and coastal flooding, alongside an increasing frequency and intensity of extreme weather events poses a serious threat to mobilisation of hazardous elements, subsequently dispersing into nearby sensitive environmental receptors including: SSSI's, RAMSAR sites, and designated bathing zones. As there are limited studies addressing the mobilisation of elements pertaining to coastal legacy waste sites in saline and representative rainwater conditions, this study focuses on establishing the total element concentrations of coastal legacy waste sites associated with colliery and/or steel waste across North West England and North Wales, and to determine the level of mobilisation of element concentrations under deionised water, artificial rainwater (ARW), and artificial seawater (ASW) conditions. It was found that across colliery and steel slag-based waste, V, Cr, Se, Ni, As, and Cu exceeded sediment guideline values across the majority of sample sites, thereby establishing these waste sites as significantly hazardous. Furthermore, leaching under deionised water conditions proved most concerning, with leached As, Pb, Al, and Mn exceeded WHO drinking water quality guideline values. Moreover, ARW and ASW leachants displayed significantly reduced leaching in contrast to deionised water leachant. As such, leaching mechanisms only attributable to deionised water conditions such as the low ionic strength of the leachant is likely the primary cause of element mobilisation. The findings of this study imply that leaching of significantly hazardous elements under saline and mildly acidic ARW conditions did not contribute to considerable leaching of elements in complex legacy waste sediments. Moreover, stark differences in concentrations seen within deionised water compared with artificial leachate highlight the need for adaptations to be made to the British standard leaching method (BS EN 12457-2-2002), as studies using this method may overestimate/underestimate element leaching potential under oxidised conditions.

1. Introduction

1.1. A global context

In recent years, global and national attention surrounding coastal legacy landfill and the subsequent impact on the coastal landscape has gained more traction, with an upsurge of media attention, government research reports, and research publications contributing to public awareness (Brand, 2017; Edwards, 2017; Hughes and Seely, 1996; BBC, 2017). Despite this, the total extent of coastal legacy waste on a global scale is unknown. Nonetheless, estimates suggest a substantial presence of such landfills within the European Union, ranging from approximately 350,000 to 500,000 sites, a considerable proportion of which are presently inactive (Willie, 2018). These landfills predate contemporary pollution prevention legislation and are present in coastal areas (Willie, 2018; Nicholls *et al,* 2021). For instance, France is estimated to harbour around 1,000 coastal landfill sites, while the German coastline accommodates 1,027 such sites (Nicholls *et al,* 2021). The potential for pollution emanating from coastal landfill sites is a matter of significant concern due to the array of associated hazards and their impact on contaminant mobility (Riley *et al,* 2022) such as the erosion and discharge of contaminated municipal solid waste, unregulated release of landfill leachate, formation of leachate plumes, and heightened exposure to bioaerosols originating from landfills (Brand, 2017; Nicholls *et al,* 2021; Zhang *et al,* 2023; Rajmohan *et al,* 2019). This paper aims to explore the pollution risk of coastal legacy waste, now labelled as 'pollution time-bombs' due to the significantly hazardous contaminants present and their continued release, and also the potential for catastrophic contaminant release exacerbated by the increasing effects of climate change (Propp *et al,* 2021; Nicholls *et al,* 2021). To classify legacy landfills, the Environment Agency has defined historic legacy waste as *"historic (closed) landfill site is one where there is no PPC [Pollution Prevention and Control] permit or waste management licence currently in force"* (Environment Agency, 2023a).

1.2. Waste type and geochemistry of coastal legacy waste

The sediment geochemistry of coastal legacy waste is multifaceted, characterised by a diverse array of pollutants. Notwithstanding this, there are similarities in detected elements across various landfill sediments, including chromium (Cr), nickel (Ni), copper (Cu), zinc (Zn), and lead (Pb) (Podlasek *et al,* 2024; Sayadi *et al,* 2015; Mavakala *et al,* 2016). Moreover, the nature of the waste itself can serve as an indicator of potential contaminants, as evidenced by the significant presence of critical raw materials such as Cr, vanadium (V), and numerous rare-earth elements within steel slag waste (Riley *et al,* 2020). However, the composition of

coastal legacy waste can reflect different origins and industrial processes, further adding to its complexity. Despite these complexities, the presence of PTEs within legacy waste are a serious concern due to the impacts on environmental receptors.

Pollutants present within coastal legacy landfill range from biological, organic, and inorganic (Siddiqua *et al,* 2022). The presence of inorganic contaminants is considered by many to be of severe concern (Nieder and Benbi, 2023; Guagliardi, 2022; Siddiqua et al, 2022). Inorganic pollutants primarily consist of heavy metals such as Cr, Pb, Zn, mercury (Hg), cadmium (Cd), and arsenic (As), which are considered potentially toxic elements (PTEs), as they are considered toxic at low concentrations (Siddiqua *et al,* 2022; Sidana *et al,* 2020). Concurrently, organic pollutants originate from the disposal of industrial chemicals, domestic, and agricultural waste. Notably, landfill sites containing chlorine (Cl) concentrations have been identified as sources of dioxins, persistent organic pollutants renowned for their longevity and high toxicity (Njoku *et al,* 2019). Additionally, the presence of biological pollution is presented in the form of bioaerosols as seen by pathogens enriched by microbes containing dust, brine water droplets, and harmful chemicals present within landfill (Zhang *et al,* 2023; Dias and Viegas, 2021; Humbal *et al,* 2018). Depending upon the waste type, the pollutants within can span across multiple pollutant categories; for instance, municipal solid waste (MSW) is a significant contributor within coastal legacy landfill sites. MSW is comprised of organic and inorganic material and in toxic concentrations., originating from general public waste, some of which include plastic, paper, food, metals, glass, and industrial material (Hong et al, 2017; Gupta, 2019). For further context, in 2014, MSW accounting for 65% of Chinas waste disposal (Hong *et al,* 2017). Furthermore, leachate production from coastal legacy landfill sites encompasses a mixture of organic and inorganic compounds alongside nutrients, often in toxic and volatile forms (Vaverková, 2019; Wdowczyk and Szymańska-Pulikowska, 2020). The hazardous nature of pollutants within coastal legacy landfills, characterized by corrosive, toxic, and ignitable properties, poses substantial risks to human and environmental health, with the exacerbation of transport mechanisms by human-induced climate change further amplifying these risks.

1.3. Potential impacts of climate change on mobilisation and risk

Given that climate change is expected to increase the of rate sea-level rise and heighten the intensities and frequencies of weather events, including coastal flooding and erosion on a global scale (Oppenheimer *et al,* 2019), this will have direct implications on coastal legacy waste sites. The repercussions will include the mobilisation of various pollutants, including

PTEs into the surrounding environment, posing substantial risks to various environmental receptors.

The leaching of potentially hazardous elements within coastal legacy waste sites, exacerbated by intensified precipitation and infiltration events, poses severe toxic implications for environmental receptors. Coastal legacy leachate, often categorised as 'old landfill leachate,' are characterised by a decrease in concentrated organic and inorganic compounds and a reduction in biochemical oxygen demand compared to younger forms of leachate (Vaverková, 2019). Youcai (2018) acknowledges precipitation, including snow and rainfall events infiltrating through landfill contents, as a primary source of leachate production. According to the UK Met Office, based on 'more likely' UKCP climate data scenarios, by 2070, precipitation events are projected to undergo significant fluctuations, with alterations in the seasonality of extremes compared to the present day. Notably, heavy precipitation events in the autumn season are expected to escalate in both intensity and frequency, and rainfall expected from a 1-in-2-year event expected to increase by approximately 29% (Met Office, 2022). Consequently, it is anticipated that the severity of leachate production from coastal legacy waste will further intensify during the autumn/winter period, recognised as the wettest period of the year in the UK.

Surface water infiltration was also acknowledged as a primary influence in leachate production (Youcai, 2018), which includes surface runoff in regions with a high-water table and/or impermeable surfaces. Brand *et al* (2017) highlights that saltwater intrusion into coastal legacy waste will likely mobilise inorganic contaminants situated within. Salinity is understood to be a key factor influencing the bioavailability of major and trace elements within sediments (Acosta *et al,* 2011; Du Laing *et al,* 2008). In soil environments containing bound inorganic contaminants, salinisation can enable mobilisation due to the high ionic strength of salts, in particular Pb and Cd (Acosta *et al,* 2011). It is therefore likely that the influence of seawater salts on inorganic contaminants within coastal legacy waste to increase metal mobilisation in various forms, including leachate. The inundation and exposure of seawater on coastal legacy landfill sites is expected to increase as a consequence of climate change. For instance, IPCC scenarios forecast a mean average sea-level rise ranging from 0.32 to 0.4 meters (RCP2.6 scenario) to 0.61 to 0.72 meters (RCP8.5 scenario) for North West England and North Wales by 2100 (NASA, 2021). Nevertheless, it is inevitable that sea-level rise will elevate the exposure of coastal legacy waste to seawater, thus increasing the mobilisation of inorganic metal pollutants. Examinations from Njue *et al* (2012) note that the attenuation of bioavailable heavy elements originating from closed landfill sites at Lodmoor

marsh, Dorset, UK, was attributed to the surrounding fine-grain sediments and fauna within the saltmarsh. This attenuation persisted beyond the peak flow of contamination from the landfill as it matured. However, the increase in ionic strength attributed to salinisation altered the bound chemical state of elements within the sediment matrix, enabling a higher degree of mobility, thus elevating the risk of nearby human and environmental receptors (Brand *et al,* 2017; Njue *et al,* 2012; Acosta *et al,* 2011; Vaverková, 2019).

With the coastal environment experiencing increasing storm conditions, compounded by enhanced coastal erosion (Oppenheimer *et al,* 2019), the distribution and dispersion potentially toxic element throughout the coastal environment is an increasing concern. The redistribution of contaminated landfill-derived materials, such as solid particulate matter, through aeolian transport mechanisms poses a significant challenge in landfill management and is considered another primary emission source of waste (Vaverková, 2019; Brand *et al,* 2017; Breshears *et al,* 2012). The increased suspension of landfill-based particulate matter and the size of the particulate matter strongly correlate with air velocity (Tian *et al,* 2008), which is further exacerbated by strong coastal weather events increasing air velocity in coastal areas, thus triggering erosion of coastal landfill; followed by the suspension; and distribution of landfill-based particulate matter and municipal solid waste, resulting in deposition of hazardous waste in areas away from the landfill source. Sea surface temperatures have risen by a global average of ~0.6°C from 1980-2020 (Fox-Kemper *et al,* 2021), which directly increases the severity and frequency of severe storm events (Aumann and Ruzmaikin, 2008). Consequently, severe storm events have the potential to structurally compromise the integrity of coastal legacy waste, thus having the potential to release bound and readily bioavailable contaminants.

1.4. The human and environmental risk of coastal legacy waste

As a consequence of mobilised toxic element concentrations, enhanced by climate change, the risk to human and environmental receptors is elevated. It is estimated that by 2055, approximately 122 coastal legacy waste sites in England are anticipated to undergo erosion into coastal waters, with this figure expected to rise to 144 sites by 2105 (Brand *et al,* 2017). The risk of human exposure towards PTE concentrations is likely to rise, as evidenced by 32% of England's total bathing water zones being within 100 meters of coastal legacy landfill sites (Brand *et al,* 2017), thus heightening the likelihood of direct human exposure through ingestion, inhalation, exposure during bathing, and contact with open wounds.

Presently, municipal solid waste landfill sites rank as the third-largest anthropogenic source of bioaerosol production (Zhang *et al,* 2023). Inhalation of these bioaerosols can induce respiratory irritation, inflammatory effects, cancers, and allergic responses. Moreover, the dispersion of bioaerosols is amplified by natural aeolian transport and human-induced climate change events and is prone to re-suspension due to inherent dynamics of particulate matter, contributing to their presence in the troposphere (Zhang *et al,* 2023; Xie *et al*, 2021).

Exposure to toxic concentrations of PTEs such as As, Cr, Cd, Zn, and iron (Fe), contained within coastal legacy landfill sites can have significant repercussions on human health (Lin *et al,* 2022). PTEs with carcinogenic properties, such as Cr, As, Cd, and beryllium (Be), can be readily ingested during bathing. Skin diseases induced by heavy metals are also of concern (Lin *et al*, 2022), with absorption through the skin serving as a primary pathway for heavy metal poisoning (Witkowska *et al,* 2021). The biophysiochemical properties of Cd, Pb, calcium (Ca), and magnesium (Mg) are similar, facilitating the replacement of Ca and Mg with Pb and Cd in the human body, thereby posing a threat to cellular integrity. Exposure is further compounded when the skin is compromised, as less penetration is required for metals, enabling easier access to the bloodstream (Magnano *et al,* 2022).

Landfill debris has been documented to inflict harm upon surrounding flora and fauna, in part due to the varied nature of legacy waste, including industrial, commercial, and domestic types. Non-biodegradable plastic waste is especially common in coastal areas (Rajmohan *et al,* 2019) and poses a detrimental impact on nearby bird and fish species. Digestion of micro-plastics can prove toxic due to chemicals used during production, as well as the absorption properties accumulating significant element concentrations (Vedolin *et al,* 2018). Whilst not always outright fatal, adverse impacts on animal species resulting from plastic ingestion include reproductive complications, reduced growth rates, inflammatory issues, and reduced digestion efficiency (Prata *et al,* 2021; Jewett *et al,* 2022; de Souza-Silva *et al,* 2022).

1.5. A UK perspective on coastal legacy waste

Inherited from a rise in industrial practices from the 19th century onwards, the issue of waste generation subsequently grew, with the need for waste storage substantially increasing (Brand *et al,* 2017; Louis, 2004). In response, areas deemed 'low-value coastal zones', for instance, saltmarshes, saw a significant increase in landfilling (Riley *et al,* 2020; Nicholls *et al,* 2021; Wadey *et al,* 2019), driven by: 1) a lack of meaning legislation regulating the composition and deposition of industrial waste (Brand *et al,* 2017); 2) the close proximity to industrial hubs; 3) a lack of environmental protection incentives, and limited understanding

of potential impacts (Jones and Tansey, 2015; Riley *et al,* 2020); and 4) the increasing industrialisation of coastal towns paired with advancements in transport infrastructure facilitating larger-scale disposal of industrial waste.

The introduction of meaningful legislative frameworks including the '*Environmental Protection Act 1990,*' '*Control of Pollution Act 1974,*' and '*House of Commons published Landfill research paper* (Hughes and Seely, 1996)' provided a modernised approach to landfill management, mandating documentation of waste deposited in landfills, to exclude significantly hazardous deposits. Subsequently, a 'Duty of Care' approach towards waste disposal was adopted to place a level of responsibility those who involved in the production, transport, and disposal of waste. Moreover, leachate control measures were introduced, with impermeable linings at landfill sites becoming mandatory to mitigate concerns regarding contaminant release (Brand *et al,* 2017). Whilst significant progress was made regarding MSW disposal, pre-legislative landfills still pose a severe risk. Furthermore, Nicholls *et al* (2021) compared the international community's approach to tackling the issue of coastal legacy waste. It was found that unlike other developed countries, policymakers in England are still not fully appreciative of the impacts and influences of coastal legacy waste.

Across England, there are approximately 420 coastal legacy waste sites within 100m proximity designated ecological sites. More specifically, 120 SSSI locations (Sites of Special Scientific Interest), 47 OSPAR marine protected areas, and 37 Ramsar sites. Furthermore, there are 128 designated UK bathing zone areas in England are situated within this proximity (Brand *et al,* 2018). Throughout England, an estimated 1264 legacy landfill sites are situated in coastal and estuarine regions vulnerable to flooding and erosion, with the associated risk linked to the shoreline management plan (SMP) adopted at each site (Brand, 2017). Predominantly, these coastal legacy landfill sites are located in areas governed by SMPs of 'managed retreat' and 'no intervention,' with notably fewer situated in regions adopting a 'hold the line' approach (Brand, 2017; Williams *et al,* 2018), coinciding with no current funding policy to protect legacy coastal landfills. (Beaven *et al,* 2020). In Wales, there are over 1,500 landfill sites, a significant proportion of which are historical and fall within coastal zones (Robbins *et al,* 2023). The majority of coastal landfill sites in Wales are situated in areas designated with a 'hold the line' SMP, with over 30% classified as 'undefended' (Robbins *et al,* 2023).

The inevitability of sea-level rise poses a substantial threat to the UK coastal zone. The Met Office (2023) annual sea-level rise projections in UK capital cities based on RCP climate

scenarios reflect different rates of sea-level rise depending on the climate scenario. Projected sea-level changes for RCP scenarios 2.6, 4.5, and 8.5 are estimated to increase by 0.4m, 0.5m, and 0.7m by 2100, respectively. Many unprotected or inadequately defended coastal legacy waste sites across the UK are already susceptible to erosion, however, the increasing intensity and frequency of weather events pose a growing concern regarding contaminant mobilisation. Moreover, legacy waste sites further inland will become increasingly at risk (Brand *et al,* 2017). While there is an ever-increasing urge to shift towards pragmatic approaches to shoreline management policies to address coastal erosion and flooding, coastal legacy waste sites present an obstacle to achieving this goal (Beaven *et al,* 2020), highlighting the need for management.

1.6. Current gaps in literature and justification of research

Despite the growing body of scientific literature on coastal legacy waste, significant knowledge gaps persist:

- There is a limited understanding of the specific contents of legacy waste, such as steelmaking slag and coal mine waste, despite the significant roles played by the steel and coal industries in regional economies (Nicholls *et al,* 2021; Riley *et al,* 2021). Further understanding of the contents of coastal legacy waste could provide further insights into potential contaminants released into surrounding coastal waters and habitats, allowing for a more pragmatic guide towards future management policies dependent on the waste type. Although recent academic literature has addressed the leaching behaviours of municipal solid waste exposed to simulated rainfall events (Linh *et al,* 2020; Takahashi and Shinaoka, 2012), deionised water has been used to represent rainwater conditions. The complexities of both aqueous matrixes are substantially different and thus are not representative of natural rainfall conditions. The identified gaps in the literature serve as the rationale for further investigation in this paper.
- Research into the interactions between saline environments and coastal landfills, as well as the environmental impacts of municipal solid waste released into the surrounding areas, remains limited (Brand *et al,* 2017). Existing studies often prioritise freshwater influences on coastal legacy waste, inadvertently disregarding the potential influence of saline salts on the mobility of elements stored within these sites (Brand, 2017; Chen and Ye, 2023; Brand and Spencer, 2020), thereby, delaying our understanding of saline water influences on leachate contaminant loads. Salinity

is known to alter the mobility of elements such as Pb, Zn, Cu, and Cd species in soils and sediments (Acosta *et al,* 2011). Moreover, the salts present in the aqueous matrix directly affect mobilization by competing with Ca for metal elements, leading to the release or precipitation of trace elements. Furthermore, acidification induced by high saline conditions provides additional opportunities for element mobilisation (Costis *et al,* 2021).

1.7. Aim and objectives

In response to the increasing concern surrounding coastal legacy waste, this research aims to *establish the environmental risk of potentially toxic elements situated within coastal legacy landfills*. To accomplish this aim, two research questions must be explored:

1. *What is the geochemical composition of coastal legacy waste sediments?*
2. *What is the leaching potential of potentially toxic elements from coastal legacy waste under various oxidised aqueous environmental matrixes?*

2. Study site

2.1. North West England and North Wales

The selection of study sites for this investigation was chosen in relation in part to reports made by Brand and Spencer (2018) highlighting the North West of England as a hotspot area for coastal legacy waste sites, due to the widespread heavy industry that once occurred in these regions. Additionally, a paper published by Riley *et al* (2022) investigating the extent of protected and unprotected coastal waste sites, and the level of prioritisation across England and Wales was also used to determine suitable study site locations. The prioritisation of coastal legacy waste sites was based on parameters such as current and predicted shoreline management policy adopted within that region; the presence of coastal flood defences; and the proximity to sensitive receptors, with areas most probable for human interaction designated higher in significance.

The extent of coastal legacy waste sites in North West England and Wales covers approximately 3,500ha, ranking it as the third-largest area of waste accumulation concerning the entirety of England and Wales. Within this region, approximately 500ha have been classified as 'unprotected,' with 55% of the total coastal steel and iron slag waste in England and Wales concentrated in North West England (Riley *et al,* 2022). The distribution of protected and unprotected coastal legacy waste sites varies across North West England and North Wales, contributing to the rationale for selecting specific sample sites. For instance, in the southern section of the Solway Firth region, protected sites range between 11 and 20, while unprotected sites range between 1 and 5. Similarly, the Duddon Sands estuary hosts between 11 and 20 protected sites and 11 and 20 unprotected sites. In North Wales, particularly the Dee Estuary, there are 24 protected sites and 6 to 10 unprotected sites (Riley *et al,* 2022).

The chosen study sites depict two distinct scenarios: legacy waste sites protected by the relevant Shoreline Management Plan (SMP) strategy and those that remain unprotected. Additionally, these sites are either situated within or adjacent to zones designated as 'Flood-Zone 3' risk areas by the Environment Agency (2023b) or classified as 'high-risk' by Natural Resources Wales (2023) (see sections 2.1.1. – 2.1.6.). Moreover, the proximity of landfill sites to culturally, scientifically, and environmentally significant areas is noteworthy. These include several SSSI locations, such as the Duddon Estuary neighbouring Borwick Rails and St. Bees Head at Whitehaven (Defra, 2023a), as well as numerous designated bathing areas like Haverigg and St. Bees (Defra, 2023b). Moreover, these study sites reflect the waste from two

prominent forms of industry, including colliery-based and steel/metalwork-based. As such, the study sites chosen include: Talacre, Bagillt, Maryport, Borwick rails, Whitehaven, and Siddick (as seen in figure 1).

Figure 1. A map of North Wales and North West England depicting the locations of each study site. Map data ©TerraMetric 2024.

2.1.1. Study site: Bagillt

As seen in figure 2, Bagillt, situated in North Wales along the banks of the Dee Estuary within the Flintshire principal area, approximately 11km upstream from the mouth of the river Dee, was a former industrialised coastal town marked by lead and iron works, as well as coal mining operations, notably the 'Bettisfield colliery.' Presently, the area contains approximately 11 coal-based coastal legacy waste sites. Furthermore, this area has been categorised as "high risk" for coastal flooding, with the likelihood of such events exceeding 1-in-30 per year (3.3%) (Natural Resources Wales, 2023). While the SMP in place adopts a partial "hold-the-line" strategy, featuring embankment defences (Environment Agency, 2023), certain coastal legacy waste sites lie beyond these defences, which are therefore more vulnerable to coastal erosion. Notably, Dee Bank, Bagillt, ranks among the ‘top 10 legacy mine spoil deposits most at risk in England and Wales,’ (Riley *et al,* 2021). Consequently, two landfill sampling sites were chosen west of the embankment defence, both displaying distinct top layer sediment colour variations, with sample site DBB1 showing a ‘black’ top layer, whereas sample site DBB2 having a ‘red-orange-based’ top layer, as seen in figure 3. In addition, very minimal vegetation was present amongst the previously eroded waste sediment within the immediate proximity to the coastline. Vegetation approximately 15m from the shoreline drastically increases where waste sediment is still yet to be eroded. These sample sites were selected due to their positioning away from the flood embankment, differences in appearance and visible exposure, as well as the accessibility and proximity of the coastal legacy waste sites to surrounding receptors including the Dee estuary SSSI.

Figure 2. Study site map of Bagillt depicting the location of the legacy waste sample sites, with the addition of the shoreline management policies and the coastal flood zone area and designation. Map data ©TerraMetric 2024.

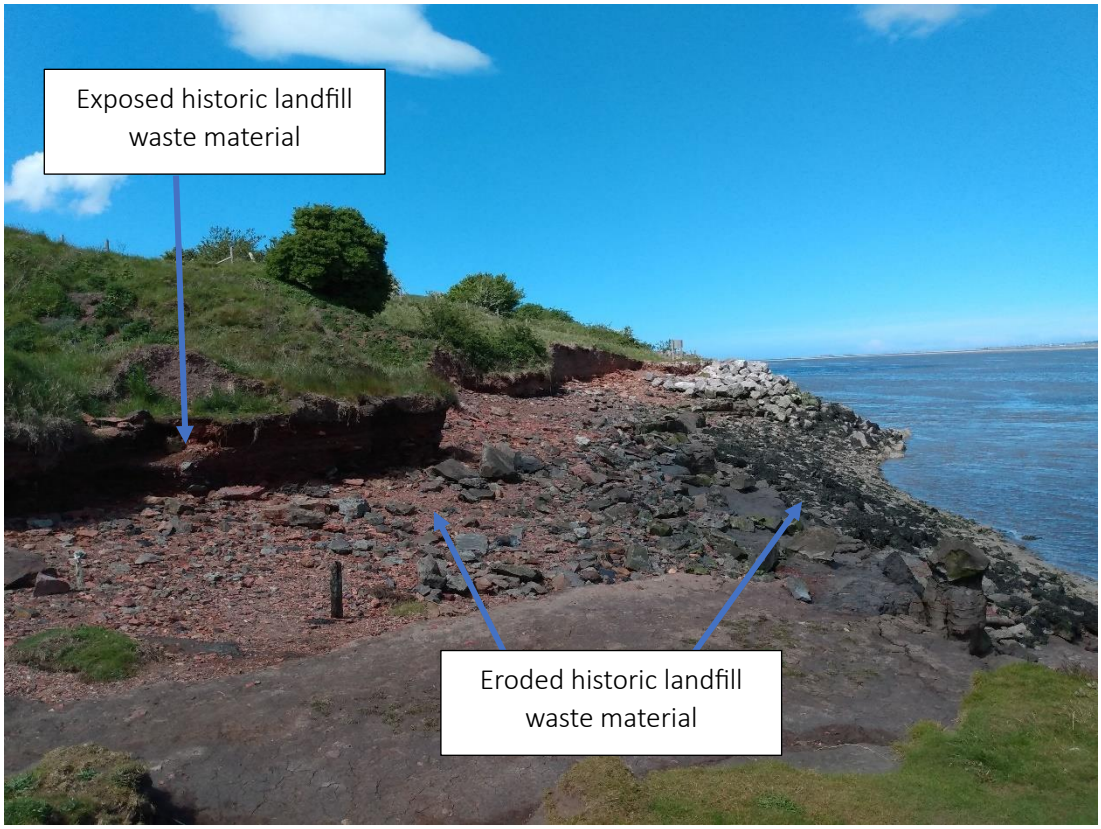

Figure 3. Erosion of coastal legacy waste sediment at Dee bank, Bagillt.

2.1.2. Study site: Talacre

As seen in figure 4, The Point of Ayr Gas Terminal, situated in Talacre, Northern Flintshire, along the Dee estuary, was previously an industrial hub located in North Wales, on the Northern outskirts of the Flintshire principal area. This region's industrial activities primarily revolved around colliery operations, notably the Point of Ayr colliery, which operated from the 1880s until 1996, undergoing modernisation in the 1950s to increase the coal extraction capacity. Consequently, substantial coal-based legacy waste remains in the surrounding coastal area, and as such the Point of Ayr site is now considered within the 'top 10 legacy mine spoil deposits most at-risk in England and Wales' as seen previously (Riley *et al,* 2021). A 'hold-the-line' approach has been adopted on the eastern side of the Talacre coastline, which can be seen by the flood embankment defence present (Environment Agency, 2023). Where coastal legacy waste is present, the embankment is situated further inland parallel to the coastline. However, coastal flood risk has been deemed 'high risk' and 'low risk' for areas further inland from the embankment and into residential areas, highlighting the risk of coastal erosion impacts on nearby settlements. Observations made at the Talacre-bound sample sites show differences between both sites. Sample site GTT1 depicts an embankment possibly composed of coal spoil, whereas sample site GTT2 is positioned central near old railway lines in the periphery of a dried-out pool. Additionally, both sample sites were similar in black/grey surface sediment colour, had minimal vegetation present, with both samples present on old industrial land (as seen in figure 5 and 6). As such, 2 sample sites were chosen where coastal flood risk is deemed 'high' and unprotected from 'hold-the-line' SMP policy and flood embankment defences, where coastal legacy waste mobilisation is high.

Figure 4. Study site map of Talacre depicting the location of the legacy waste sample sites, with the addition of the shoreline management policies and the coastal flood zone area and designation. Map data ©TerraMetric 2024.

Figure 5. Exposed legacy waste surface at sample site GTT1 in Talacre gas terminal.

Figure 6. Exposed legacy waste surface at sample site GTT2 in Talacre gas terminal

2.1.3. Study site: Maryport

Maryport is a town located in Western Allerdale, Northern Cumbria with significant industrial, maritime, and historical heritage (figure 7). The period of industrialization from the 1860s onwards enabled a diverse array of industries, including iron and metal works, colliery operations, timber yards, and dockyards, alongside significant improvements in transportation infrastructure such as the railway network. Industrial practices dominated the region until the 1940s, and as a result, is partially responsible for the >55 million cubic metres of slag waste identified in Cumbria recognised by Riley *et al* (2020), making Cumbria the county with the highest amount of slag waste deposit in the UK; with North Lincolnshire 2nd at 17.5 million cubic meters. The SMP for Maryport is segmented into two sections: North of Maryport Dockyard, adopts a 'hold-the-line' approach, while the southern section adopts a 'no active intervention' strategy in the short, medium, and long terms. Additionally, the entire coastline of Maryport falls within the 'Flood Zone 3' designation set by the Environment Agency (2023), signifying a 0.5% or greater chance of sea-induced flooding in any given year. Four sample sites were chosen in the southern section of the coastal area of Maryport, once neighbouring the ‘Solway Iron Works’ and the ‘Risehow Colliery.’ Additionally, observations of legacy waste material at sample sites MPC1 and MPC3 depict white eroding steel slag material with soil cap intermixed with ochreous gravels, whereas sample sites MPC2 and MPC4 appeared to show eroding waste sediment alongside ochreous soil cap/overburden. With no active sea defence or suitable management policies, these sites remain entirely exposed, presenting significant risks to nearby residents and environmental receptors.

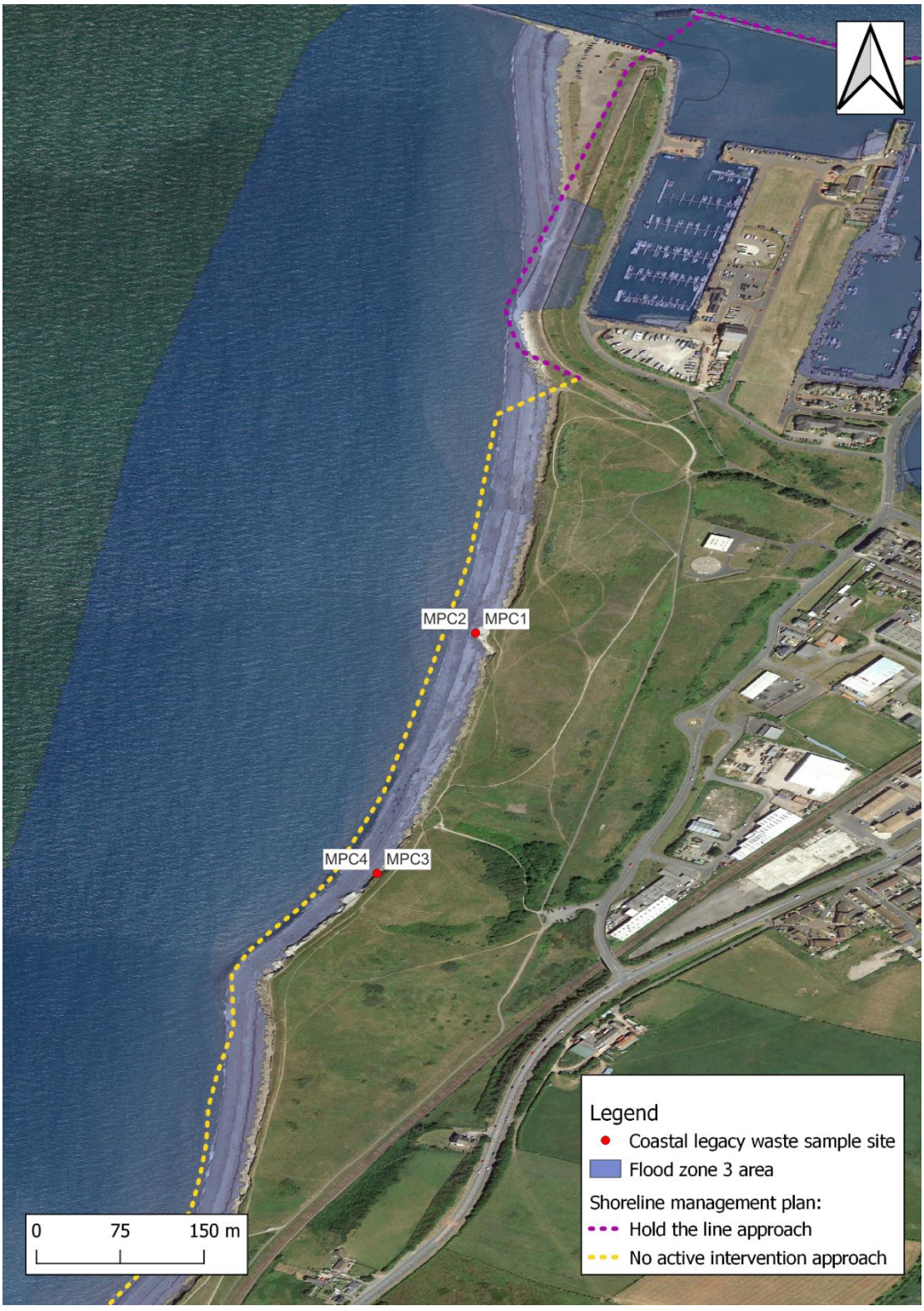

Figure 7. Study site map of Maryport depicting the location of the legacy waste sample sites, with the addition of the shoreline management policies and the coastal flood zone area and designation. Map data ©TerraMetric 2024.

2.1.4. Study site: Whitehaven

Whitehaven is a coastal port town located south of Maryport, situated in the North West of Copeland Borough, Northern Cumbria (as seen in figure 8). Similar to previous study sites, industrialisation in Whitehaven from the 1840s onwards was predominately colliery-based, with examples including Wellington Pit, Haig Colliery, and Saltom Pit. The SMP for the Whitehaven coastline south of the harbour predominantly adopts a 'no active intervention' strategy, with limited areas implementing a 'hold-the-line' approach (Cumbria County Council, no date; Environment Agency, 2024). Concurrently, this area holds a ‘Flood Zone 3’ designation, similar to previous study sites. The accelerated erosion of coastal areas, particularly those housing colliery and metal slag coastal legacy waste, presents a significant concern as the Whitehaven coastline is currently eroding at approximately 1.5m per year (Cumbria County Council, no date). Moreover, the degradation of coastal defences within the Saltom Pit area highlights the escalating risk of contaminant mobilization in the event of defence failure. Consequently, four sample sites situated south of Whitehaven harbour were chosen, adjacent to former colliery sites, all of which are within areas of ‘no active intervention’ SMP. Furthermore, observations at sample site HC1 reveal an eroding escarpment characterised by layers of coal spoil, soil, sand, gravel, and cobble. In contrast, sample site HC2 exhibits a coal spoil outcrop positioned west of the Haig Colliery. Sample sites HC3 and HC4 display an eroded cliff face predominantly composed of black coal spoil, with red gravel deposits and an underlying clay layer also observed.

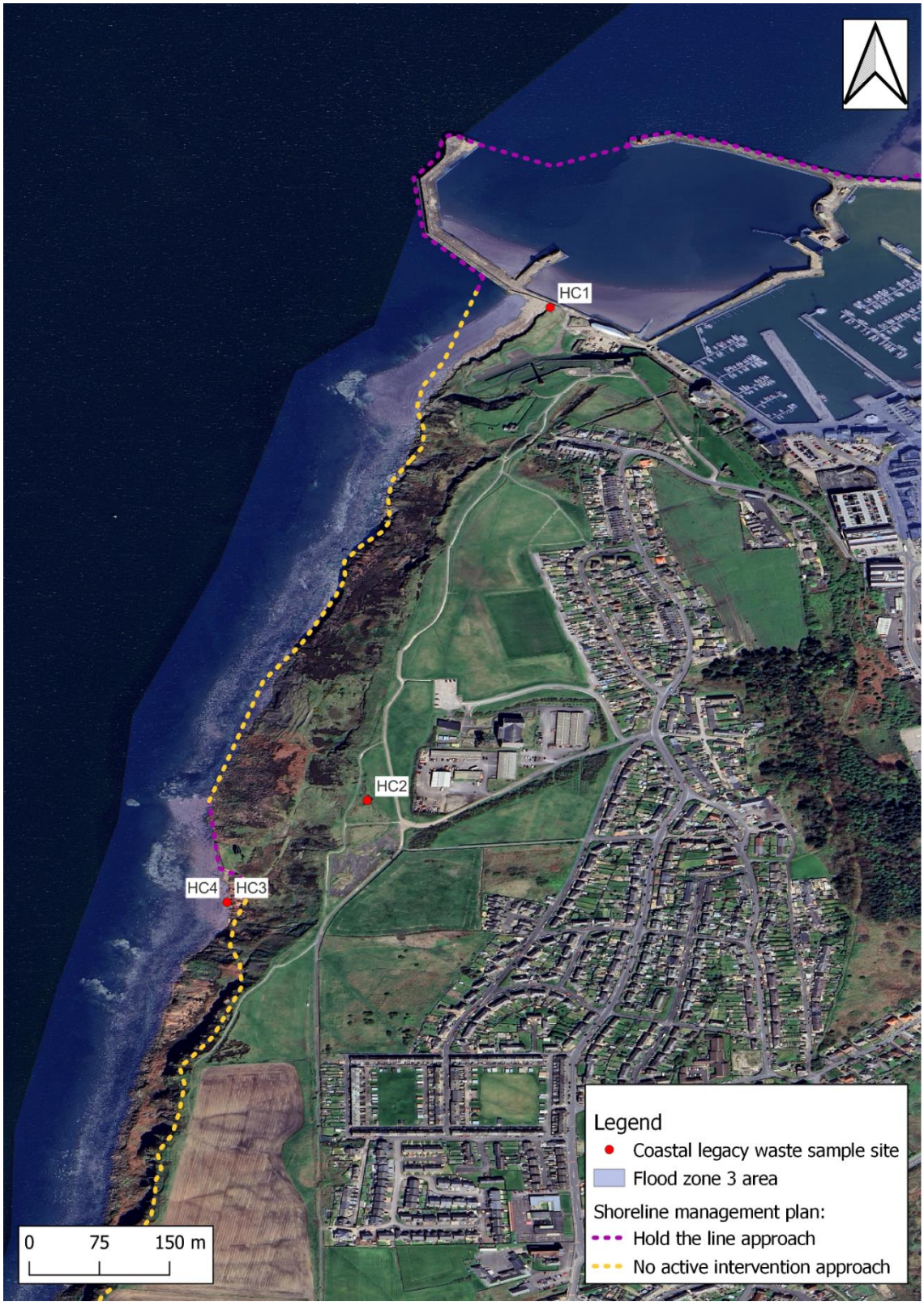

Figure 8. Study site map of Whitehaven depicting the location of the legacy waste sample sites, with the addition of the shoreline management policies and the coastal flood zone area and designation. Map data ©TerraMetric 2024.

2.1.5. Study site: Borwick Rails

The period of industrialisation in Borwick Rails mirrors the sites aforementioned across Cumbria. Located in the southern region of Copeland Borough, Cumbria, the industry is primarily centred on ironworks. The consequence of this led to extensive slag deposits (Riley *et al,* 2020) encircling the outskirts of the 'salting zone.' The SMP for this area is a 'no active intervention' strategy (Cumbria County Council, no date) due to the limited economic significance and the presence of established flood defences westward of the former ironworks. However, unlike previous sites across Cumbria, the study site does not lie within any designated flood zone. Nonetheless, the surrounding environs are encompassed within 'Flood-Zone 3' (Environment Agency, 2021), indicating that heightened coastal erosion and rising sea levels could potentially expose these sites, mobilising bound contaminants and redistributing them to receptors. Observations made at the study site reveal both similarities and differences among each sampled location. Coastal erosion is present across all sample site locations, characterised by eroding slag faces and scattered rubble. Variations in soil texture at each site was also noticeable, and as a consequence, six sampling sites were identified along the periphery of the "salting zone," where slag deposition occurred (as seen in figure 9). Specifically, sample sites MP1, MP2, and MP5 exhibit eroding slag faces with loose rubble and minimal soil coverage. Sample sites MP3 and MP4 present similar eroding slag features, distinguished by a darker red tinge in the eroded sediment. Lastly, sample site MP6 is visually distinguished by ferrocrete sediments with a distinctive orange to purple colouration.

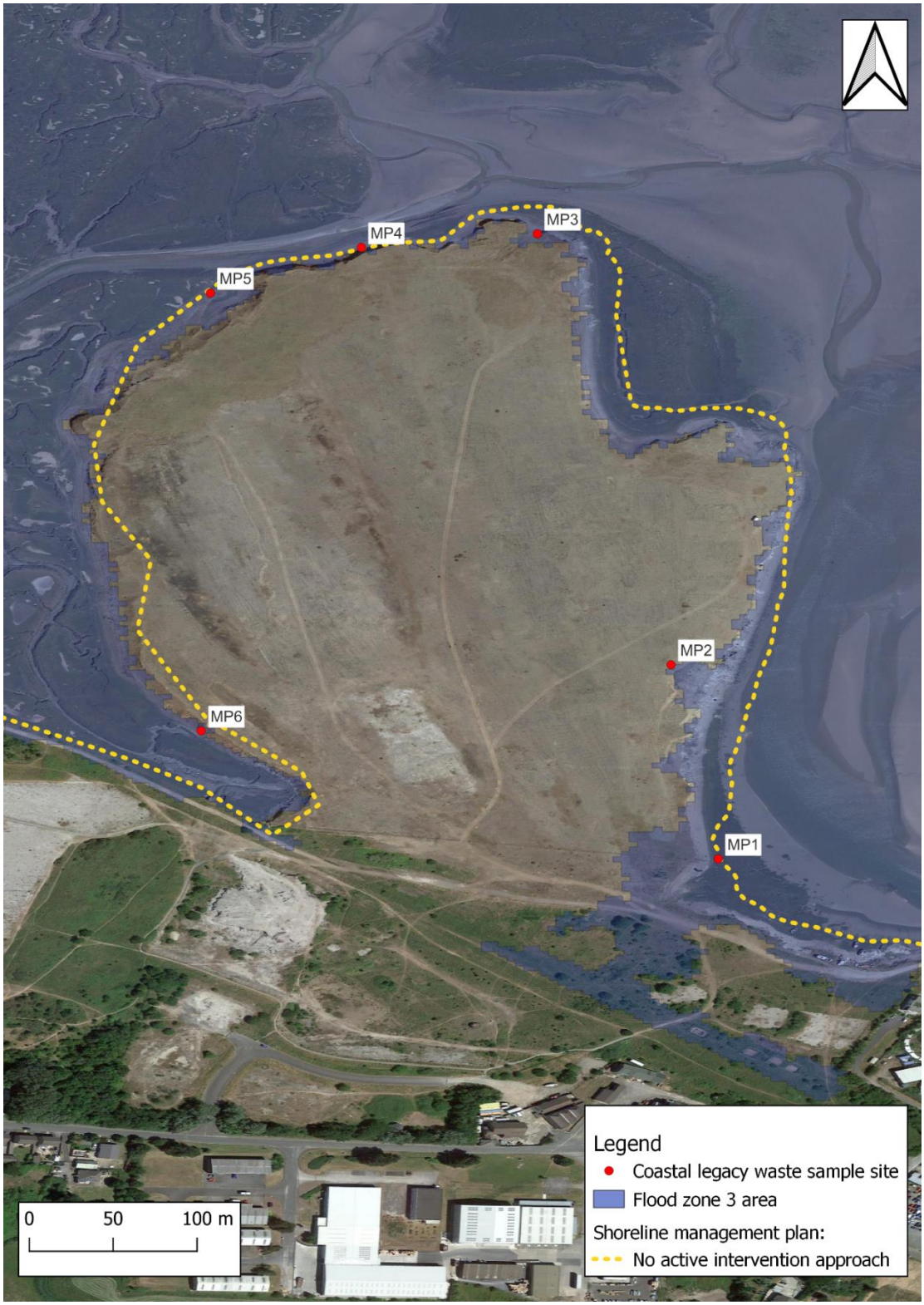

Figure 9. Study site map of Borwick rails depicting the location of the legacy waste sample sites, with the addition of the shoreline management policies and the coastal flood zone area and designation. Map data ©TerraMetric 2024.

2.1.6. Study site: Siddick

Situated along the western coastline of Allerdale in Northern Cumbria, Siddick underwent industrialisation, giving rise to industries such as the 'Oldside Iron and Steel Works' and 'St. Helens Colliery.' The addition of railway infrastructure at these sites facilitated the transportation and disposal of generated waste, which was subsequently deposited along the coastal periphery of these railways. In contrast to previous study sites, the SMP adopted at the Siddick study site is a 'hold-the-line' strategy (Cumbria County Council, no date; Environment Agency, 2024), due to the surrounding land value, elevated by the nearby ‘Siddick wind farm.’ However, the coastal legacy waste sites along the Siddick coastline are not within this designation and coupled with the designation of 'Flood Zone 3' (Environment Agency, 2021), the risk of mobilisation of bound contaminants will only increase. Five sampling sites were chosen, of which, three were situated in areas once occupied by 'St. Helens Colliery' and the remaining two near to the 'Oldside Iron and Steel Works' (as seen in figure 10). Specifically, sample sites WWF1 and WWF2 exhibit erosion of legacy waste sediment with visible white and black concrete layers and ochreous nodules inside. Additionally, sample sites WWF 3 and WWF4 depict an eroding ‘black gravel’ legacy waste spoil, with ochreous nodules inside and yellow clays dispersed throughout. Finally, sample site WWF5 depicts an eroding white concrete waste deposit.

Figure 10. Study site map of Siddick depicting the location of the legacy waste sample sites, with the addition of the shoreline management policies and the coastal flood zone area and designation. Map data ©TerraMetric 2024.

.

3. Methodology

3.1. Sample collection

To address the outlined research questions, six study site locations (as mentioned in section 2.1) corresponding to coastal legacy landfill sites in North West England and North Wales were selected, from which a total of 23 sediment samples were collected. Sediment samples were selected through a targeted sampling strategy of cluster sampling and point sampling of legacy waste sediments. For the initial cluster sample, 5 surface sediment samples within a ~10m^2 area was collected using a trowel until 5kg of mixed sample was reached. Subsequently, the sediment was thoroughly mixed, followed by the coning of quartering of the sample to collect ~0.5 kg of the homogenous sample matrix, which were then sealed within plastic sample bags and ready for laboratory preparation.

3.1.1. Sample preparation

Before any laboratory analysis, the preparation of samples required thorough cleaning of all glassware and plasticware with 5% nitric acid rinse to ensure no contamination of samples. This follows a similar protocol to that of Brand and Spencer (2020). Furthermore, in preparation for acid digestion, scanning electron microscopy, and leachate generation, the landfill samples underwent initial compaction followed by pulverization to ensure sample homogenization, making them suitable for analysis.

Proctor compaction was utilised as a crushing technique to alter the sample specimen by reducing the clast and aggregate size of samples unable to be initially pulverised to due size restraints, also seen in Choi *et al* (2018). A minimum of 100g rock samples extracted from legacy coastal landfill sites were crushed to a size fraction <2mm in preparation for further crushing through a "Fritsch mortar grinder Pulverisette." To prevent cross-contamination during the grinding process, the equipment was thoroughly cleaned after processing each sample.

Samples crushed to <2mm were placed into the Pulveriser, whereby the samples were further grounded down to a size fraction of <63µm resulting in the production of a microfine powder (Erdoğan *et al,* 2007). Subsequently, sieve analysis using a plastic sieve was performed to separate any particulate matter >63µ that are unsuitable for analysis.

3.2. Major element analysis by scanning electron microscopy

Scanning electron microscopy (SEM) is a routine forensic method of analysis used in numerous studies in the past to identify the characteristics of various soils and minerals. The application of SEM is an appropriate method for coastal legacy waste samples for compositional and geochemical analysis. (Huliselan *et al,* 2010; Östürk and Sevimoğlu, 2021). Following the initial preparation of landfill samples, each sample was attached to an aluminium stud using a small amount of graphite adhesive. Subsequently, samples were sputter coated in gold to standardise the surface of the sample to provide adequate electrical charging of elements within the sample, given that most geological materials are primarily non-conductive (Echlin, 2011; Leslie and Mitchell, 2007). Analysis of major element concentrations in legacy waste sediments was conducted using a "FEI Quanta200 SEM" with an inspect S range of 0.1-30kv, while also equipped with secondary electron, backscattering, and large field detectors.

Analysis of the samples involved examining 8-10 'sites of interest' per sample, consisting of 23 samples obtained from coastal legacy landfills. SEM analysis utilised the 'secondary electron mode,' an accepted method of element analysis (Dai *et al,* 2020; Pina *et al,* 2000). However, a backscattering approach was also employed to identify heavier elements within the sample images (Goldstein *et al.* 2017). Careful consideration was given to the 'spot size' during sample analysis, as variations in spot size directly influenced the intensity of emitted x-rays. Consequently, an increase in spot size could potentially disrupt or redistribute the sample under examination, while a reduction in spot size might compromise image resolution (ThermoFisher, 2023). Hence, spot size adjustments were made to balance the need to minimize sample disturbance whilst achieving satisfactory imaging resolution. The elements detected through SEM are considered major elements for this study due to the high detection limits, in comparison to other analytical methods of element analysis (mentioned below in section 3.3).

3.3. Trace metal analysis by acid digestion and ICP-MS

3.3.1. Acid digestion

The reverse Aqua regia method in a 4:1 ratio of nitric acid (HNO3) to hydrochloric acid (HCl) was selected to dissolve the landfill sediments into a liquid for, due to previous publications establishing this method as highly effective in extracting metals while preserving their integrity (Lu *et al,* 2007; Siaka *et al,* 1998). Initially, 1g of landfill sample was dispensed into a standard microwave digestion tube, with triplicate digestions conducted for each sample. An additional set of duplicate sets for two landfill samples and four blanks were also produced alongside the batch.

Following sample deposition, the samples were moistened with 2 mL of deionized water, followed by the injection of 3ml HCl and 12ml HNO_3. To mitigate foam formation during acid introduction, a gradual drop-by-drop approach was adopted upon initial signs of foaming. Subsequently, the samples were allowed to rest for 30 minutes in a fume cupboard to alleviate pressure on safety valves during the digestion process, thereby minimizing the release of hot acid vapor. White pressure caps and screwcaps were then placed on each digestor tube after the rest period to complete the preparation for digestion.

Microwave digestion was selected as the appropriate method for converting geological samples into a liquid matrix. This method enables complete sample digestion in less than two hours, requiring a reduced volume of acid relative to traditional wet-digestion techniques (Papp and Fischer, 1987). The use of microwave digestion was also conducted in guidance with procedures from Lamble and Hill (1998).

Digestion was carried out using the "1600w MARS CEM" microwave digestion system, with the temperature set at 170°C and maintained for 20 minutes, preceded by a 10-minute ramp time for the microwave to reach the desired temperature. Following the digestion process, a 30-minute cooling-off period was allowed before continuing further.

Digested samples were decanted from the digestor tubes onto filter paper to separate precipitates. In the few cases where insoluble mixtures were present, <1ml nitric acid was applied to the samples until the filtrate had completely passed through. Subsequently, sample dilution of acid-based samples was carried out in preparation for sample analysis. Diluting digested samples by a factor of 1000x was carried out to achieve suitable results within the calibration range generated with use of external standards (referred to below), and to protect the integrity of the analytical instruments.

3.3.2. ICP-MS and ICP-OES

Inductively Coupled Plasma Mass Spectrometry (ICP-MS) and Optical Emission Spectroscopy (ICP-OES) are designed to detect and quantify elements at trace levels often corresponding to regulatory limits within the parts per billion (ppb) range. Now a widely adopted method since its inception in the 1980s (Lum and Leung, 2016), this technique of element analysis has been implemented vastly throughout the literature and also used in similar studies, as seen in Khan *et al,* (2017) and Brand and Spencer (2019).

Following guidance outlined by Prichard and Barwick (2003), a calibration range comprising eight calibration standards, along with one blank and two duplicates was produced. As such, minimising the level of prediction and estimations and increased the level of confidence in the obtained results. Calibration standards were prepared using the 'SPEX Certiprep' multi-element solution 2 (Spex Certiprep, 2023) certified reference material (external standard). Depending on the nature of the samples under analysis, such as leachate or digested samples, adjustments to the calibration ranges were made to ensure that the analysed concentrations fell within the calibration range.

3.3.3. ICP quality control: total dissolved metals

An Agilent Technologies 7900 ICP-MS was utilised to determine the element concentrations of the aforementioned digested samples, of which the elements analysed included As, Cu, V, Pb, Ni, Zn, Cr, Co, Be, Sb, Tl, and Se. Prior to sample injection, calibration standards were introduced to establish a suitable R^2 value and detection limit, as seen in table 1. The limit of detection varies depending on the analytical instrument used. For instance, ICP-MS is well-suited for detecting analyte concentrations ranging from low ppb to low parts per million (ppm), contrasting with ICP-OES, which is more adept at analysing concentrations within a higher ppm range. Subsequently, diluted digested landfill samples were introduced to the ICP-based instrument. Notably, a blank sample was analysed after every set of ten digested samples, with two check standard measures performed after each blank analysis.

Total dissolved elements	R^2 Value	Limit of detection (mg/kg)
Al	0.976	0.1
K	0.999	0.3
Mg	0.982	0.6
Fe	0.987	0.05
Mn	9999	0.001
As	9999	0.001
Ba	998	0.02
Cd	998	0.02
Co	0.9999	0.0006
Cr	0.999	0.007
Cu	0.998	0.01
Ni	0.9999	0.003
Pb	0.9999	0.009
Zn	0.998	0.1
V	0.999	0.0008
Tl	0.999	<0.001
Se	0.9999	0.07
Sb	0.999	0.0003
Be	0.999	0.001

Table 1. R^2 value and limit off detection (mg/kg) results of total dissolved elements prior to ICP analysis.

3.4. Leaching experiments

Leaching experiments were undertaken to assess the leachable forms of elements from coastal legacy waste sediments. These experiments were performed in accordance with the British standard leaching test (BS EN 12457-2-2002), also seen in Brand and Spencer (2020), and Little *et al* (2008). Adaptations to the British standing leachate test were implemented by integrating artificial rainwater (ARW) (section 3.4.2) and artificial seawater (ASW) (section 3.4.1), as the current British standard method does not entirely reflect real-world conditions. Notably, the differences in composition between deionised water, ASW, and ARW could significantly influence the mobility of elements, justifying such adjustments.

3.4.1. Artificial seawater production

ASW was produced using manufactured synthetic sea salt from 'Aquarium Systems.' A 2L batch of artificial seawater was produced by measuring out 33g (with precision up to three decimal places) of the aforementioned artificial sea salts and thoroughly mixing with 2L of deionised water. This formulation yielded artificial seawater with an approximate density of 1.020 g/ml at 24 degrees Celsius, with magnesium (1200 mg/L), calcium (370 mg/L), and potassium (350 mg/L) concentrations falling within appropriate ranges.

3.4.2. Artificial rainwater production

ARW was generated in accordance with an ARW recipe used in academic literature to depict rainfall precipitated in Plynlimon, mid-Wales (Lynch, 2015; Neal *et al,* 2001), of which can be seen in table 2 below.

Salt	(mg/L)
K_2SO_4	0.2
$CaSO_42H_2O$	0.74
$MgSO_47H_2O$	0.56
NaCl	4.47
$MgCl_26H_2O$	1.36
NH_4NO3	0.726
$(NH_4)2SO_4$	0.18

Table 2. List of ingredients and quantity needed to produce artificial rainwater based on Plynlimon precipitation, Mid-Wales (Lynch, 2015).

3.4.3. Deionised water production

Deionised water throughout the project was produced at 18.2MΩ using a 'Suez water purification system.'

3.4.4. Leachate sample preparation

The finely prepared sample used for ICP and SEM analysis was also utilised for the leaching sample as it was within particulate size required by the BS EN 12457-2-2002 leaching method, whilst it also allowed to save on potential legacy waste sample should the need for re-running of tests be necessary. 10g of sample was partitioned into thirds, approximately 3.33 grams each. To determine the dry matter content, each sub-sample was placed in a 105°C oven for 3 hours, then followed by weighing. Following this, each sub-sample was transferred into a 50ml clean bottle, where leachant was added in accordance with the 10l/kg of leachant water ratio to comply with leaching standards. This method was carried out three times, employing deionised water, ASW, and ARW as leachants separately. Moreover, measurements of temperature and pH (EUTECH Instruments pH 700), Oxygen Reduction Potential (ORP) (EUTECH Instruments Ion 2700), and electrical conductivity (EUTECH Instruments CON 2700) were conducted both before and after leaching.

3.4.5. Leaching test

The batch leaching method, in accordance with the BS EN 12457-2-2002 method, was performed to assess the leaching of hazardous element concentrations within coastal legacy waste sediments. A total of 90 samples were subjected to leaching (30 samples per leachant type), with 10 sample sites selected and an additional two duplicates for each sample. Furthermore, a blank sample was included for each sample site, containing only leachant, to assess background conditions and identify potential contamination. Leachate samples were agitated on an orbital shaker (Adolf Kühner AG Schweiz Lab-Shaker) for 24 hours at 95 rpm. Following agitation, each sub-sample was allowed to settle for 15 minutes. Subsequently, samples that did not settle within one hour were centrifuged (HERMLE Labortechnik model Z 446) at 2000 rpm for 10 minutes to separate suspended sediments from leachate, as seen in Brand and Spencer (2020). The samples were then filtered through a 0.45 µm cellulose filter using the syringe filtering method. The volume of filtered eluate was measured, and the temperature, ORP, pH, and electrical conductivity of the eluate were determined as previously described.

In preparation for ICP-MS analysis, the leachate samples were acidified with 2% nitric acid to stabilise the elements within the sample matrix and prevent alteration of analytes before

analysis. Deionised leachate samples were initially diluted by a factor of 2, followed by a subsequent dilution by a factor of 5 to ensure that the results fell within the calibration range established. ASW and ARW were not diluted, as the ICP-MS instrument was equipped with a 'Mira Mist nebuliser,' allowing it to withstand total dissolved solid concentrations exceeding 35,000 mg/l. The samples were then refrigerated pending ICP-MS analysis of dissolved metal concentrations.

3.4.6. ICP-MS quality control: leaching test

Similar to quality control measures for total dissolved metals (seen in section 3.3.3), limits of detection and R^2 value results for the leaching tests are displayed in table 3 below.

Element	R^2 value			Limit of detection (mg/kg)		
	Deionised leachate	ARW leachate	ASW leachate	Deionised leachate	ARW leachate	ASW leachate
Al	0.996	0.999	0.999	0.001	0.003	0.003
K	0.998	0.998	n/a	0.001	0.03	n/a
Mg	0.999	0.998	n/a	0.006	0.006	n/a
Fe	0.999	0.999	n/a	0.002	0.003	n/a
Mn	0.999	0.999	0.9996	0.002	0.0002	<0.001
As	0.9996	0.999	0.9997	0.001	0.0004	<0.001
Ba	0.999	0.999	0.999	0.02	0.001	<0.001
Co	0.999	0.999	0.999	0.001	<0.0001	<0.001
Cr	0.999	>0.999	0.9998	0.003	<0.0001	<0.001
Cu	0.999	0.999	0.9994	0.001	0.0018	0.001
Ni	0.999	0.9996	0.9997	0.003	0.0003	<0.001
Pb	>0.999	0.9996	0.999	0.009	0.0001	<0.001
Zn	0.999	0.9996	0.9997	0.01	0.004	0.001
V	0.9998	0.9992	0.9998	0.007	0.0001	<0.001

Table 3. R^2value and limit of detection (mg/kg) results of elements throughout all leachant types prior to ICP-MS analysis.

3.5. Statistical analysis

Statistical analysis was performed using OriginPro 9 (OriginLab, 2012) scientific graphing and data analysis software to identify differences in element concentrations between colliery and steel-based waste types. Regarding the first research question, total digest concentration data was plotted using box-and-whisker plots, displaying the elements present within each study site. Moreover, element data was separated into two distinct groups based on the waste type of the sample, either colliery-based or steel slag-based waste. A subsequent assessment of normality was performed using the Shapiro-Wilk normality test to determine if the null hypothesis regarding data distribution can be rejected or not, followed by a Mann-Whitney test to determine differences between waste types. Similarly, in addressing the second research question, element leachate data was represented through box-and-whisker plots along with conducting distribution and difference tests on leached elements based on waste type. Furthermore, an analysis of distribution and differences was carried out using the previously mentioned analysis methods for pH, Oxygen Reduction Potential (ORP), and Electrical Conductivity (EC) values before and after leaching. Additionally, Pearson's correlation coefficient was conducted to evaluate potential associations among leached elements within specific leachants.

4. Results and Discussion

4.1. Geochemistry of legacy waste sediments

4.1.1. Major element concentrations

SEM analysis of elements in to colliery sediments (seen in figure 11 and table 4) is listed in order from highest average concentrations: O (53wt%) > Si (18wt%) > Al (12wt%) > Fe (8wt%) > Ca (3wt%) > K (2wt%) > Mg (1wt%) > Mn (0.6wt%) > Ti (0.4wt%). Additionally, the highest average element concentrations in steel waste sediments are listed as: O (53wt%) > Si (13wt%) > Ca (11wt%) > Al (8.2wt%) > Fe (8wt%) > Mn (3.5wt%) > Mg (1wt%) > K (1wt%) (seen in figure 12 and table 4). The distribution of element concentrations across colliery-based and steel slag-based waste sediments can be seen in table 5. The distribution of elements within colliery-based sediments, K, Ca, Ti, Si, Mn, and Mg concentrations are indicative of non-normal distribution, whereas O, Mn, Al, and Fe are representative of normal distribution. As for steel-slag based waste, distribution of O, and Mg concentrations were indicative of non-normal distribution, with Al, Si, K, Ca, and Fe representative of normal distribution. Moreover, Mann-Whitney U analysis of major element concentrations across both waste types illustrate significant differences in Mg, Al, Si, and Ca concentrations, whereas similarities in Fe, K, and O concentrations were apparent (as seen in table 6).

Focusing on major metal concentrations, Aluminium (Al) concentrations make up the largest proportion within landfill sediment matrix across the majority of sample sites across steel and colliery waste. Al concentrations detected across all waste sites fall within typical Al concentrations detected within soils according to US EPA (2003a) (1-30wt%). This is indicative of feldspars and aluminosilicates present in soil, which are also used in the steel-making process (EPA, 2003). Whilst abundant in soil, Al is typically not readily bioavailable, with the majority of the concentration bound to minerals and sediments (BGS, 2012). Furthermore, concentrations are of relatively low risk seen by no sediment quality guidelines values available. Whilst Sediment guideline values (SGVs) are not a direct indicator for element toxicity within soils and sediment (O'Connor, 2004), they provide a basis for the likelihood of toxic effects to occur if the SGV is used as a threshold, with the likelihood increasing further as concentrations increasingly exceed the guideline value.

Iron (Fe) made up the 2nd largest proportion of total metal concentrations across most sample sites. Similarly to Al, Fe concentrations present in soil range from 2-55wt% (EPA, 2003), of which concentrations detected did not exceed. Fe is ubiquitous in soil and sediments, and is also considered a major constituent in coal ash (USGS, 2015) and iron and

steel slag waste (Piatak *et al,* 2019). Although only a small fraction of the overall Fe concentrations in soils and sediments may be deemed bioavailable (BGS, 2012), in aerobic soils and sediments characterized by moderately neutral to high pH levels, Fe primarily exists in a relatively insoluble form as ferric oxide (Fe_2O_3) (Morrisey and Guerinot, 2009). Under saline conditions, whilst dissolved Fe can be present within seawater, the solubility of Fe(III) limits total dissolved Fe concentrations present within seawater (Liu and Millero, 2002). Similarly to Al, no Fe sediment quality guidelines have been established, and as such, are less of a concern in contrast to more toxic PTEs at lower at trace level concentrations.

Average potassium (K) concentrations across both colliery and steel-based waste types constitute the 3rd largest proportion of total metal concentrations. Potassium concentrations in soils and sediments vary, typically falling within the range of approximately 0.15-5wt% at the surface layer of soil down to 0.2 metres. K is predominantly integrated within the soil and sediment structure, making it largely unavailable for uptake by surrounding vegetation (Sparks, 2001; Kaiser, 2018). Furthermore, K concentrations within both waste types are comparable to the aforementioned approximate K range in surface layer sediments. The fraction of readily available K within soils represents a minor portion of the total K content, with certain soils in Nebraska containing single-digit percentages (Shaver, 2014), highlighting the immobile nature of K within the soil matrix. Nevertheless, K oxide species are present within coal ash waste (USGS, 2015). The risk associated with K contamination is relatively low, and no established guideline values for K in soils and sediments have been determined.

Average Magnesium (Mg) concentrations seen across both colliery and steel slag-based waste types make up a considerable portion of the sediment matrix. Mg concentrations were within typical values found in terrestrial soils, typically falling between 0.5-4wt% (Yan and Hou, 2018). In coal ash, Mg oxides are present, although the proportion can vary depending on internal and external factors, such as sample specificity, and industrial processes (USGS, 2015). Mg in oxide form is also a prevalent constituent in steel slag waste, alongside FeO, SiO_2, and CaO (Wang, 2016). Similarly to K, only a small fraction of total Mg in soils exist in an exchangeable form. The absence of Mg SGVs reflects a lower level of concern of toxic implications towards receptors in relation to more toxic PTEs at lower at trace level concentrations.

Manganese (Mn) concentrations make up a considerable fraction in both steel slag-based coastal legacy waste sediments and colliery-based sediments. Mn is ubiquitous in soil, however concentrations in this study drastically exceed general background Mn

concentrations in soils of 0.004-0.09wt% (ATSDR, 2012). Elevated concentrations are associated with industrial activities, particularly steel production, which generates Silicon Manganese slag as a by-product, along with manganese oxide resulting from combustion processes (Ji *et al,* 2022; BGS, 2012). The readily available Mn fraction is regulated by microorganisms and the biological activity of plant life (Schulte and Kelling, 2004). Mn SGVs have not been established due to the primary routes of exposure leading to health effects being inhalation and ingestion. Moreover, ingestion or inhalation of large quantities of Mn may result in symptoms such as gastrointestinal irritation, nausea, vomiting, headaches, and myalgia. Typically, these symptoms resolve within a 48-hour period (PHE, 2015). As such, like the aforementioned elements, Mn concentrations are of low concern in contrast to more toxic PTEs at lower at trace level concentrations.

The major element fraction of Ti was only detected in colliery-based sediments. Ti concentrations in soils vary considerably in nature as a result of rock type (Aubert and Pinta, 1977). Additionally, Ti concentrations typically in soils can range from 0.01-1wt%, of which colliery concentrations detected did not exceed. Whilst concentrations are not insignificant, mobility is limited due to the high weathering resistance of Ti (Cornu et al, 1999), and to coincide with no clear toxic health implications at low concentrations (Tarpada et al, 2020), Ti concentrations within coastal waste sediments are of low risk.

Some major elements detected such as Oxygen (O), Silica (Si), and Calcium (Ca) are indicative of nutrients and potential mineral composition within the sediment. Whilst SEM has provided geochemical insight, analysis through XRD would identify mineral compositions present within colliery sediments (Ali *et al,* 2022), with substantial O, Al, Si, and Fe concentrations indicative of oxide, pyrite, and silica-based minerals within the legacy waste sediments.

	Colliery		Steel slag	
Major elements	**Average concentration (wt%)**	**Concentration range (wt%)**	**Average concentration (wt%)**	**Average concentration (wt%)**
O	53	46-57	53	42-57
Al	12	9-18	8.2	1-19
Si	18	11-21	13	7-21
Fe	8	0.4-11	8	0.2-21
Mg	1	0.5-2	1	0.7-4
K	2	0.3-3	1	0.1-3
Ca	3	0.4-17	11	0.5-25
Ti	0.4	0.2-0.5	n/a	n/a
Mn	0.6	0.1-2	3.5	0.3-9.3

Table 4. Major element concentrations detected through SEM analysis of colliery-based coastal legacy waste sediments (n=11), and steel slag-based coastal legacy waste sediments, presenting average element concentrations and concentration ranges (wt%) (n=11).

	Colliery waste type			Steel slag waste type		
Elements	Statistic	df	*p*	df	Statistic	*p*
O	11	0.94883	>0.05	12	0.70516	<0.01*
Mg	11	0.65509	<0.01*	12	0.65455	<0.01*
Al	11	0.95332	>0.05	12	0.87577	>0.05
Si	11	0.80671	<0.05*	12	0.86679	>0.05
K	11	0.62855	<0.01*	12	0.91771	>0.05
Ca	8	0.53707	<0.01*	12	0.94054	>0.05
Ti	11	0.82378	<0.05*	n/a	n/a	n/a
Fe	11	0.95662	>0.05	12	0.92456	>0.05
Mn	11	0.76039	<0.01	9	0.50795	<0.01

Table 5. Shapiro-Wilk test of normality results of individual major elements across both waste type data sets to determine whether data was drawn from a normally distributed population (p< 0.05).

	Colliery waste type		Steel slag waste type			
Element	Median	IQR	Median	IQR	U	*p*
O	52.83	46.33-54.31	54.7	41.7-55.14	48	>0.05
Mg	0.72	0.59-0.87	1.02	0.67-1.37	22.5	<0.01*
Al	12.36	10-14.12	5.96	4.06-13.72	98	0.05
Si	18.9	15.81-19.63	14.58	8.04-17.85	100	<0.05*
K	2.73	2.38-2.89	1.07	0.45-2.45	77	>0.05
Ca	0.79	0.42-2.5	5	0.48-16.05	18	<0.05*
Fe	7.23	4.63-11.08	5.5	3.81-13.93	63	>0.05

Table 6. Mann-Whitney U analysis of individual major element concentrations (wt%) detected through SEM analysis across both colliery-based waste (n=11) and steel slag-based waste (n=12) sediment types (p< 0.05).

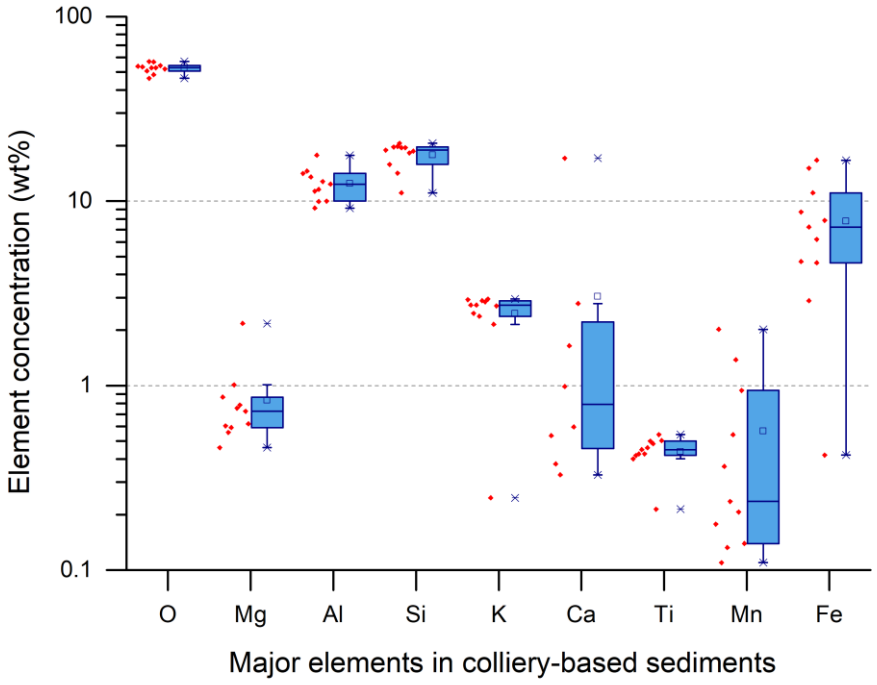

Figure 11. A box-and-whisker plot depicting major elements and concentrations (wt%) detected in colliery-based coastal legacy waste sediments (n=11).

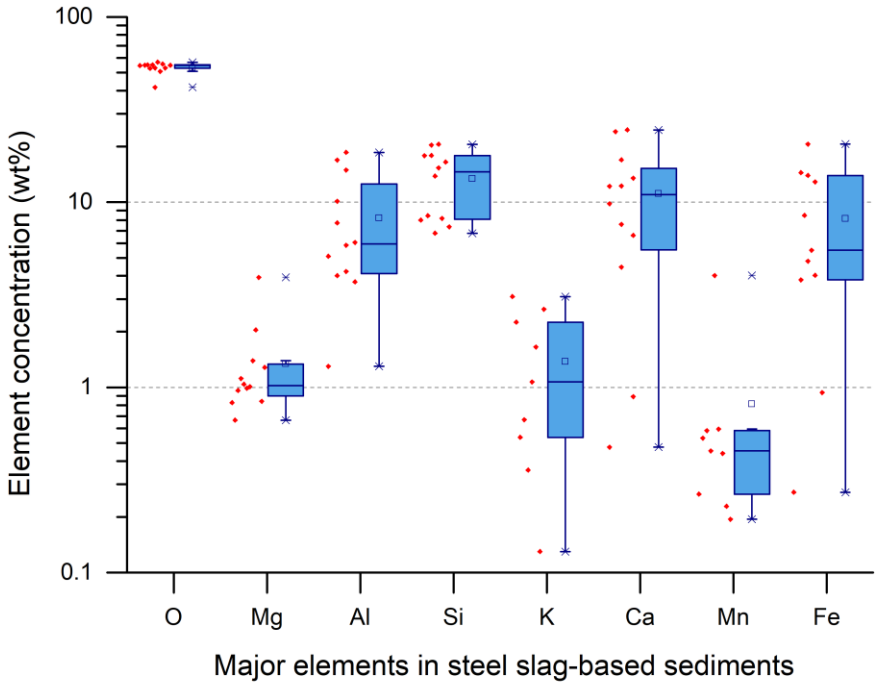

Figure 12. A box-and-whisker plot depicting major elements and concentrations (wt%) detected in steel slag-based coastal legacy waste sediments (n=12).

4.1.2. Trace element concentrations

Trace element analysis through ICP-MS detected twelve elements within colliery and steel waste matrixes. The highest average element concentrations within colliery waste are listed as: As (925ppm) > Cu (532ppm) > V (527ppm) > Pb (494ppm) > Ni (416ppm) > Zn (365ppm) > Cr (344ppm) > Co (134ppm) > Be (17ppm) > Sb (12ppm) > Tl (10ppm) > Se (8ppm) (seen in figure 13 and table 7). As for steel slag waste, the highest average element concentrations are listed as: Zn (1966ppm) > Pb (1080ppm) > As (353ppm) > Cu (286ppm) > V (236ppm) > Cr (182ppm) > Ni (146ppm) > Sb (85ppm) > Co (55ppm) > Be (40ppm) > Se (10ppm) > Tl (3ppm) (seen in figure 13 and table 7). As highlighted by Brand and Spencer (2019), studies on variability surrounding total element concentrations within numerous waste types is limited. Nevertheless, statistical analyses reveal both similarities and disparities in concentrations between elements amongst waste types. Trace element distributions across colliery-based and steel-slag based waste sediments can be seen in table 8. The distribution of Cr, Be, Co, and As concentrations in colliery-based sediments are indicative of non-normal distribution, whereas, V, Ni, Cu, Zn, Se, Sb, and Pb concentrations are representative of normal distribution. As for steel-slag based waste, distribution of Be, Ni, Zn, and Pb concentrations were indicative of non-normal distribution, with V, Cr, Co, Cu, Se, Sb, and As concentrations representative of normal distribution. Moreover, Mann-Whitney U analysis of trace element concentrations across both waste types illustrate significant differences in V, Cr, Be, Co, Ni, and Sb concentrations, whereas similarities in Cu, Zn, Se, Pb, and As concentrations were apparent (seen in table 9). The differences underline the elements of greater potential concern based on waste type. For example, in colliery waste sediments, elevated concentrations of V, Cr, Co, and Ni are more concerning compared to steel slag waste. Conversely, Be, and Sb are more prominent concerns in steel slag sediments.

It was determined that across both waste types, V concentrations exceeded Canadian sediment quality guideline values for a majority of sample sites with, 9 of 11 sample sites for colliery waste and 8 of 12 sample sites for steel slag waste exceeding the limit More specifically, exceeded values for colliery sample sites include DBB2 (545ppm), GTT1 (511ppm), GTT2 (487ppm), WWF3 (594ppm), WWF4 (913ppm), HC1 (801ppm), HC2 (803ppm), HC3 (683ppm), and HC4 (323ppm), with steel slag waste sample sites being MP1 (178ppm), MP2 (162ppm), MP3 (320ppm), MP4 (175ppm), MP5 (280ppm), MP6 (361ppm), MPC2 (549ppm), and MPC4 (632ppm). Mann-Whitney U analysis of V concentrations between each waste type revealed a significant difference, with colliery waste presenting higher concentrations. While concentrations are further elevated in colliery waste, the

significance of the hazardous nature of V concentrations across both waste categories should not be underestimated. V enters the soil environment through natural and anthropogenic means, from parent material to metal industry and mine tailings (Chen *et al,* 2021). In oxic conditions, tetravalent V and pentavalent V are the most likely forms of V in the soil environment (Chen *et al,* 2021). Additionally, V is highly absorbent to Fe, Mn, and Al hydroxides, which can directly influence the level of V mobility seen within the environment (Wnuk, 2023; Yang *et al,* 2017). As the major elements within waste sites include Al, Fe, and Mn (see section 4.1.1.), it is reasonable to assume these minerals are constituents within the sediments, storing significant amounts of V. The fate of V can be directly tied to these major elements, with changes in sediment geochemistry a potential mobilising factor, posing a significant environmental risk. In terms of toxicity towards receptors, V pentoxide (a form of pentavalent V) is a notably toxic form of V (Ścibior *et al,* 2021), which is extremely hazardous to human health. Ingestion of V can result in allergic responses, respiratory issues, DNA damage, birth defects, and more serious conditions such as pulmonary tumours (Zhang *et al,* 2019; Ścibior *et al,* 2021; Cseh *et al,*2012). Additionally, high concentrations of V in soils can disturb and impede important physiological processes (Aihemaiti *et al,* 2020) leading to deformities in plant and root growth, and subsequently plant death.

Similar to V, Cr concentrations across the majority of colliery and steel slag waste sites exceeded Canadian sediment quality guideline values, with 9 of 11 colliery sites and 10 of 12 steel slag waste sites exceed values. More specifically, exceeded colliery sample sites include DBB2 (417ppm), GTT1 (441ppm), GTT2 (422ppm), WWF3 (397ppm), WWF4 (496ppm), HC1 (512ppm), HC2 (438ppm), HC3 (329ppm), and HC4 (226ppm), whereas with steel slag waste sites, this includes sample sites WWF2 (142ppm), MP1 (169ppm), MP2 (113ppm), MP3 (152ppm), MP4 (125ppm), MP5 (199ppm), MP6 (302ppm), MPC2 (388ppm), MPC3 (168ppm), and MPC4 (389ppm). Mann-Whitney U analysis of Cr concentrations between each waste type revealed a significant difference, with colliery waste presenting higher concentrations. Even though concentrations are higher at colliery waste sites, concern regarding Cr concentrations across both waste types is important. Recognised as a common metal contaminant in soils and sediments (Liu *et al,* 2021), Cr contamination is a widespread issue for many environments globally and elevated Cr concentrations are a result of industrial metal work practices, tanneries, fossil fuel combustion mine tailings, and parent rock material (Ullah *et al,* 2023; Liu *et al,* 2021). Oxidised forms of Cr typically found in the environment range from Cr^{2-} to Cr^{6+}, of which trivalent Cr (Cr III) and hexavalent Cr (Cr VI) are most commonly found in soil and sediment environments (Liu *et al,* 2021; EPA, 2000b). In

soils and sediments above 5.5 pH, Cr (III) is relatively stable, typically forming Cr-hydroxide, Cr-oxide, with Cr-hydroxide relatively immobile (Kim and Dixon, 2002). Unlike Cr (III), Cr (VI) is more readily mobile and is more toxic, as it is considered a human carcinogenic (Jabasingh *et al,* 2015). Sorption of Cr (VI) onto Fe-oxide has been documented and has also been utilised in remediation efforts (Park *et al,* 2022; Kim and Dixon, 2002), however, seeing as there is a reasonable assumption of Fe-oxide minerals within legacy waste sediments (see section 4.1.1.), Fe-oxide minerals in sediments are likely to contain Cr (VI). Furthermore, Bartlett and James (1988) highlight that the presence of Mn-oxides can further oxidise Cr (III) into Cr (VI), which is also likely present in legacy waste sediments suggesting that Cr (VI) is more prevalent in waste sediments. Other than the carcinogenic properties of Cr, physiological impacts of Cr toxicity include respiratory implications such as asthma, chronic bronchitis, and irritation; skin conditions including swelling, and erythema; alongside severe liver damage, gastrointestinal implications, and mutagenic effects (Dianyi, no date). Additionally, as documented by Yan *et al* (2023), Cr (VI) can be toxic to soils, sediments, and plants and microorganisms living in the soil, by impeding plant development and productivity, decreasing rates of photosynthesis, and accumulation of Cr enabling bioaccumulation into local wildlife. As such, Cr concentrations across both waste types are potentially hazardous, and the potential release of Cr, especially Cr (VI), can have serious implications for the surrounding environment.

Nickel concentrations detected across both waste types exceed Canadian sediment guideline values, with 10 of 11 colliery sites and 10 of 12 steel slag-based sites exceeding the value set. More specifically, colliery waste sample sites that exceed the guideline limits include DBB1 (57ppm), DBB2 (513ppm), GTT1 (295ppm), GTT2 (284ppm), WWF3 (667ppm), WWF4 (931ppm), HC1 (398ppm), HC2 (802ppm), HC3 (332ppm), and HC4 (268ppm), with steel slag sample sites including WWF1 (55ppm), WWF2 (117ppm), MP1 (132ppm), MP2 (68ppm), MP3 (155ppm), MP4 (108ppm), MP5 (169ppm), MP6 (126ppm), MPC2 (2644ppm), and MPC4 (521ppm). Mann-Whitney U analysis of Ni concentrations between each waste type revealed a significant difference, with colliery waste presenting higher concentrations. Nevertheless, concentrations at both sites are of hazardous concern. The origins of Ni in soil and sediment environments can be attributed to natural and anthropogenic influences including parent rock material, natural existence in flora, consumption of fossil fuels, alloying agents during the steel-making process, and agriculture (Iyaka, 2011). Nickel from anthropogenic sources is primarily soluble in oxide (Ni^{2+}), sulphide, and silicate form, which, as seen in section 4.1.1. is more likely prevalent in the waste sediment, as opposed to

naturally occurring insoluble Ni-based minerals, though soluble forms of Ni can also be present in nature (Begum *et al,* 2022). The mobility of Ni is notably dependent upon pH conditions. Whilst Ni-oxide is resistant to alkaline corrosion, at pH <6.5, Ni becomes readily soluble in natural oxidising acids (Genchi *et al,* 2020), which can be present in landfill leachate (Chou *et al,* 2013). In addition, Ni in chloride and/or sulphate form is easily water-soluble (Genchi *et al,* 2020). The compound of Ni can determine the nature of toxic implications, with Ni salts able to remain within the human body for a prolonged period (Gates *et al,* 2023). The primary pathways for Ni toxicity in humans include ingestion, inhalation, and absorption onto the skin (Gates *et al,* 2023; Genchi *et al,* 2020; Das *et al,* 2019). Additionally, Ni toxicity is not cumulative and will not effectively bioaccumulate in the human body for a prolonged period, however, Ni can bind to the blood and lead to organ and tissue damage throughout the body, leading to potential cardiac arrest and respiratory distress (Das *et al,* 2019). Even though Ni is an essential element for plant development, chronic and acute toxicity can lead to restricted growth and plant development, limited seed germination, chlorosis, and necrosis (Hassan *et al,* 2019). As such, Ni sediment concentrations are of high concern, although to determine a risk level, leaching tests to determine the mobile fraction is required (see section 4.2).

Selenium (Se) concentrations across 10 of 11 colliery-based waste sites and all steel slag-based waste sites exceed Canadian sediment quality guideline values established. More specifically, exceeded colliery waste sample sites include DBB2 (9ppm), GTT1 (5ppm), GTT2 (7ppm), WWF3 (9ppm), WWF4 (8ppm), WWF5 (12ppm), HC1 (13ppm), HC2 (7ppm), HC3 (12ppm), and HC4 (6ppm), whereas steel slag waste sample sites include WWF1 (20ppm), WWF2 (13ppm), MP1 (14ppm), MP2 (16ppm), MP3 (6ppm), MP4 (4ppm), MP5 (3ppm), MP6 (5ppm), MPC1 (14ppm), MPC2 (6ppm), MPC3 (10ppm), and MPC4 (7ppm). Mann-Whitney U analysis revealed no significant difference in Se concentrations between each waste type, suggesting that concentrations are equally concerning in both waste types. Se in the soil environment can pose as inorganic SeO_4^{2-} (Selenate), Se^{2-} (Selenide), and $HSeO_3^-$/SeO_3^{2-} (Selenite) (Puhakka *et al,* 2019; Mehdi *et al,* 2013) which can sorb onto Mg and Ca-based minerals present such as phlogopite and calcite (Tolu *et al,* 2022). Erosion of sulphide minerals known to contain selenite and selenide is responsible for initial Se in soils. As a result, anionic selenate salts and free Se which are sorbed onto Fe leading to Fe(III) selenite, which are the common forms of Se in soil. Furthermore, anionic Se has high solubility and mobility and recognised as a bioavailable fraction of Se (Mehdi *et al,* 2013). As Fe is a major element within both waste sediments, it is reasonable for Fe(III) selenite to be present within

the sediment matrixes alongside selenate salts. The fate of Se in waste sediment depends upon various external geochemical variables which may mobilise a specific fraction of bound Se. Investigation of which can be seen in section 4.2. Regarding toxicity in humans, Se is primarily cytotoxic and genotoxic, with documented side effects including impaired cell growth and damage to DNA structure, in addition to cardiovascular disease, diabetes, and hepatocarcinogenesis (Sun *et al,* 2014). As for surrounding flora, 2 main processes cause toxicity in plant life; oxidative stress and malformed selenoproteins (Gupta and Gupta, 2017), causing significant damage to protein function and decreased glutathione levels leading to plant growth limitations. It is apparent that Se concentrations in legacy waste sediments are potentially hazardous and may pose a severe risk to the coastal environment if mobilised.

Canadian sediment quality guideline value for Thallium (Tl) was exceeded at sample sites across both waste types. Of colliery waste sites, 9 of 11 sample sites exceeded the SGVs, with specific sample sites including DBB2 (3ppm), GTT1 (6ppm), GTT2 (5ppm), WWF3 (8ppm), WWF4 (34ppm), HC1 (15ppm), HC2 (8ppm), HC3 (20ppm), and HC4 (8ppm), whereas 6 of 12 steel slag-based waste sites exceeded the established Canadian values. More specifically, these include sample sites MP3 (5ppm), MP4 (6ppm), MP5 (3ppm), MP6 (2ppm), MPC2 (5ppm), and MPC4 (12ppm). Additionally, Mann-Whitney U analysis of Tl concentrations between each waste type revealed a significant difference, with colliery waste presenting higher concentrations. Whilst found naturally in the environment, elevated Tl concentrations directly correlate with industrial practices including coal burning and mineral smelting (Karbowska, 2016). As a result of steel smelting and coal combustion, the majority of Tl present, bound to sulphides and to a lesser extent aluminosilicates and organic compounds are subsequently oxidised through combustion, make up a considerable portion of Tl(I) to a lesser extent Tl(III)in sediments (Karbowska, 2016). Due to Tl's resemblance with alkali metals, cation exchanges between Tl(I) and K ions can occur, causing elevated Tl concentrations in environmental and biological organisms to occur, enabling concentrations to exceed guideline values (Hodorowicz *et al,* 2022; Belzile and Chen, 2017). It is reasonable to suggest significant concentrations of Tl(I) in legacy waste sediments, more prevalent in colliery waste based on Tl concentrations and O concentrations seen in section 4.1.1. Whilst considered toxic in low concentrations, further information regarding the geochemical fraction and mobility of Tl is recommended (Liu *et al,* 2019), what is known is that even though Tl(III) is more toxic than Tl(I), it is less bioavailable in circumneutral conditions (Belzile and Chen, 2017). Secondly, human symptoms of acute human toxicity can include gastrointestinal issues, degeneration of internal organs including the heart and liver,

haemorrhaging, hallucinations, and dementia also documented (Saddique and Peterson, 1983). Thirdly, on plant toxicity, a study by Mazur *et al* (2016) found that increases in Tl(I) in the soil lead to initial leaf discolouration and subsequent tissue damage. Consequently, Tl is a known bioaccumulative element in soil organisms and plants (Health Canada, 2020), there is potential for considerable environmental repercussions if currently bound Tl is dispersed into the widespread coastal environment. Whilst colliery waste appears more potentially hazardous than steel slag-based waste, both waste types are of concern. To determine whether Tl concentrations are less likely on average to exceed SGVs at steel slag-based legacy waste sites, further investigation of concentrations of additional sites is required to be more representative of general concentrations. This also applies to all elements across both waste types.

Arsenic concentrations across all colliery and steel slag-based waste sites exceeded Canadian sediment quality guideline values More specifically, concentrations of colliery waste sample sites are as follows: DBB1 (788ppm), DBB2 (399ppm), GTT1 (285ppm), GTT2 (206ppm), WWF3 (500ppm), WWF4 (4526ppm), WWF5 (328ppm), HC1 (89ppm), HC2 (815ppm), HC3 (977ppm), and HC4 (1266ppm). Additionally, steel slag waste sample concentrations include WWF1 (65ppm), WWF2 (435ppm), MP1 (343ppm), MP2 (155ppm), MP3 (343ppm), MP4 (514ppm), MP5 (403ppm), MP6 (768ppm), MPC1 (70ppm), MPC2 (402ppm), MPC3 (66ppm), and MPC4 (674ppm). However, using the UK Environment Agency commercial land guideline values, only 5 of 11 colliery waste (sample sites DBB1, WWF4, HC2, HC3, and HC4) and 2 of 12 steel slag-based waste sites (sample sites MP6, and MPC4) As concentrations exceed guideline values. Mann-Whitney U analysis revealed no significant difference in As concentrations between each waste type, suggesting that concentrations are equally concerning in both waste types. Resulting As concentrations in soil is primarily caused by anthropogenic means, of which a large fraction can be attributed to the unrecovered As portion in mine and smelted ores (Nriagu *et al,* 2007). Even though the form of As cannot be specifically determined, Makowska *et al* (2019) noted significant correlations between As and pyritic S contents. Whilst there are considerable amounts of Fe in waste sediments (see section 4.1.1.), it is reasonable that waste sites pertain S concentrations, although, As bound to pyritic-S may not make up a major portion of the sediment matrix. Additionally, the probability of As in sulphide minerals in colliery waste was also documented, of which has been detected (Makowska *et al* (2019). There is a strong association between inorganic As (arsenate) and Fe(III) oxide/hydroxide due to highly efficient equilibrium processes, which is therefore commonly seen in soils (Aftabtalab *et al,* 2022; Frazer, 2005). Furthermore, it is

likely that considerable portions of pyrite-based As are currently stored in both waste-type sediments. In regard to As toxicity, it is well-documented that As in arsenate and arsenite form is a human carcinogenic and is also responsible for neurotoxicity, skin lesions and blisters, cognitive impairment, and neurodegeneration (Muzaffar *et al,* 2023; Nail *et al,* 2023). As for flora, As can bioaccumulate in plants whilst also causing morphological changes, necrosis, growth limitations, and chlorophyll degradation to plant species (Abbas *et al,* 2018). With climate change influencing the coastal environment, potentially hazardous As concentrations currently immobilised in the soil is a growing concern, as increasing mobilising influences are interacting with coastal legacy waste sites, As is a serious concern, as displacement is increasingly likely in the coastal environment.

Beryllium concentrations across both waste-type sediments exceeded Canadian sediment quality guideline values at a minority of sample sites, with 1 of 11 colliery sediments and 5 of 12 steel slag-based sediments exceeding guideline values. More specifically, at colliery sample site WWF5 (61ppm) and steel slag sample sites WWF1 (61ppm), WWF2 (68ppm), MP1 (73ppm), MP2 (84ppm), and MPC1 (68ppm). Mann-Whitney U analysis of Be concentrations between each waste type revealed a significant difference, with steel slag-based waste presenting higher concentrations. In natural soil and sediment environments, Be is relatively sparse with low background concentrations (Gehle, 2011). Elevated Be concentrations are attributed to fossil fuel combustion. Be association with Fe and Mn hydroxides is reportedly high, with reported Fe-oxide precipitation correlating with increased particulate Fe and Be concentrations in the sediment (Bolan *et al,* 2023). Based on Mn, Fe, and O concentrations in section 4.1.1., it is reasonable that a considerable portion of Be is sorbed onto the aforementioned minerals, though further analysis to determine specific mineral fractions is required. As for toxicity, Be is documented as a probable human carcinogen (EPA, 2000a) with acute toxicity leading to high likelihood of developing CDB, inflammation of airways, and chronic beryllium disease, however, toxicity is dependent upon the level of solubility (Stearney *et al,* 2023). Flora response to Be toxicity is dependent on exposure level. Whilst concentrations at a micromolar level is beneficial to plant life, elevated accumulation can replace Mg which is essential for effective phosphoglucomutase, causing an imbalance in plant metabolism (Tanveer and Wang, 2019). Beryllium concentrations at a minority of steel slag-based waste sites are potentially hazardous and can potentially pose a high environmental risk if concentrations are mobilised into the surrounding environment. Whilst concentrations at colliery waste sites are elevated, sediment concentrations are less

of a concern. Additionally, determining risk level requires investigation of the mobile fraction of Be (see section 4.2).

Cobalt (Co) concentrations in coastal legacy waste sediments do not exceed the established Netherlands soil remediation intervention value. Specifically, only 1 of 11 colliery-based waste sites exceed value set, at sample site WWF3 (289ppm). There is a significant difference in Co concentrations between each waste type, with colliery waste presenting higher concentrations according to Mann-Whitney U analysis. The speciation of anthropogenically sourced Co in soils and sediments is an oxidative state, with divalent Co^{2+} (cobaltous) as the most likely state, notable for complexations with carbonate and ferromanganese oxides (Srivastava *et al,* 2022). It is reasonable that Co speciation in coastal legacy waste sites for this study to be in a ferromanganese oxide state, based on concentration data from section 4.1.1., and ferromanganese oxide is known to inhabit waste sediments relating to fossil fuel consumption and further industrial practices. Whilst concentrations do not predominately exceed intervention values present, Co is not as potentially hazardous compared to the aforementioned elements. Although, clarification of mobility within leachate will help determine risk levels associated with Co in coastal legacy waste sediment, which can be seen in section 4.2.

Colliery and steel slag-based coastal legacy waste sites present elevated Antimony (Sb). Specifically, 4 of 11 colliery sample sites including DBB2 (16ppm), GTT2 (18ppm), WWF4 (27ppm), and HC3 (20ppm) and 8 of 12 steel slag-based waste sample sites including WWF2 (105ppm), MP1 (79ppm), MP2 (440ppm), MP3 (132ppm), MP4 (183ppm), MP5 (206ppm), MP6 (188ppm), and MPC2 (63ppm) exceed the established Netherlands soil remediation intervention value. Mann-Whitney U analysis of Sb concentrations between each waste type revealed a significant difference, with steel slag-based waste presenting higher concentrations. In soil and sediment environments, Sb occurs in oxidised states including –III, 0, +III, and +V, of which trivalent Sb(III) and pentavalent Sb(V) including antimonite and antimonate are most commonly seen (Bolan *et al,* 2022; Diquattro *et al,* 2020). Additionally, the toxicity of Sb species is as follows: antimonite (Sb(III)) > antimonate (Sb(V)) > organoantimonials (Wei *et al,* 2015), with antimonite 10x higher than antimonate. Sorption of Sb in sediments, especially Sb(III) is highly influenced Mn and Fe oxides, transforming Sb(III) to Sb(V), documented to have increased solubility and mobility potential (Liu *et al,* 2015; Bolan *et al,* 2022). Human exposure to toxic Sb concentrations towards humans has been documented to cause pneumoconiosis, increased blood pressure and cardiovascular abnormalities, internal ulcers, and “antimony spots.” (Sundar and Chakravarty, 2010; Cooper

and Harrison, 2009) As for flora, as recognised by Vidya *et al* (2022), elevated Sb concentrations are known to inhibit rates of photosynthesis, upset plant membrane systems, and alter root and leaf composition, and as such pose considerable harm to plant health and well-being (Tang *et al,* 2022). Sb concentrations in steel slag-based waste sites should be considered potentially hazardous, with the need for awareness of concentrations at colliery waste sites also necessary. Determining the risk towards the surrounding environment requires assessments of Sb mobility, which can be seen in section 4.2.

Across both waste types, Cu concentrations in the waste sediments predominately exceed the Canadian sediment quality guideline value. More specifically, 10 of 11 colliery waste sites including DBB1 (180ppm), DBB2 (528ppm), GTT1 (220ppm), GTT2 (262ppm), WWF3 (1017ppm), WWF4 (347ppm), HC1 (1244ppm), HC2 (893ppm), HC3 (771ppm), and HC4 (340ppm) and 9 of 12 steel slag-based waste sample sites including WWF2 (196ppm), MP1 (244ppm), MP2 (181ppm), MP3 (596ppm), MP4 (370ppm), MP5 (301ppm), MP6 (96ppm), MPC2 (587ppm), and MPC4 (742ppm) exceed the value. Mann-Whitney U analysis of Cu concluded no significant difference in concentrations across colliery and steel slag-based legacy waste. Copper species in the soil and sediment environment from anthropogenic industrial waste are almost entirely present in a divalent form, primarily crystal lattices of primary and secondary minerals (Mengel *et al,* 2001). More specifically, Cu has an affinity towards sorption onto carbonate, phyllosilicates, and/ Fe, al, and Mn hydroxide-based complexes (Reed and Martens, 1996). Copper is likely present in the aforementioned complexes, which is further supported by major concentrations present in section 4.1.1. however, mineralogic analysis is required to make detailed assertions. Human toxicity involving Cu is predominantly a result of ingestion of Cu through contaminated aqueous sources. Neurological side effects of Cu toxicity include fatigue and depression, while physical side effects include abdominal pain, hematemesis, and jaundice, with severe implications including hepatic necrosis, renal failure, and death (Royer and Sharman, 2023). As for plant life, whilst an essential micronutrient, Cu toxicity can result in considerable root damage and deformation, and decreasing photosynthesis rates (Chen *et al,* 2022), although Cu-resilient flora is less susceptible. Total Cu concentrations across both waste types are potentially hazardous in coastal legacy waste sediments. Additionally, mobility assessments of bound Cu are required to determine the current level of risk to the coastal environment (see section 4.2).

Zinc concentrations in legacy waste sediments from 11 colliery and 12 steel slag-based sites were compared to the Canadian sediment quality guideline. 4 colliery sample sites including

DBB2 (575ppm), GTT2 (736ppm), HC1 (678ppm), and HC2 (587ppm) and 6 steel slag-based waste sites including MP3 (2560ppm), MP4 (3984ppm), MP5 (4156ppm), MP6 (413ppm), MPC2 (411ppm), and MPC4 (9746ppm) exceeded the threshold. Mann-Whitney U analysis determined that there is no significant difference in the Zn concentrations between each waste type. Zinc speciation in soils and sediments is very diverse, and Zn form and total sediment concentration is dependent upon industrial practices, the geochemistry of soils, and geology, which are significantly impacted by smelter slag waste and coal ash waste (Vodyanitskii, 2010). Zinc minerals in the earth's crust including sphalerite, franklinite, zinc hydrosilicate, and smithsonite are commonly found in many regions (Vodyanitskii, 2010). In steel slag waste, Zn is usually in the form of Zn ferrite (ZnFe2O4) and Zincite (ZnO) (Smith *et al,* 2021), though can also be present in a Zn sulphide form given that it is the main source of Zn metal (Ma *et al,* 2018). As for colliery waste, a study by Struis *et al* (2004) determined that fly ash from municipal solid waste sites was predominately comprised of approximately 60% Zn oxide, specifically hydrozincite (Zn5(OH)6(CO3)2), with the remaining fraction made up of willemite (Zn2SiO4) and gahnite (ZnAl2O4). It is reasonable that the aforementioned Zn species are likely present amongst coastal legacy waste sediments, however further analysis as mentioned previously is required to remove assumptions. Zinc toxicity and human health implications are tied to the presence of Zn in the environment. Acute exposure to Zn oxide through ingestion/inhalation can result in 'metal fume fever' (NJDHSS, 2007), with Zn sulfate and chloride resulting in hematemesis, nausea, and potential renal injury (Agnew and Slesinger, 2022). Chronic Zn exposure has been known to result similar acute implications though to a lesser extent (Plum *et al,* 2010). Flora toxicity on the other hand has been documented to cause similar growth and development, photosynthesis, and structural abnormalities that previous elements can cause, although the precursing factors leading to these implications can differ (Kaur and Garg, 2021). Given the fluctuating concentrations across steel slag-based waste sediments, and to a lesser extent colliery waste sediments, Zn concentrations can be potentially hazardous across coastal legacy waste sites, and sites where Zn concentrations do not exceed the guideline value, attention should be given to these sites also, as concentrations are not too dissimilar to the guideline value. However, assessing risk requires analysis of Zn leaching, which can be seen in section 4.2.

Concentrations of Pb in coastal legacy waste sediments were compared to the Canadian sediment quality guideline value, including sites DBB2 (419ppm), GTT2 (386ppm), WWF3 (316ppm), WWF4 (806ppm), WWF5 (386ppm), HC1 (734ppm), HC2 (659ppm), HC3 (844ppm), and HC4 (534ppm). On the other hand, out of 12 steel slag-based waste

sediments, 5 exceeded the guideline value, including sample sites MP3 (2617ppm), MP4 (3107ppm), MP5 (1166ppm), MPC2 (468ppm), and MPC4 (5209ppm). Through Mann-Whitney U analysis, no significant difference was found in Pb concentrations between waste sediments based on colliery and steel slag. It should be noted that concentrations vary notably more in steel slag-based sediments, and as such, the relatively small sample size could have impacted the outcome. Pb speciation can vary depending upon natural and anthropogenic influences. Within coal, Pb is typically found in sulphide form, specifically galena and pyrite (Cui *et al,* 2019). Sauvé *et al* (1997) assessed the Pb complexes in contaminated soils including agricultural and sewage sludge-based soils and found that between 60-80% of Pb is associated with organo–Pb complexes. It is reasonable that the soil fraction within coastal legacy waste sediments is less than typical residential and rural soils, thus the inorganic fraction within legacy waste sediments should theoretically be higher. During the lead refinement and process, at the PbS stage, PbS is oxidised, separating S and producing PbO. As the refinement process cannot produce perfect yields, PbO and PbS is present amongst the blast furnace slag waste, subsequently deposited through landfilling (Pan *et al,* 2019). In addition, a study by Funatsuki *et al* (2012) determining lead speciation in fly ash in Japan noted that amongst the samples analysed, XANES analysis found $PbSiO_3$, $PbCl_2$, and $Pb_2O(OH)_2$ dominated Pb speciation in the sediment matrixes. It is reasonable that based on the major elements identified, $PbSiO_3$ and $Pb_2O(OH)_2$ could make up a notable fraction of Pb in coastal legacy waste sediments. Additionally, Cl concentrations were detected across a minority of sites, so $PbCl_2$ cannot be categorically ruled out. In terms of human health implications, inorganic Pb can pose a severe human health hazard. Neurological effects of Pb toxicity have been documented. Mild toxicity can affect behaviour and temperament, and lead to cognitive and motor skill impairment, whereas moderate to severe toxicity can result in dizziness, tremors, seizures, and unconsciousness. Other known effects are known to include reduced fertility rates, renal impairment, and smoothing of intestinal muscle lining. More severely, Pb is reasonably anticipated to be a human carcinogen (ATSDR, 2020; Patočka and Černý, 2003). Documented flora implications have been set out by Ravipati *et al* (2021) whereby elevated Pb concentrations in soils and sediments can inhibit photosynthesis rates, impede growth rates, interfere with cell division and water retention, and root abnormalities. There are PTE concentrations across the majority of colliery-based waste sediments. Attention should also go to steel slag-based waste sites as a minor proportion of sites exceed the guideline value.

	Colliery		Steel slag		Sediment Quality Guideline value (mg/kg)
Trace elements	**Average concentration (wt%)**	**Concentration range (wt%)**	**Average concentration (wt%)**	**Average concentration (wt%)**	
Be	17	2-61	40	13-84	30***
V	527	58-913	236	17-632	130*
Cr	344	31-512	182	10-389	87*
Co	134	8-289	55	4-203	240***
Ni	416	31-931	146	20-521	50* 1,800**
Cu	532	52-1244	286	16-742	91*
Zn	365	47-736	1966	23-4156	360*
Se	8	1-13	10	3-20	2.9*
Sb	12	0.5-27	85	3-206	15***
Tl	10	0.4-34	3	0.1-12	1*
Pb	494	113-844	1080	14-5209	260*
As	925	89-4526	353	66-768	12* 640**

Table 7. Trace elements detected through ICP-MS analysis of colliery-based and steel slag-based waste sediments across all study sites, presenting average element concentrations and concentration ranges (mg/kg), with the inclusion of sediment guideline values.

**Canadian sediment quality guideline value (CCME, 2007)*

***UK Environment Agency sediment quality guideline value for commercial land (EA, 2009)*

****Netherlands soil remediation intervention value (ESDAT, 2000).*

	Colliery waste type			Steel slag waste type		
Elements	Statistic	df	*p*	df	Statistic	*p*
V	11	0.93276	>0.05	12	0.90447	>0.05
Cr	11	0.84182	<0.05*	12	0.90845	>0.05
Be	11	0.72556	<0.01*	12	0.81124	0.01*
Co	11	0.84182	<0.05*	12	0.91744	>0.05
Ni	11	0.94141	>0.05	12	0.77475	<0.01*
Cu	11	0.91759	>0.05	12	0.90487	>0.05
Zn	11	0.91554	>0.05	12	0.69595	<0.01*
Se	11	0.95111	>0.05	12	0.93512	>0.05
Sb	11	0.94712	>0.05	12	0.88259	>0.05
Pb	11	0.95227	>0.05	12	0.70322	<0.01*
As	11	0.6135	<0.01*	12	0.92359	>0.05

Table 8. Shapiro-Wilk test of normality results of individual trace elements across both waste type data sets to determine whether data was drawn from a normally distributed population (p< 0.05).

	Colliery waste type		Steel slag waste type			
Elements	Median	IQR	Median	IQR	U	*p*
V	544.84	322.55-913.25	176.13	51.19-350.64	104	<0.05*
Cr	417.31	225.83-440.92	160.22	115.99-276.42	107	0.01*
Be	14.04	8.84-21.07	24.6	16.03-67.79	24	0.01*
Co	417.31	225.83-440.92	44.44	10.41-83.69	122	<0.01*
Ni	331.51	267.64-666.77	121.57	57.92-163.93	107	0.01*
Cu	346.58	219.76-893.04	220.01	82.48-532.42	92	>0.05
Zn	329.45	147.87-587.13	272.02	64.05-2915.7	58	>0.05
Se	8.31	6.14-12.18	8.69	5.57-14.27	56	>0.05
Sb	14.24	3.11-18.03	70.83	8.71-170.2	30	<0.05*
Pb	418.95	316.48-734.59	98.82	47.32-2254.16	81	>0.05
As	500.31	285.19-976.54	372.54	91.32-493.89	90	>0.05

Table 9. Mann-Whitney U analysis of individual trace element concentrations (mg/kg) detected through ICP-MS analysis across both colliery-based waste (n=11) and steel slag-based waste (n=12) sediment types (p< 0.05).

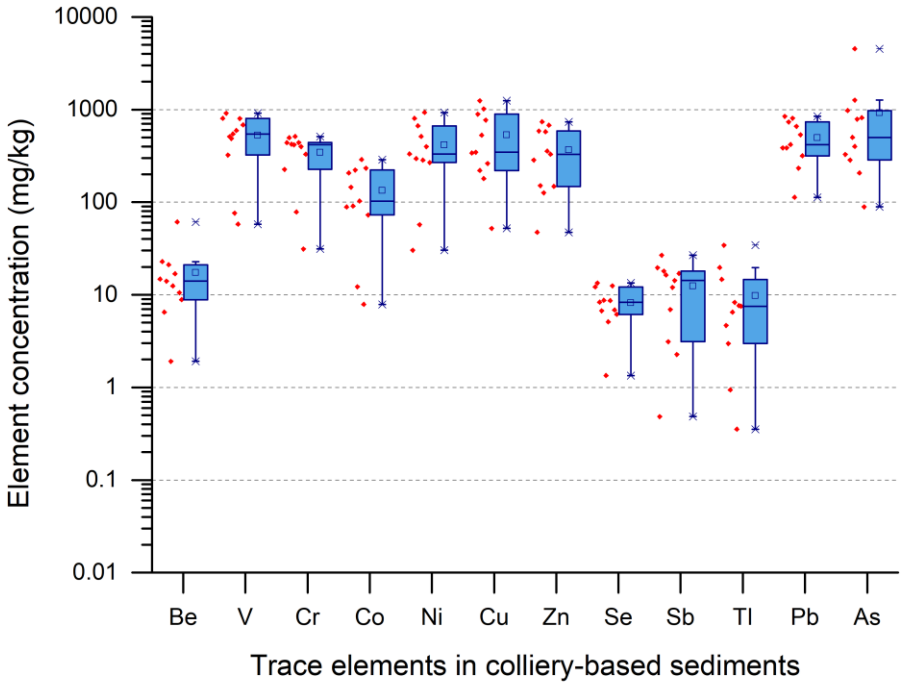

Figure 13. A box-and-whisker plot depicting trace elements and concentrations (wt%) detected in colliery-based coastal legacy waste sediments (n=11).

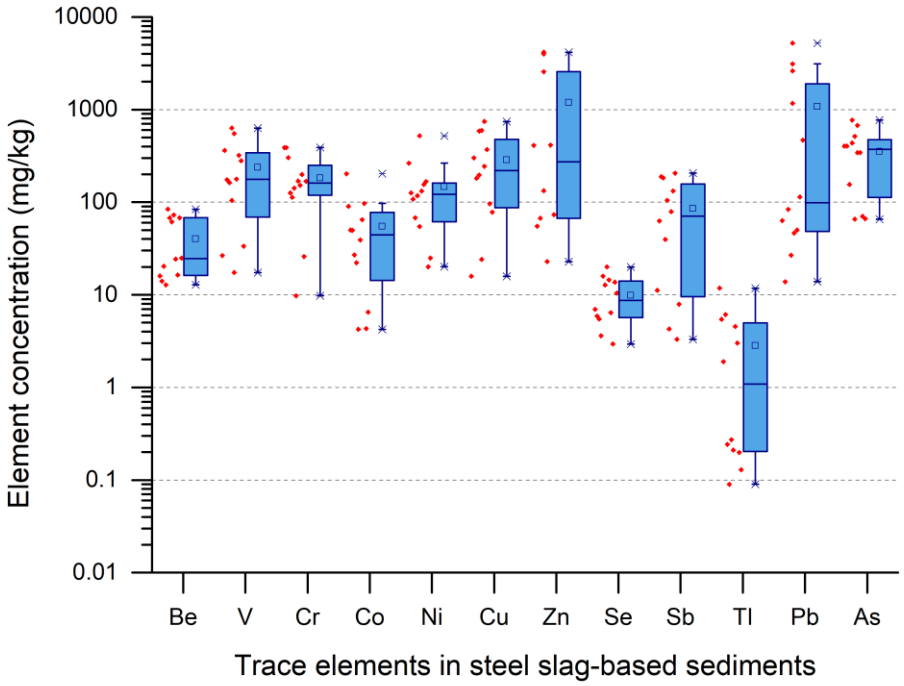

Figure 14. A box-and-whisker plot depicting trace elements and concentrations (wt%) detected in steel slag-based coastal legacy waste sediments (n=12).

4.2. Leaching under oxidising conditions

4.2.1. Concentration and leaching behaviour of elements within deionised water leachant

Leaching of legacy waste sediments in deionised water presented considerable leaching potential of elements For instance, average dissolved element concentrations within colliery-based leachate are as follows: K (112.86mg/l) > Al (47.55mg/l) > Mn (4.4mg/l) > Fe (2.28mg/l) > Pb (1mg/l) > As (0.63mg/l) > Cu (0.34mg/l) > Ni (0.25mg/l) > Zn (0.2mg/l) > V (0.19mg/l) > Co (0.09mg/l) > Cr (0.07mg/l). Conversely, elements in steel slag-based deionised leachate are listed as: K (113.74mg/l) > Al (18.97mg/l) > Mn (8.24mg/l) > Zn (2.8mg/l) > Pb (1.07mg/l) > Mg (0.39mg/l) > Cu (0.38mg/l) > As (0.12mg/l) > Ni (0.09mg/l) > V (0.07mg/l) > Co (0.04mg/l) > Cr (0.03mg/l).

The distribution of element concentrations seen within deionised water leachate pertaining to colliery-based and steel-slag based waste sediments can be seen in table 10. The distribution of Cr, Co, Ni, Mn, Pb, and As concentrations in colliery-based leachate are indicative of non-normal distribution, whereas K, Cu, Zn, Al, and V concentrations are representative of normal distribution. As for steel-slag based leachate, the distribution of V, Al, Zn, Mn, Pb, and As concentrations were indicative of non-normal distribution, with Cr, Co, Cu, Ni, and K concentrations representative of normal distribution (seen in table 10). Moreover, Mann-Whitney U analysis of leached element concentrations across both waste types illustrate no significant differences in individual element concentrations (seen in table 11), indicating that waste type had a minimal influence on element mobility. However, no definitive conclusions can be made due to the limited sample size per waste type.

	Colliery waste type			Steel slag waste type		
Element	df	statistic	*p*	df	Statistic	*p*
V	5	0.77689	>0.05	5	0.58456	<0.01*
Cr	4	0.64164	<0.01*	4	0.88121	>0.05
Al	5	0.86546	>0.05	5	0.66337	<0.01*
Co	5	0.62181	<0.01*	4	0.83532	>0.05
Zn	4	0.99659	>0.05	5	0.67677	<0.01*
Cu	5	0.86324	>0.05	5	0.87774	>0.05
Ni	5	0.63951	<0.01*	4	0.84921	>0.05
K	4	0.9248	>0.05	5	0.94933	>0.05
Mn	5	0.6728	<0.01*	5	0.71726	<0.05*
Pb	5	0.60585	<0.01*	5	0.56102	<0.01*
As	5	0.57251	<0.01*	5	0.58882	<0.01*

Table 10. Shapiro-Wilk test of normality results of individual leached elements in deionised water leachant across both waste type data sets to determine whether data was drawn from a normally distributed population (p< 0.05).

	Colliery waste type		Steel slag waste type			
Element	Median	IQR	Median	IQR	U	*p*
V	0.09	0.02-0.42	0.01	0.004-0.17	21	>0.05
Cr	0.03	0.03-0.14	0.02	0.01-0.06	10	>0.05
Al	26.34	13.71-92.01	6.89	3.88-40.11	20	>0.05
Co	0.02	0.01-0.19	0.02	0.001-0.1	12	>0.05
Ni	0.02	0.02-0.58	0.07	0.05-0.13	8	>0.05
Cu	0.19	0.1-0.7	0.22	0.09-0.82	4	>0.05
Zn	0.2	0.13-0.28	0.22	0.16-6.74	8	>0.05
K	106.23	58.54-146.81	119.05	53.12-171.71	8	>0.05
Mn	2.7	1.78-7.86	3.97	0.6-18.01	12	>0.05
Pb	0.13	0.03-2.4	0.02	0.01-2.65	17	>0.05
As	0.07	0.03-1.51	0.01	0.01-0.28	19	>0.05

Table 11. Mann-Whitney U analysis of individual leached element concentrations (mg/kg) under deionised water conditions detected through ICP-MS analysis of both colliery-based waste (n=5) and steel slag-based waste (n=5) sediment types (p< 0.05).

The abundance of dissolved trace element concentrations in deionised leachate can be influenced by geochemical properties such as pH, EC (electrical conductivity), and ORP (Lévesque *et al,* 2023; Zhang *et al,* 2016; Farahat *et al,* 2019; Mahedi *et al,* 2019; Kommonweeraket *et al,* 2015; Bhaat *et al,* 2019; Schlieker *et al,* 2001), with small adjustments having potentially notable consequences on solubility. The Shapiro-Wilk distribution test carried out on geochemical parameters including pH, EC, and ORP for each individual waste type pre and post leaching alongside Mann-Whitney U test of difference concluded no significant difference in pH, ORP, and EC values between pre-leaching and post-leaching values of colliery sediment, and also steel slag-based sediments. Additionally, no differences in values relating to sediment types. (seen in tables 12-16). The pH levels observed in deionised leachate range from acidic to alkaline (seen in tables 17 and 18 and figures 15 and 16). Roy and Berger (2011) conducted a study on the pH variability of coal fly ash leachate, observing significant variations in pH values during sediment introduction and mixing, with pH levels ranging from strongly acidic (pH 4) to alkaline (pH 12) conditions. These variations are likely attributed to the sorption rate of SO_2 onto particulate surfaces, hydrolysis of Al^{3+} from $Al_2(SO_4)_3$, and Ca content. An initial cause for acidic/alkalinity is a result of the Ca and S ratio within sediments (Bhaat *et al,* 2019; Izquierdo and Querol, 2012). Over time, acidic and alkaline leachates neutralise, as the dissolution of CaO and MgO under acidic conditions increases negatively charged ions present in leachate (Mahedi *et al,* 2019; Kommonweeraket *et al,* 2015), whereas alkaline leachates often decrease in pH with increased exposure to atmospheric CO_2. The Electrical conductivity (EC) results (seen in table 17 and table 18) indicate no considerable disparity in values before and after leaching. However, EC levels observed are considerably higher than normal deionised water EC levels under unexposed conditions of approximately 0.055µS (MyronL, no date), with only marginal increased in EC detected post leaching. Elevated EC values are comparable to normal background levels for a majority of rivers (200-1000µS/cm) (CCME, no date), with a minority of sites presenting values beyond this value, values far higher than pure deionised water. The increase in EC is attributed to the mineral fraction within the sediment, salt dissolution, high iron content, and temperature (Karato and Wang, 2013). Slag EC reportedly increases with increasing temperatures, and also the increase in FeO and/or CaO contents, whereas increased SiO_2 contents reduce slag EC (Farahat *et al,* 2019). The contents of Ca and Fe detected in section 4.1 present a reasonable explanation for increased EC values. In all instances except for sample MPC1, positive oxygen reduction potential (ORP) ORP values were observed (seen in tables 17 and 18). Notably, a reduction in ORP was observed at pH

levels exceeding 10 at sample sites MPC1 and WWF1, contrasting with more neutral conditions. Zhang *et al* (2016) determined that ORP typically decrease as pH increases due to higher reducing agents present, with ORP increasing under lower pH conditions are there are more oxidising metal oxide agents present.

	Pre-leaching colliery sediment waste type			Pre leaching steel slag sediment waste type		
	df	statistic	*p*	df	statistic	*p*
pH	5	0.98857	0.97447	5	0.92548	0.56591
ORP	5	0.93054	0.60004	5	0.97623	0.91353
EC	5	0.66243	0.00371	5	0.85776	0.2203

Table 12. Shapiro-Wilk normality test of individual geochemical factors in deionised water from colliery-based and steel slag-based waste sediments including pH, ORP (R.mv), and EC (mS cm-1) prior to leaching, to determine whether data was drawn from a normally distributed population (p< 0.05).

	Pre-leaching colliery sediment waste type (n=5)		Post-leaching colliery sediment waste type (n=5)			
	Median	IQR	Median	IQR	U	*p*
pH	7	6.25-8.05	7.6	6.35-7.8	10.5	0.75
ORP	173.7	102.8-198.45	163.2	156.65-180.85	14	0.83
EC	0.32	0.22-1.07	0.49	0.26-1.26	8	0.4

Table 13. Mann-Whitney U analysis of colliery-based sediment pre (n=5) and post-leaching (n=5) data sets for geochemical parameters including pH, EC, and ORP pre and post leaching under deionised water conditions (p< 0.05).

	Pre-leaching steel slag sediment waste type (n=5)		Post-leaching steel slag sediment waste type (n=5)			
	Median	IQR	Median	IQR	U	*p*
pH	9.2	7.15-11.05	8.1	7.05-10.55	15	0.68
ORP	82.3	-3.2-182.75	114.5	6.45-163.55	12	1
EC	2.2	0.74-2.8	2.43	0.79-3.05	9	0.53

Table 14. Mann-Whitney U analysis of steel-slag-based sediment pre (n=5) and post-leaching (n=5) data sets for geochemical parameters including pH, EC, and ORP pre and post leaching under deionised water conditions (p< 0.05).

	Post-leaching colliery sediment waste type			Post leaching steel slag sediment waste type		
	df	statistic	*p*	df	statistic	*p*
pH	5	0.83216	0.1444	5	0.96352	0.83229
ORP	5	0.953	0.75862	5	0.94395	0.69399
EC	5	0.71524	0.01373	5	0.79311	0.07112

Table 15. Shapiro-Wilk normality test of individual geochemical factors in deionised water from colliery-based and steel slag-based waste sediments including pH, ORP (R.mv), and EC (mS cm-1) post leaching, to determine whether data was drawn from a normally distributed population (p< 0.05).

	Pre-leaching of both sediment waste types (n=10)		Post-leaching of both sediment waste types (n=10)			
	Median	IQR	Median	IQR	U	*p*
pH	8.05	6.48-9.53	7.8	6.6-8.58	51.5	0.94
ORP	140.15	61.73-193.58	156.65	95.25-174.5	50	1
EC	0.74	0.3-2.31	0.79	0.44-2.58	42	0.57

Table 16. Mann-Whitney U analysis of the combined data set of colliery (n=5) and steel slag-based (n=5) geochemical parameters including pH, EC, and ORP pre and post leaching (p< 0.05) under deionised water conditions.

	ORP (R.mv)			pH			EC (mS cm-1)		
Sample site	*Pre-agitation mean value*	*Post-agitation mean value*	*Difference after agitation*	*Pre-agitation mean value*	*Post-agitation mean value*	*Difference after agitation*	*Pre-agitation mean value*	*Post-agitation mean value*	*Difference after agitation*
GTT1	208.2	163.2	-45	7	7.8	0.8	0.3	0.5	0.2
MP1	75.5	152.2	76.7	8.6	7.6	-1.1	0.2	0.3	0.1
DBB2	130.1	173.1	43.1	6.7	6.7	0.0	0.2	0.2	0
HC1	173.7	161.1	-12.6	7.5	7.8	0.3	0.4	0.5	0.1
WWF4	188.7	188.6	-0.1	5.8	6	0.2	1.7	2	0.3

Table 17. Mean ORP (R.mv), pH, and EC (mS cm-1) values for colliery-based coastal legacy waste samples in deionised water before and after leaching (n=5).

	ORP (R.mv)			pH			EC (mS cm-1)		
Sample site	*Pre-agitation mean value*	*Post-agitation mean value*	*Difference after agitation*	*Pre-agitation mean value*	*Post-agitation mean value*	*Difference after agitation*	*Pre-agitation mean value*	*Post-agitation mean value*	*Difference after agitation*
MP5	150.2	148.4	-1.9	8.9	7.8	-1.1	2.2	2.4	0.2
HC4	215.3	178.7	-36.6	5.4	6.3	0.9	0.8	0.8	0
MPC1	-26.8	-24.6	2.2	11.6	11.1	-0.4	2.6	3	0.4
MPC4	82.3	114.5	32.2	9.2	8.1	-1.1	0.7	0.8	0.1
WWF1	20.4	37.5	17.1	10.5	10	-0.5	3	3	0

Table 18. Mean ORP (R.mv), pH, and EC (mS cm-1) values for steel slag-based coastal legacy waste samples in deionised water before and after leaching (n=5).

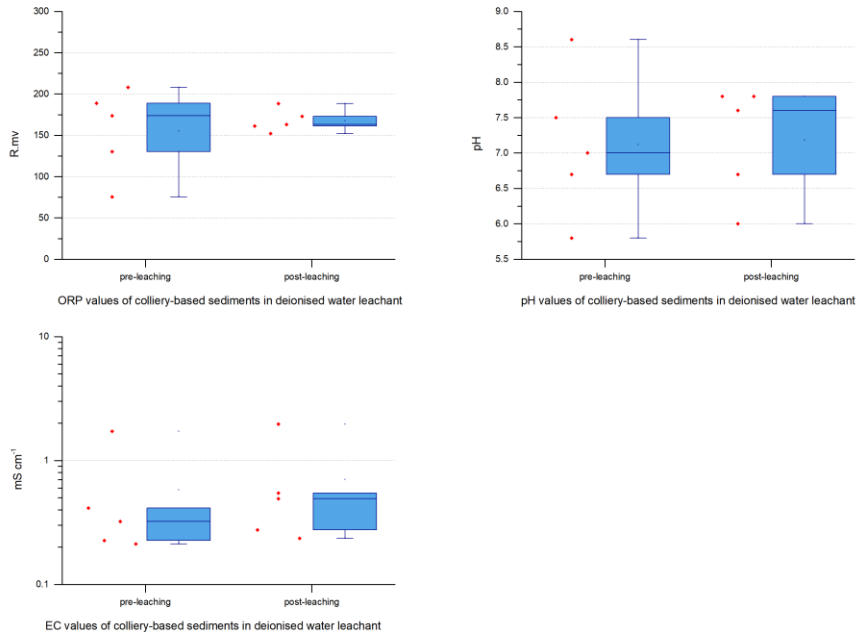

Figure 11. A box-and-whisker plot depicting ORP (R.mv), pH, and EC (mS cm-1) values for colliery-based coastal legacy waste samples in deionised water before and after leaching (n=5).

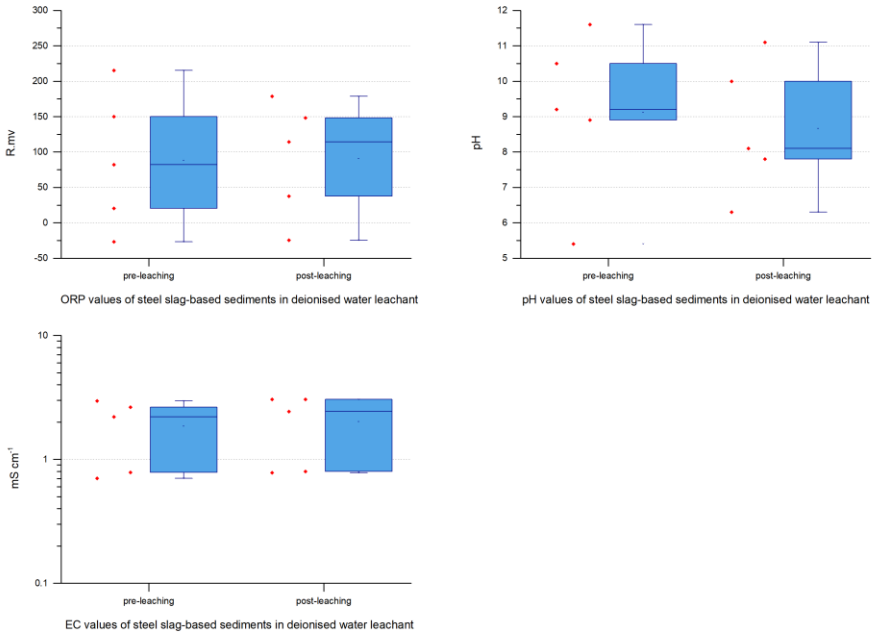

Figure 12. A box-and-whisker plot depicting ORP (R.mv), pH, and EC (mS cm-1) values for steel slag-based coastal legacy waste samples in deionised water before and after leaching (n=5).

Pearsons's correlation coefficients analysis was carried out on the combined datasets to illustrate the inter-elemental relationship of dissolved trace elements (seen in table 19). Very high positive correlation coefficients with Al and Pb, Al and Cr, Al and Co, Al and Ni, As and Cr, As and V, Pb and Cu, V and Cr, Mn and Co, Mn and Cu, and Co and Ni. As Al and Mn are major elements (see section 4.1), this suggests that the dissolution/precipitation of Al/Mn in the sediment is an influential mechanism for related trace element mobility. This also appears the case for high positive correlation coefficients such as Cr and Ni, Al and V, Pb and Zn, and Co and Pb.

		Zn	As	Pb	Al	K	V	Cr	Mn	Co	Ni	Cu
Zn	Pearsons corr.	1.00	0.01	**0.70**	0.28	-0.07	0.28	0.11	-0.05	0.13	-0.07	0.66
	Sig	--	0.97	0.04	0.47	0.85	0.47	0.82	0.91	0.76	0.88	0.23
As	Pearsons corr.		1.00	0.01	0.38	0.31	**0.92**	**0.98**	-0.20	-0.10	-0.02	-0.27
	Sig		--	0.99	0.28	0.41	<0.01	<0.01	0.57	0.81	0.97	0.61
Pb	Pearsons corr.			1.00	**0.82**	-0.29	0.40	0.20	0.16	**0.79**	0.66	**0.98**
	Sig			--	<0.01	0.45	0.26	0.64	0.66	0.01	0.05	<0.01
Al	Pearsons corr.				1.00	-0.20	**0.67**	**0.81**	0.10	**0.87**	**0.84**	0.71
	Sig				--	0.61	0.03	0.02	0.79	<0.01	<0.01	0.11
K	Pearsons corr.					1.00	0.16	0.41	-0.04	-0.23	-0.47	-0.17
	Sig					--	0.69	0.36	0.91	0.58	0.24	0.78
V	Pearsons corr.						1.00	**0.97**	-0.13	0.22	0.24	0.14
	Sig						--	<0.01	0.72	0.57	0.54	0.79
Cr	Pearsons corr.							1.00	-0.31	0.18	**0.77**	-0.05
	Sig							--	0.46	0.71	0.04	0.94
Mn	Pearsons corr.								1.00	**0.97**	0.22	**0.82**
	Sig								--	<0.01	0.56	0.04
Co	Pearsons corr.									1.00	**0.97**	0.76
	Sig									--	<0.01	0.08
Ni	Pearsons corr.										1.00	0.56
	Sig										--	0.33
Cu	Pearsons corr.											1.00
	Sig											--

Table 19. Pearsons's correlation coefficient values of dissolved element concentrations in deionised leachate, with high and very high positive correlations highlighted in bold. The significant correlation is tested on the level of p< 0.05 (n=10).

The unique constitution of deionised water presents significant differences compared with forms of water seen in the environment (Verma and Kushwaha, 2014), including rainwater and seawater. As such, studies investigating element leaching potential in deionised water are not necessarily transferable to environmental waters. Furthermore, average element concentrations alongside concentration range and water quality guideline values for colliery sediment and steel slag leachate can be seen in tables 20 and 21, and figures 17 and 18.

Potassium concentrations show the highest average concentrations of elements leached in deionised water, with 112.86mg/l in leached colliery sediments and 113.75mg/l in leached steel slag-based sediments. The Soluble K^+ fraction in solutions has been investigated throughout the literature (Jalali and Jalali, 2022; Goulding *et al,* 2021) and can be attributed to the solubility potential of K salts in aqueous conditions (Merck, no date). The presence of K_2CO_3, KCl, and K_2SO_4 in coal fly ash has been documented by Wang *et al* (2019a). The subsequent mixing of salts can promote the dissolution of K salts, resulting in elevated leaching concentrations. The interaction between carbonic acid generated in deionised water through air exposure and (H_2CO_3) and K_2CO_3 is also worth considering (Izquierdo and Querol, 2012).

Aluminium concentrations within deionised leachate make up the 2nd highest proportion of all detected elements, with an average concentration of 47.55mg/l in colliery sediments and 18.97mg/l in steel slag sediments. The release of Al into a soluble form (Al^{3+}), and other trace elements including Ni, Cr, Pb, Cu, and Zn throughout the literature illustrates that solubility is severely limited at near-neutral pH conditions, with the rate of solubility increasing approximately at <pH 6 and >pH 12 conditions (Kròl *et al,* 2020; Mahedi *et al,* 2019; Kryzevicius *et al,* 2019 Kommonweeraket *et al,* 2015; Garrabrants *et al,* 2004). An inverse pattern regarding Al is reflected in this study within deionised water, whereby dissolved Al concentrations are higher in near-neutral pH conditions than an acidic and basic pH, with other trace elements suggesting no pattern with pH. Studies investigating Al solubility reflect notable differences with this study during their leaching investigation, whereby Al leaching is investigated within a more homogenised matrix or through fundamental differences in the design of the leaching test (Mahedi *et al,* 2019; Semwal *et al,* 2006). This study presents very complex heterogeneous sediment matrixes, likely containing various large-scale inorganic impurities (such as $Al(OH)_3$), which can inhibit changes in morphology, altering the solubility equilibrium when exposed to water (Wei *et al,* 2014). Soluble Al (Al^{3+}) and other soluble trace elements within deionised water can be attributed to complex interactions between deionised water and metals within waste sediments, through the drawing of ions from

neighbouring metals. Changes enabling Al release into water can directly induce changes in other trace metal mobility (Vojteková *et al,* 2010). Furthermore, as mentioned previously, the significant correlation coefficient of Al with Cr, Co, Ni, and Pb suggests the release of Al increases the leached concentrations of the other metals. Additionally, within deionised water, a galvanic corrosion electrochemical process can occur when two dissimilar metals (primarily in their metallic form) are in contact while immersed in an electrolyte (enabled by elevated EC and temperature) (Selwyn, 2021; Hao *et al,* 2020; Gustafsson, 2011; Yang *et al,* 2021). Additionally, galvanic corrosion has also been documented to occur between metals in their mineral form (Liu *et al,* 2008), suggesting the possibility of galvanic corrosion also having an influence on leachate concentrations from waste sediments, although the extent to which in this study is unknown. pH values were a result of ion exchange between deionised water and waste sediments, therefore had minimal influence on leachate concentrations. It is therefore hypothesised that initial ion exchange between deionised water and all elements detected contributed towards element mobility, especially with elements that highly correlate with each other (Sankar and Das, 2013; Velling, 2020; NASA, no date), with galvanic corrosion reactions potentially contributing to leached element concentrations in deionised leachate.

No correlation coefficients could be established for Fe as concentrations were undetectable in steel slag-based waste type. Soluble Fe concentrations present elevated leachate concentrations in comparison to trace elements detected. Similar to Al, Fe compounds solubility in aqueous conditions are influenced by pH, with minimal solubility seen at pH 8-9 (Baumgartner and Faivre, 2015). It is known that Fe-oxides and hydroxides play important roles within environmental chemistry, through element sorption and redox buffering (Baumgartner and Faivre, 2015) further influenced by the co-occurrence of Ca and Sulphate. The cooperation with Ca and Fe on trace element sorption can result in decreased dissolved trace element concentrations. As Ca concentrations were abundant in sediments, Fe and Ca cooperation may have resulted in the buffering of dissolved trace elements, more so at pH above neutral (Wikkie and Hering, 1996).

Concentrations of Mn in deionised leachate represent the 3rd most leached element behind K and Al. More specifically, colliery leachate presents an average concentration of 4.4mg/l, whereas steel slag leachate presents an average concentration of 8.24mg/l. Manganese solubility is dependent on various factors including species, pH, ORP, and available anion characteristics (WHO, 2020). Typically, Mn^{2+} is the dominant aqueous form of Mn in water, with inorganic Mn present in oxide form. In < pH 6 waters, the favoured Mn form is very

soluble, whereas > pH 8.5 is indicative of insoluble Mn (Chriswell and Huang, 2006). Although, as Mn oxides and Mn silicate-based minerals are known to pertain to legacy waste (see section 4.1), Mn oxides and silicates are relatively insoluble in neutral waters, therefore processes previously hypothesised likely account for Mn concentration release alongside Co and Cu which positively correlate with Mn.

Whilst Mg concentrations account for a considerable fraction in coastal legacy waste sediments (see section 4.1), the release of Mg was minimal across both waste types. Moreover, concentrations in colliery-based sediments were below detection limits, whereas steel slag leachate presented average concentrations of 0.39mg/l. This suggest that Mg-based minerals were insoluble under deionised leachate conditions, and mechanisms hypothesised to mobilise elements were non-consequential on Mg. Moreover, the solubility of Mg differs depending on the Mg compound. Magnesium oxides are relatively water-insoluble, suggesting that either Mg oxide makes up a significant majority of the Mg fraction in waste sediments and/or the presence of complex oxide species and Mg absorption, for instance binding onto Fe-based minerals (Wang *et al,* 2020) and gibbsite minerals (Katz *et al,* 2013). It is evident that the mobilising influences pertaining to deionised water were non-influential towards Mg, although further investigation is recommended to ascertain the mechanisms prohibiting Mg mobility in deionised leachate in complex waste sediment matrixes.

Regarding trace elements, the availability of As and Cr in reservoir sediments was limited by the presence of Al, Fe, and total C, with Al oxides and hydroxides able to rapidly absorb As (Ngatia *et al,* 2021). More specifically, As concentrations in colliery leachate averaging 0.63mg/l, with steel slag leachate averaging 0.12mg/l, whereas average Cr concentrations in colliery leachate and steel slag leachate averaging 0.07mg/l and 0.03mg/l. Whilst no significant correlations between As and Al were detected, this suggests Al dissolution can enable the release of bound As. Therefore, a relationship between Al and As cannot be definitively ruled out. In addition, Cr, As, and V participate in redox reactions between major elements Al, Mn, and Fe, with oxide major elements directly contributing to the oxidation of V, Cr, and As (Peel *et al,* 2022; Pahlevaninezhad *et al,* 2022). Elevated Cr concentrations is typical of Cr(VI) due to its relatively higher solubility and bioavailability than the more stable Cr(III) (Huggins *et al,* 2016; IARC, 2012) which is insoluble at near-neutral pH (Rai *et al,* 1987). Lead concentrations in deionised leachate are reflective of predominately insoluble Pb species within legacy waste sediments, dictating the overall speciation of Pb(II) speciation in water, with an average colliery concentration of 1mg/l and an average steel slag leachate

concentration of 1.07mg/l. $PbCO_3$ or $Pb(CO_3)_2$ are known for their potential solubility (Zha *et al,* 2021; Lenntech, no date), of which can pertain to coal/fly ash (Abdulla, 2020) and slag waste (Xu and Yi, 2022). Sample sites MPC4 and HC1 present Pb concentration anomalies of >4mg/l, however the pH range from near-neutral to mildly alkaline, indicative of reduced Pb solubility (Australian and New Zealand Guidelines for Fresh and Marine Water Quality, 2000), suggesting that pH is not the primary cause of Pb solubility, suggesting a higher proportion of $PbCO_3$ or $Pb(CO_3)_2$ than in other waste sediments. Leaching of Co in trace amounts was present across both colliery and slag waste types. More specifically, an average colliery leachate concentration of 0.09mg/l and 0.04mg/l for steel slag leachate. More specifically, an average colliery leachate concentration of 0.09mg/l and 0.04mg/l for steel slag leachate. The leaching of Co was dictated by pH conditions, with leaching near-neutral pH conditions limited. The differing Co species across all waste sediments could explain increased Co leachate concentrations in certain leachate samples, irrespective of pH. Cobalt chloride hexahydrate (CoCl2·6H2O) in room temperature is soluble in water (83.5g/100g H_2O) (Merck, no date), whereas Co-based metals are predominately insoluble in water at room temperature. Moreover, alterations towards the silicate and glass fraction in waste sediments can also contribute to the dissolution of Co (Vítková *et al,* 2013). Trace amounts of dissolved Ni was detected within deionised leachate across both waste types. For example, an average colliery leachate concentration of 0.25mg/l and 0.09mg/l for steel slag leachate. The compound state also dictates the relative solubility of Ni, with NiO displaying leaching under distilled water conditions higher than saline conditions, as amino acids, proteins, and coexisting salts act as a leaching suppressant (Yamada *et al,* 1993). The lack of which, and the fluctuating pH conditions of the deionised water leachate explains leaching of Ni. Furthermore, significantly positive correlation relationships between Ni and Cr, and Ni and Co, suggesting the fate of these elements are tied to one-another, and the mechanisms enabling release into a soluble fraction are directly linked. Additionally, anomalies in trace metal concentrations within the leachate can be attributed to the complex composition of the sediment, still impacted by the same leaching processes as seen across the other deionised leachate samples.

As mentioned previously regarding the composition and mobility mechanisms of deionised waters, it is unreasonable to determine the risk towards human and environmental receptors. Nevertheless, concentrations were compared to water quality guideline values to assess the hazard potential (see tables 20 and 21). As, Pb, Al, and Mn exceeded guideline values across a majority of leachate samples, whereas Cr, V, Ni, and Cu were exceeded in a

minority. Additionally, screening values established by the National Oceanic and Atmospheric Administration (NOAA) for Zn, K, Co, Fe, and Mg were also not exceeded amongst all leachate samples across both waste types. Nevertheless, concern for those elements is less than As, Pb, Al, and Mn. Leaching of elements within coastal legacy waste sediments under deionised water conditions presents hazardous element concentrations that exceed water quality guideline values. Whilst these results are not representative of rainwater and seawater conditions, this can serve as a warning about the possibility of leaching in legacy sites if action is not taken.

Leached elements	Zn	As	Pb	Al	K	V	Cr	Mn	Co	Ni	Cu	Fe
Average concentration (mg/l)	0.2	0.63	1	47.55	112.86	0.19	0.07	4.4	0.09	0.25	0.34	2.28
Concentration range (mg/l)	0.11-0.3	0.01-2.95	0.01-4.47	10-117.36	79.73-159.25	0.02-0.63	0.03-0.18	1.22-12.93	0.002-0.36	0.02-1.01	0.1-0.72	0.98-4.68
Drinking water quality guideline value (mg/l)	120**	0.01*	0.01*	0.9*	373,000**	0.12*	0.05*	0.08*	1,500**	0.07*	2*	1,000**

Table 20. Leached elements in a deionised water matrix detected through ICP-MS analysis of colliery-based waste sediments, presenting average element concentrations and concentration ranges (mg/kg) (n=5), in addition to the WHO drinking water quality guideline values and National Oceanic and Atmospheric Administration freshwater screening values (Buchman, 2008)**.*

Leached elements	Zn	As	Pb	Al	K	V	Cr	Mn	Co	Ni	Cu	Mg
Average concentration (mg/l)	2.8	0.12	1.07	18.97	113.74	0.07	0.03	8.24	0.04	0.09	0.38	0.39
Concentration range (mg/l)	0.13-11.19	0.01-0.52	0.01-5.22	1.37-69.5	15.21-181.57	0.006-0.33	0.01-0.07	0.44-29.86	0.001-0.11	0.05-0.15	0.09-0.82	0.09-0.82
Drinking water quality guideline value (mg/l)	120**	0.01	0.01	0.9	373,000**	0.12	0.05	0.08	1,500**	0.07	2	1,000**

Table 21. Leached elements in a deionised water matrix detected through ICP-MS analysis of steel slag-based waste sediments, presenting average element concentrations and concentration ranges (mg/kg) (n=5), in addition to the WHO drinking water quality guideline values and National Oceanic and Atmospheric Administration freshwater screening values (Buchman, 2008)**.*

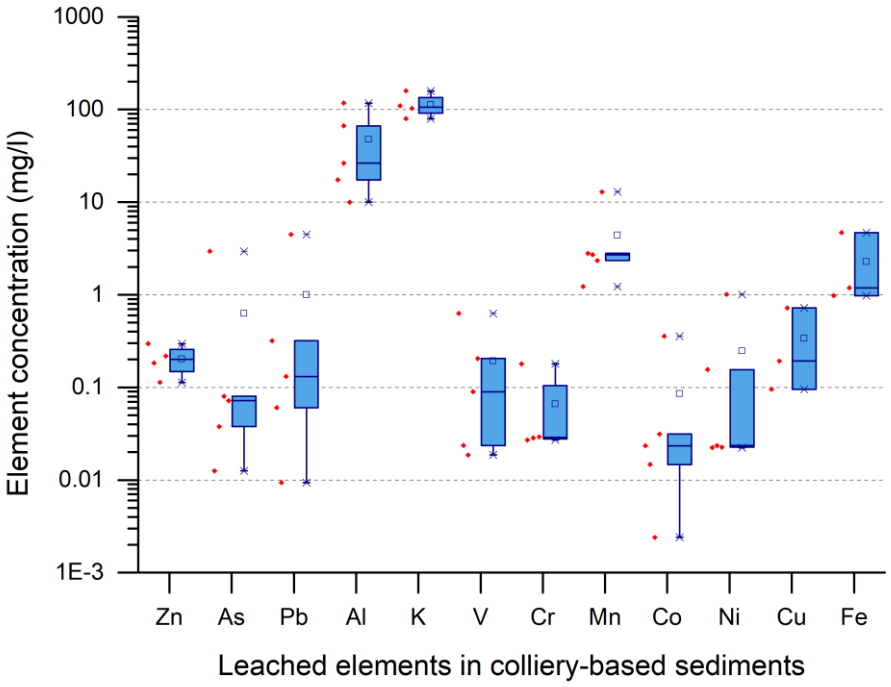

Figure 17. A box-and-whisker plot depicting the elements and their concentrations under an oxidising leaching experiment in deionised water conditions (mg/l) from colliery-based sediments (n=5).

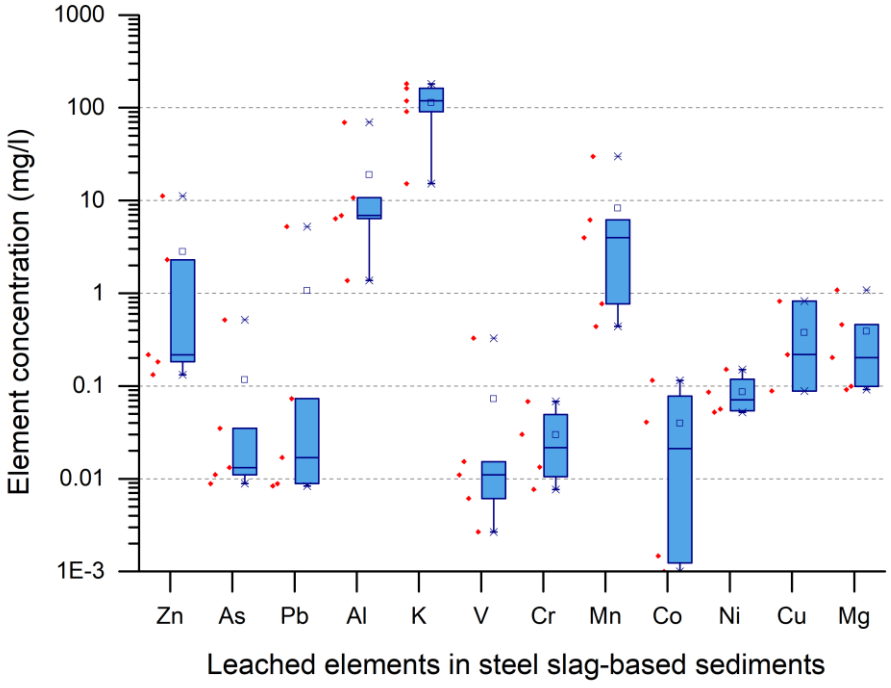

Figure 18. A box-and-whisker plot depicting the elements and their concentrations under an oxidising leaching experiment in deionised water conditions (mg/l) from steel slag-based sediments (n=5).

4.2.2. Concentration and leaching behaviour of elements within ARW leachant

Element leaching under ARW conditions presents considerably reduced element concentrations in comparison to the deionised water leachant. The highest average dissolved element concentrations within colliery-based leachate are as follows: K (8.2mg/l) > Mn (0.9mg/l) > Co (0.004mg/l) > Ni (0.003mg/l), whereas K (12.3mg/l), whereas K was the only element found to have leached from steel slag-based sediments. Across both waste sediments, the majority of trace and major elements including Zn, As, Pb, Al, V, Cr, Cu, and Fe were below detection limits and were immobilised under ARW conditions, with Co, Ni, Mn, and Mg leaching from colliery-based sediments rather than steel slag-based.

Geochemical factors influencing element mobility in aqueous conditions are similar across all aqueous leachants including ORP, pH, and EC, however, leaching mechanisms can differ between deionised water and rainwater, for example, the leaching strength of low ionic strength deionised water can leach directly from the soil and sediment matrix whilst significantly changing the chemical composition of bioretention media (Stahnke and Poor, 2017), unlike other forms of water. ARW pH before introduction to leachate introduction was 5.6. The Shapiro-Wilk distribution test carried out on geochemical parameters including pH, EC, and ORP for each individual waste type pre and post leaching alongside Mann-Whitney U test of difference concluded significant difference in EC values between pre-leaching and post-leaching values of colliery sediment, and also steel slag-based sediments. Additionally, EC values significantly differed between post-leaching colliery sediments and post-leaching steel slag-based sediments. Furthermore, no significant differences in pH, and ORP pre and post leaching, and also no difference between sediment types (see tables 22-26). pH values vary from acidic to alkaline across both waste types, indicating that pH values are a result of the complexities of individual sediments rather than waste type (seen in tables 27 and 28, and figures 19 and 20). No statistical difference was determined between waste types, however notable changes in pH of >2 were found in samples GTT1, MP1, DBB2, MP5, and MPC1. As mentioned previously, pH variability in waste sediments can vary drastically, with pH reaching more neutral conditions over an extended period of time (Roy and Berger, 2011). The readily available Ca and S fraction under ARW conditions in sediments explains variations in pH, with agitation altering Ca and S ratio within sediments (as mentioned previously). Similar to deionised leachate, ORP decreased to near neutral/negative as pH increases (seen in tables 27 and 28, and figures 19 and 20). As mentioned previously, ORP decreases as pH increases due to the reducing agents present. EC values were similar across all ARW leachate samples (seen in tables 27 and 28, and figures 19 and 20). ARW EC values

are above EC values within other studies (Zdeb et al, 2018; Jonsson and Vonnegut, 1991) due to salts consumed to replicate rainwater.

Furthermore, regarding EC and pH values of steel slag-based leachate, post leaching displayed a reduction across the majority of leachate samples. This is contradictory to previous literature establishing elevated values of pH and EC post leaching in deionised water and seawater conditions (Riley *et al,* 2024; Hobson *et al,* 2018), as there is a positive correlation between dissolved Ca and increases in pH. One potential explanation is that dissolution of soluble Na hydroxides tends to initially buffer the increase in pH associated with slower reacting Ca silicates pertaining to steel slag waste (at >pH12). However, carbonate dissolution over a prolonged period becomes the more dominant factor altering pH (Gomes *et al,* 2016). However, further research is necessary to accurately determine the cause of reduced pH and EC values post leaching within steel slag leachate. Nevertheless, this highlights the complexities of real-world environmental conditions.

It is worth noting that traces of contamination were detected throughout some ARW leachate samples, likely due to constraints with instruments to determine ORP, EC, and pH. Whilst thorough cleaning was carried out, special attention is required during the cleaning process. However, cross-contamination concentrations were minimal and therefore had little to no significant consequences on the discussion.

	Pre-leaching colliery sediment waste type			Pre leaching steel slag sediment waste type		
	df	statisitc	*p*	df	statistic	*p*
pH	5	0.93499	0.6308	5	0.95509	0.77345
ORP	5	0.94036	0.66847	5	0.87099	0.27044
EC	5	0.80563	0.08999	5	0.84238	0.17162

Table 22. Shapiro-Wilk normality test of individual geochemical factors in ARW from colliery-based and steel slag-based waste sediments including pH, ORP (R.mv), and EC (mS cm-1) prior to leaching, to determine whether data was drawn from a normally distributed population (p< 0.05).

	Pre-leaching colliery sediment waste type (n=5)		Post-leaching colliery sediment waste type (n=5)			
	Median	IQR	Median	IQR	U	*p*
pH	6.9	5.8-7.65	8.3	6.6-10.55	6	0.21
ORP	145.6	103.7-159.6	101.3	-50.3-162.4	17	0.4
EC	12.2	12-12.6	13.2	12.45-13.8	2	0.04

Table 23. Mann-Whitney U analysis of colliery-based sediment pre (n=5) and post-leaching (n=5) data sets for geochemical parameters including pH, EC, and ORP pre and post leaching under ARW conditions (p< 0.05).

	Pre-leaching steel slag sediment waste type (n=5)		Post-leaching steel slag sediment waste type (n=5)			
	Median	IQR	Median	IQR	U	*p*
pH	8.4	6.5-10.3	7.6	6.05-7.85	19	0.2
ORP	69	-105.7-123	134.2	118-171.15	3	0.06
EC	13.6	12.5-13.8	12.1	11.95-12.65	23	0.03

Table 24. Mann-Whitney U analysis of steel-slag-based sediment pre (n=5) and post-leaching (n=5) data sets for geochemical parameters including pH, EC, and ORP pre and post leaching under ARW conditions (p< 0.05).

	Post-leaching colliery sediment waste type			Post leaching steel slag sediment waste type		
	df	statistic	*p*	df	statistic	*p*
pH	5	0.94845	0.73	5	0.88678	0.34
ORP	5	0.96324	0.83	5	0.97515	0.91
EC	5	0.8938	0.38	5	0.76764	0.04

Table 25. Shapiro-Wilk normality test of individual geochemical factors in ARW from colliery-based and steel slag-based waste sediments including pH, ORP (R.mv), and EC (mS cm-1) post leaching, to determine whether data was drawn from a normally distributed population (p< 0.05).

	Pre-leaching of both sediment waste types (n=10)		Post-leaching of both sediment waste types (n=10)			
	Median	IQR	Median	IQR	U	*p*
pH	7.45	5.85-8.78	7.75	6.18-8.78	46	0.79
ORP	106.3	55.53-152.13	126.9	78.88-164.28	40	0.47
EC	12.5	12.18-13.63	12.45	12.08-13.33	52.5	0.88

Table 26. Mann-Whitney U analysis of the combined data set of colliery (n=5) and steel slag-based (n=5) geochemical parameters including pH, EC, and ORP pre and post leaching (p< 0.05) under ARW conditions.

	ORP (R.mv)			pH			EC (mS cm-1)		
Sample site	*Pre-agitation mean value*	*Post-agitation mean value*	*Difference after agitation*	*Pre-agitation mean value*	*Post-agitation mean value*	*Difference after agitation*	*Pre-agitation mean value*	*Post-agitation mean value*	*Difference after agitation*
GTT1	145.6	-112.2	-257.8	6.9	10.9	4	12.2	13.2	1
MP1	86.2	11.6	-74.6	8.2	10.2	2	11.9	13.9	2
DBB2	167.9	101.3	-66.6	5.9	8.3	2.4	12.1	13.7	1.6
HC1	121.2	122.4	1.2	7.1	7.9	0.8	12.2	12.4	0.2
WWF4	151.3	202.4	51.1	5.7	5.3	-0.4	13	12.5	-0.5

Table 27. Mean ORP (R.mv), pH, and EC (mS cm-1) values for colliery-based coastal legacy waste samples in ARW before and after leaching (n=5).

	ORP (R.mv)			pH			EC (mS cm-1)		
Sample site	*Pre-agitation mean value*	*Post-agitation mean value*	*Difference after agitation*	*Pre-agitation mean value*	*Post-agitation mean value*	*Difference after agitation*	*Pre-agitation mean value*	*Post-agitation mean value*	*Difference after agitation*
MP5	69	157.4	88.4	8.4	6.3	-2.1	13.7	12	-1.7
HC4	154.6	184.9	30.3	5.2	5.8	0.6	12.6	13.1	0.5
MPC1	-218.5	134.2	352.7	10.7	7.6	-3.1	13.6	12.1	-1.5
MPC4	91.4	131.4	40.1	7.8	7.6	-0.2	12.4	12.2	-0.2
WWF1	7.1	104.6	97.5	9.9	8.1	1.8	13.9	11.9	-2

Table 28. Mean ORP (R.mv), pH, and EC (mS cm-1) values for steel slag-based coastal legacy waste samples in ARW before and after leaching (n=5).

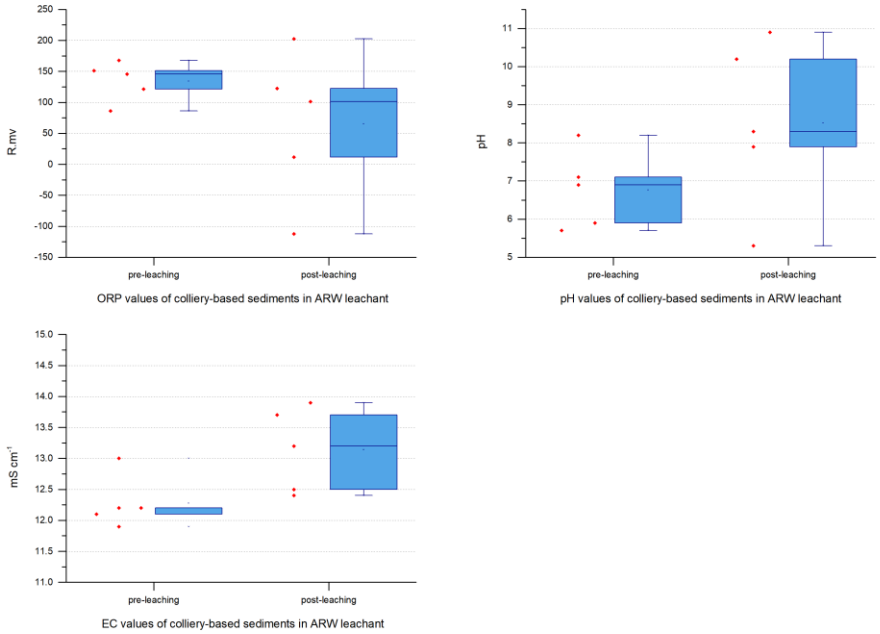

Figure 19. A box-and-whisker plot depicting ORP (R.mv), pH, and EC (mS cm-1) values for colliery-based coastal legacy waste samples in ARW before and after leaching (n=5).

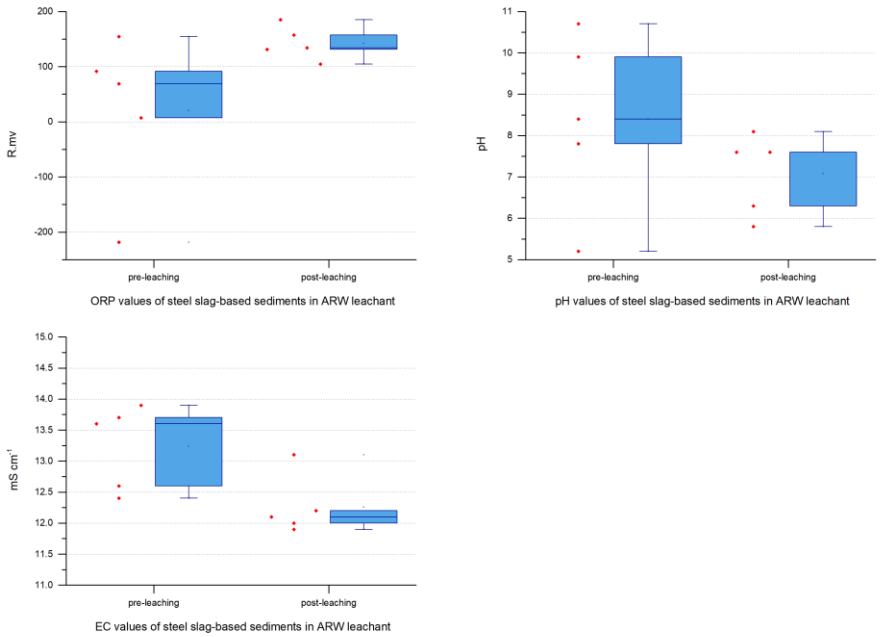

Figure 20. A box-and-whisker plot depicting ORP (R.mv), pH, and EC (mS cm-1) values for steel slag-based coastal legacy waste samples in ARW before and after leaching (n=5).

Potassium concentrations similarly to deionised leachate account for the majority of total dissolved elements leached from the sediment matrix, with the aforementioned average element concentrations for both waste sediments in ARW leachant seen in tables 29 and 30. However, concentrations are considerably different across both waste types in comparison between deionised and ARW, with K concentrations notably higher in deionised water leachate than ARW leachate. Leaching of colliery sediments presented concentrations of dissolved Mn, Co, Ni, and Mg. Significant differences in Mn and Ni concentrations were observed between ARW and deionised leachate, with the exception of Co concentrations (see table 31).

The sorption of trace elements including As, V, Cu, Pb, and Cd is greatly increased with the presence of Ca, with the release of readily soluble K^+, Na^+, Ca^{2+} and Mg^{2+} cations, facilitating the bonding of trace elements to negatively charged surfaces (Zheng *et al,* 2012). This aligns with previous investigations examining element mobility in coal fly ash sediments (Hartuti *et al,* 2018). The elevated Ca^{2+} concentrations detected in steel slag-based waste suggests sorption is further pronounced in steel slag-based leachate, explaining the further lack of leaching in comparison to colliery waste. Additionally, contrary to prior literature (Ghisman *et al,* 2022), in this scenario, pH does not appear to be a significant influence on element mobility, as seen be pH values increasing when in contact with legacy waste sediments. Furthermore, the leachability of Fe in fly ash sediments can restricted, due to strong bonding of Fe to ash particulates (Verma and Verma, 2019). There are variations throughout the literature regarding element mobility, concerning elevated and reduced element concentration in leachates. For instance, Singh *et al* (2007) performed leaching experiments on pond fly ash collected from numerous thermal power plants. Leached elements differed from site to site, with Mn and Cu below detection limits at the Durgapur power plant, though differed at the remaining stations, and moreover, Pb was also found to not be detected amongst all leachates. Whilst no definitive conclusions on the precise mechanisms were found, it was determined that the leachate characteristics are attributed to sediment properties, hence the differences in leached elements and concentrations found across the sites. Similarly, the unique sediment characteristics across coastal legacy waste sites in this study are limiting the leaching of elements under ARW conditions.

In terms of toxicity, leached concentrations in ARW were less hazardous than in deionised leachate. More specifically, only Mg in 3 of 5 leachate samples in colliery leachate exceeded WHO drinking water quality guideline values (2022), and as such suggesting that oxidised rainwater leaching is of low concern under pH 5.6 conditions.

The chemical composition of rainwater differs across regions and countries (Kassamba-Diaby et al, 2022; Sanusi et al, 1996). The ARW produced in this study is more representative of rural conditions in North Wales and therefore anthropogenic sources of pollution are less influential on rainwater composition, and the occurrence of marine salts in rainwater was not considered (Kassamba-Diaby et al, 2022; Al Obaidy et al, 2006). Nevertheless, rainwater produced for this study is more representative than deionised water, which has been used throughout the literature to represent rainwater (Linh et al, 2020; Takahashi and Shinaoka, 2012). Leaching under ARW conditions presents reduced concentrations compared to deionised water, likely explained by the interactions only occurring in deionised water such as its instability and dissolution of minerals to achieve equilibrium, and a lesser extent corrosion. The hypothesised mechanisms for dissolution in deionised water do not apply due to the severe differences in the water matrixes. Furthermore, it is hypothesised that the release of Ca facilitates the bonding process of trace metals, prohibiting mobilisation into a readily available form.

Leached elements	Zn	As	Pb	Al	K	V	Cr	Mn	Co	Ni	Cu	Fe
Average concentration (mg/l)	n/a	n/a	n/a	n/a	8.2	n/a	n/a	0.9	0.004	0.003	n/a	n/a
Concentration range (mg/l)	n/a	n/a	n/a	n/a	0.5-21.6	n/a	n/a	0.08-1.8	0.003-0.005	0.002-0.004	n/a	n/a
Drinking water quality guideline value (mg/l)	120**	0.01*	0.01*	0.9*	373,000**	0.12*	0.05*	0.08*	1,500**	0.07*	2*	1,000**

Table 29. Leached elements in ARW matrix detected through ICP-MS analysis of colliery-based waste sediments, presenting average element concentrations and concentration ranges (mg/kg) (n=5), in addition to the WHO drinking water quality guideline values and National Oceanic and Atmospheric Administration freshwater screening values (Buchman, 2008)**.*

Leached elements	Zn	As	Pb	Al	K	V	Cr	Mn	Co	Ni	Cu	Fe
Average concentration (mg/l)	n/a	n/a	n/a	n/a	12.3	n/a	n/a	n/a	n/a	n/a	n/a	n/a
Concentration range (mg/l)	n/a	n/a	n/a	n/a	6-18.5	n/a	n/a	n/a	n/a	n/a	n/a	n/a
Drinking water quality guideline value (mg/l)	120**	0.01*	0.01*	0.9*	373,000**	0.12*	0.05*	0.08*	1,500**	0.07*	2*	1,000**

Table 30. Leached elements in ARW matrix detected through ICP-MS analysis of steel slag-based waste sediments, presenting average element concentrations and concentration ranges (mg/kg) (n=5), in addition to the WHO drinking water quality guideline values and National Oceanic and Atmospheric Administration freshwater screening values (Buchman, 2008)**.*

	Deionised leachate		ARW leachate			
Elements	Median	IQR	Median	IQR	U	*p*
Mn	2.7	1.78-7.86	0.87	0.39-1.38	24	0.02
Co	0.02	0.008-0.19	0.003	0-0.004	22	0.06
Ni	0.02	0.02-0.58	0.003	0.001-0.004	25	0.01

Table 31. Mann-Whitney U analysis of individual elements leached in deionised water (n=5) and ARW (n=5) conditions from colliery-based sediments (p< 0.05).

4.2.3. Concentration and leaching behaviour of elements within ASW leachant

The leaching of hazardous sediments under ASW was the lowest across all leachants in this study. More specifically, across both waste sediments, all elements leached except Mn were undetected, with Mn concentrations presenting minimal leaching. More specifically, average leached Mn colliery was 0.4mg/l, whereas steel slag leachate was 0.08mg/l.

The Shapiro-Wilk distribution test carried out on geochemical parameters including pH, EC, and ORP for each individual waste type pre and post leaching alongside Mann-Whitney U test of difference concluded no significant differences detected in pH, EC, and ORP across different sediment types, and prior and post leaching (seen in tables 32-36). The majority of ASW leachate samples (8 of 10) present a decrease in pH from the blank ASW sample of 8.4. pH values are near-neutral, with samples sites MPC1 and WWF1 are within mild alkalinity range (seen in tables 32-36, and figures 21 and 22). Moreover, there was no statistical difference between pH before and after leaching. As mentioned previously, the leaching mechanisms differ from previous leachants, and changes in pH are a result of individual waste sediments rather than waste type specific, as pH varies across all leachate samples. Whilst not considered a substantial contributor to the decrease of ASW pH, aged plastic particulates are exposed to weathering and sunlight (Romera-Castillo et al, 2023).

Nevertheless, whilst not hypothesised to have a significant influence on pH conditions in a laboratory setting, environmental conditions where waste plastics are more apparent may notably contribute to a reduction in pH, having additional consequences on the mobilisation of elements with lower pH solubility. Additionally, EC values (seen in tables 32-36, and figures 21 and 22) fall within surface conductivity values seen in UK seawaters (Tyler et al, 2017). The presence of waste sediments did not impact conductivity values pre and post-leaching. As for ORP, similar to previous leachants, ORP values (seen in tables 32-36, and figures 21 and 22) decreased to near neutral/negative as pH increases. ORP values remain positive post leaching, although sample WWF1 presents differs, as ORP values post-leaching increase to 97.7 R.mv at pH 9.5, suggesting the absence of reducing agents available within this individual sediment matrix. Furthermore, there was no statistical difference between ORP, and EC before and after sample leaching, and additionally, no statistical differences in geochemical parameters between waste types.

	Pre-leaching colliery sediment waste type			Pre leaching steel slag sediment waste type		
	df	statistic	*p*	df	statistic	*p*
pH	5	0.94888	0.7292	5	0.95104	0.74459
ORP	5	0.80994	0.09742	5	0.76979	0.04493
EC	5	0.82827	0.13502	5	0.87247	0.27658

Table 32. Shapiro-Wilk normality test of individual geochemical factors in ASW from colliery-based and steel slag-based waste sediments including pH, ORP (R.mv), and EC (mS cm-1) prior to leaching, to determine whether data was drawn from a normally distributed population (p< 0.05).

	Pre-leaching colliery sediment waste type (n=5)		Post-leaching colliery sediment waste type (n=5)			
	Median	IQR	Median	IQR	U	*p*
pH	7.5	6.95-7.8	7.3	6.65-7.75	15.5	0.6
ORP	124.9	120.6-167	133.2	120.5-160.7	11	0.83
EC	43.6	43.5-43.8	43.3	43.2-43.8	19	0.2

Table 33. Mann-Whitney U analysis of colliery-based sediment pre (n=5) and post-leaching (n=5) data sets for geochemical parameters including pH, EC, and ORP pre and post leaching under ASW conditions (p< 0.05).

	Pre-leaching steel slag sediment waste type (n=5)		Post-leaching steel slag sediment waste type (n=5)			
	Median	IQR	Median	IQR	U	*p*
pH	8.1	7.25-9.45	8.1	7.15-9.85	12	1
ORP	116.6	-117.45-131.5	107	48.95-161.95	9	0.53
EC	44.3	43.95-44.65	44.1	43.65-44.7	13.5	0.92

Table 34. Mann-Whitney U analysis of steel-slag-based sediment pre (n=5) and post-leaching (n=5) data sets for geochemical parameters including pH, EC, and ORP pre and post leaching under ASW conditions (p< 0.05).

	Post-leaching colliery sediment waste type			Post leaching steel slag sediment waste type		
	df	statistic	*p*	df	statistic	*p*
pH	5	0.99444	0.99271	5	0.96778	0.86084
ORP	5	0.97026	0.87691	5	0.94056	0.66987
EC	5	0.78616	0.0622	5	0.85044	0.1959

Table 35. Shapiro-Wilk normality test of individual geochemical factors in ASW from colliery-based and steel slag-based waste sediments including pH, ORP (R.mv), and EC (mS cm-1) post leaching, to determine whether data was drawn from a normally distributed population (p< 0.05).

	Pre-leaching of both sediment waste types (n=10)		Post-leaching of both sediment waste types (n=10)			
	Median	IQR	Median	IQR	U	*p*
pH	7.8	7.13-8.38	7.65	6.8-8.45	54	0.79
ORP	124.4	86.63-135.35	132.85	104.68-156.75	41	0.52
EC	43.8	43.6-44.38	43.65	43.28-44.25	60	0.47

Table 36. Mann-Whitney U analysis of the combined data set of colliery (n=5) and steel slag-based (n=5) geochemical parameters including pH, EC, and ORP pre and post leaching ($p < 0.05$) under ASW conditions.

	ORP (R.mv)			pH			EC (mS cm-1)		
Sample site	*Pre-agitation mean value*	*Post-agitation mean value*	*Difference after agitation*	*Pre-agitation mean value*	*Post-agitation mean value*	*Difference after agitation*	*Pre-agitation mean value*	*Post-agitation mean value*	*Difference after agitation*
GTT1	117.3	133.2	15.9	7.5	7.3	-0.2	43.4	43.2	-0.2
MP1	124.9	108.5	-16.4	8	8	0	43.6	43.2	-0.4
DBB2	189.2	132.5	-56.7	7.3	6.9	-0.4	43.6	43.5	-0.1
HC1	123.9	152.8	28.9	7.6	7.5	-0.1	43.6	43.3	-0.3
WWF4	144.8	168.6	23.8	6.6	6.4	-0.2	44	44.1	0.1

Table 37. Mean ORP (R.mv), pH, and EC (mS cm-1) values for colliery-based coastal legacy waste samples in ASW before and after leaching (n=5).

	ORP (R.mv)			pH			EC (mS cm-1)		
Sample site	*Pre-agitation mean value*	*Post-agitation mean value*	*Difference after agitation*	*Pre-agitation mean value*	*Post-agitation mean value*	*Difference after agitation*	*Pre-agitation mean value*	*Post-agitation mean value*	*Difference after agitation*
MP5	116.6	107	-9.6	8	8.1	0.1	44.3	44.7	0.4
HC4	132.2	180.6	48.4	6.5	6.5	0	44.3	43.6	-0.6
MPC1	-231.6	0.2	231.8	9.7	10.2	0.5	44.7	44.1	-0.6
MPC4	130.8	143.3	12.5	8.1	7.8	0.3	43.6	43.7	0.1
WWF1	-3.3	97.7	100.7	9.2	9.5	0.3	44.6	44.7	0.1

Table 38. Mean ORP (R.mv), pH, and EC (mS cm-1) values for steel slag-based coastal legacy waste samples in ASW before and after leaching (n=5).

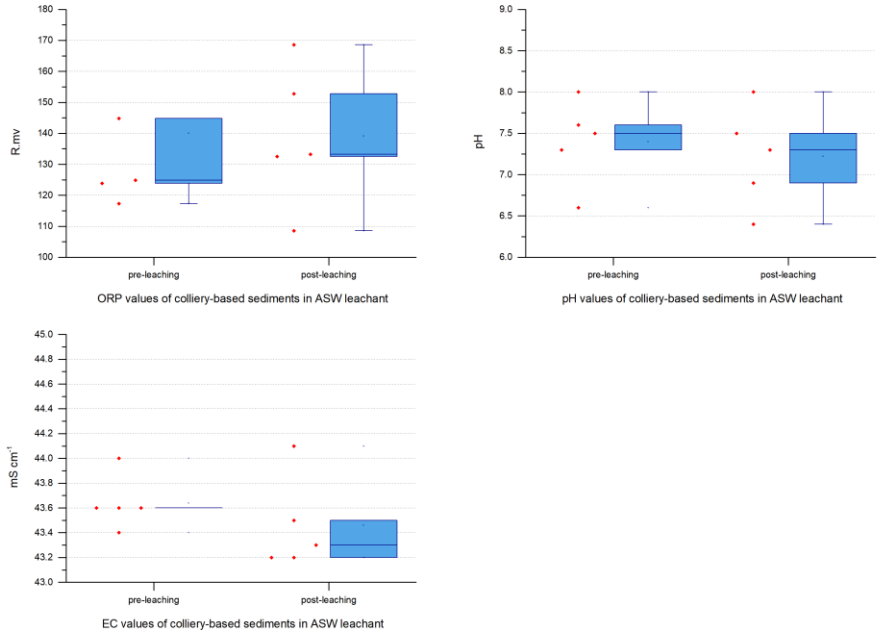

Figure 13. A box-and-whisker plot depicting ORP (R.mv), pH, and EC (mS cm-1) values for colliery-based coastal legacy waste samples in ASW before and after leaching (n=5).

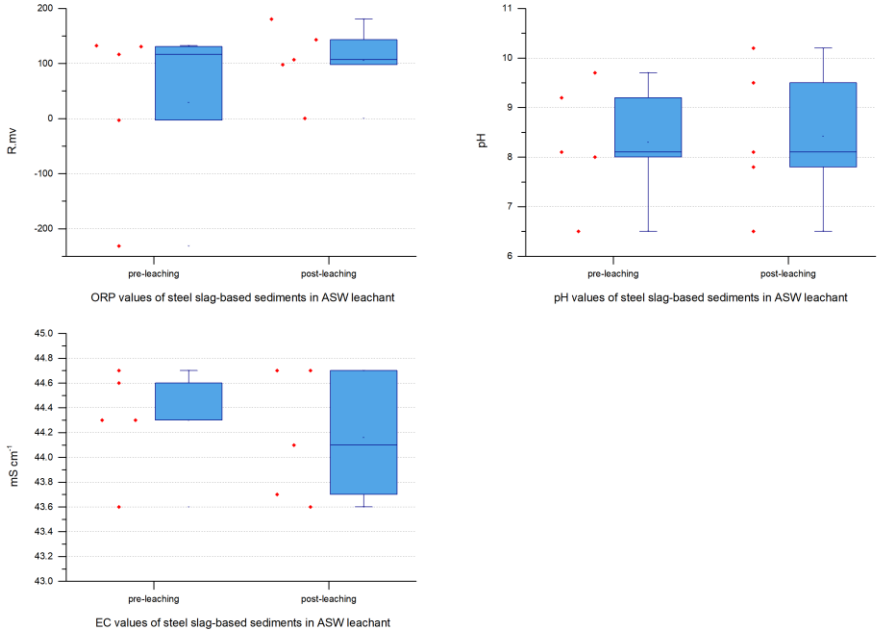

Figure 14. A box-and-whisker plot depicting ORP (R.mv), pH, and EC (mS cm-1) values for steel slag-based coastal legacy waste samples in ASW before and after leaching (n=5).

The aforementioned average leached element concentrations within ASW leachate can be seen in tables 39 and 40. The release of element concentrations in waste sediments through the inundation of seawater has been linked to soluble metal complexes Cl^- and SO_4^{2-} anions and competition for sorption sites (Brand and Spencer, 2020). This study contrasts previous suggestions made under saline conditions, with a lack of released metals present in the leachate. The biogeochemical properties of carbonate minerals can prohibit the sorption of trace elements and incorporate them into the mineral constitution (Smrzka *et al,* 2019; Wang *et al,* 2019b). $CaCO_3$ is soluble under seawater conditions, forming Ca and Hydrogen carbonate ions (Anderson, 2013), and the presence of Ca can enable sorption mechanisms with trace elements in a precipitate form, altering the solubility state, and adding to the complexity of the sediment (Wise and Gilburt, 1981). Furthermore, the precipitation of poorly soluble carbonates and hydroxides presents sorption opportunities for heavy metals including As, Zn, Cu, Cd, and As through ion exchanges (Wierzba *et al,* 2022; Hunter *et al,* 2020). Additionally, as mentioned previously, Cl concentrations were detected using SEM analysis, although only within a small minority of sites, suggesting the Cl-based minerals were less abundant overall in waste sediments. It is therefore hypothesised that the lack of competition for sorption sites between trace elements with Ca^{2+} is enabling the precipitation of trace elements, thus immobilising hazardous element concentrations within the waste sediment. It is worth mentioning that there were ICP-MS detection issues when investigating Mg and K concentrations, likely attributable to the exceedingly high concentrations of dissolved Mg and K solids from sea salts used to produce the ASW leachant. Mg concentrations were therefore undetectable, whereas K concentrations were exceedingly high.

Leached concentrations fall within WHO (2022) drinking water quality guideline values and National Oceanic and Atmospheric Administration screening values (see tables 39 and 40). Whilst seawater consumption is not necessarily a concern, guideline values can be used utilised to make judgements on either accidental consumption or concentrations that can potentially re-attenuate into sediments. Overall, this study presents oxidised ASW leachate concentrations as non-hazardous in relation to the elements analysed. However, it is recommended that further leachate tests be carried out under different conditions at different timescales to determine the risk factors in a wider variety, as this method only represents one controlled transport pathway. For instance, batch leaching tests with changes in timescales could reflect real-world conditions rather than constant stable exposure in a laboratory setting. Secondly, simulating weather events would help to determine whether

changes in leached concentrations are detected, thereby reflecting the influence of real-world weather variability on leaching rates. Additionally, the use of column leaching tests to simulate the movement of water percolating through porous and granular waste material and the fate of PTEs transported (Siddique *et al,* 2010).

Leached elements	Zn	As	Pb	Al	K	V	Cr	Mn	Co	Ni	Cu	Fe
Average concentration (mg/l)	n/a	n/a	n/a	n/a	n/a	n/a	n/a	0.4	n/a	n/a	n/a	n/a
Concentration range (mg/l)	n/a	n/a	n/a	n/a	n/a	n/a	n/a	0.1-0.8	n/a	n/a	n/a	n/a
Drinking water quality guideline value (mg/l)	90**	0.01*	0.01*	0.9*	n/a	0.12*	0.05*	0.08*	1**	0.07*	2*	300**

Table 39. Leached elements in ASW matrix detected through ICP-MS analysis of colliery-based waste sediments, presenting average element concentrations and concentration ranges (mg/kg) (n=5), in addition to the WHO drinking water quality guideline values and National Oceanic and Atmospheric Administration marine water screening values (Buchman, 2008)**.*

Leached elements	Zn	As	Pb	Al	K	V	Cr	Mn	Co	Ni	Cu	Fe
Average concentration (mg/l)	n/a	n/a	n/a	n/a	n/a	n/a	n/a	0.08	n/a	n/a	n/a	n/a
Concentration range (mg/l)	n/a	n/a	n/a	n/a	n/a	n/a	n/a	0.01-0.14	n/a	n/a	n/a	n/a
Drinking water quality guideline value (mg/l)	90**	0.01*	0.01*	0.9*	n/a	0.12*	0.05*	0.08*	1**	0.07*	2*	300**

Table 40. Leached elements in ASW matrix detected through ICP-MS analysis of steel slag-based waste sediments, presenting average element concentrations and concentration ranges (mg/kg) (n=5), in addition to the drinking water quality guideline values and National Oceanic and Atmospheric Administration marine water screening values (Buchman, 2008)**.*

4.3. Implications

This study examines the levels of PTEs found in coastal waste sites in the North West of England and North Wales which are comprised of colliery and steel slag. The findings align with previous research that describes these sites as "significantly hazardous waste" (Brand *et al,* 2018), indicating that they are a major source of inorganic contaminant pollution. Out of the 12 trace elements that were detected, 7 of them in steel slag-based waste and 8 of them in colliery-based waste exceed Canadian sediment quality guideline values, highlighting the potential of toxic implications on human and other environmental receptors through interaction with the contaminated sediments. To add further perspective, there are approximately 420 coastal legacy waste sites within 100m proximity of designated ecological sites. This includes 120 SSSI locations, 47 OSPAR marine protected areas, and 37 Ramsar sites. Additionally, 128 designated UK bathing zone areas in England are situated within this proximity (Irfan, 2019; Brand *et al,* 2018), thus supporting the statement by Riley *et al* (2022) labelling coastal legacy waste sites as “ticking time bombs.” It is unreasonable to generalise element concentrations by waste type at this stage, as element concentrations vary across sample sites, with instances of exceeded guideline values present at a minority of sample sites. It is vital for further assessments of element concentrations across coastal legacy waste sites across England and Wales given the hazardous waste present. Further investigation with a larger and broader sample size will provide a further in-depth understanding of total element concentrations and element speciation, thus potentially identifying further similarities and differences between waste types. Unfortunately, it was not possible to determine the forms of each specific element and the minerals present in colliery and steel slag waste sediments. Therefore, this study recommends using X-ray diffraction spectrometry for mineralogical analysis and X-ray absorption spectroscopy for element species identification (as seen in Byrne *et al,* 2016) for future analysis. This will allow for less speculative insight into element mobility potential. Furthermore, identifying element species will provide greater clarity regarding the level of toxicity, therefore providing a further understanding of the hazardous contents present in coastal legacy waste sediments, and also the risk to environmental receptors.

The findings from the leaching experiments emphasise the limited leaching potential of PTEs within highly contaminated sediments under oxidating ARW and ASW conditions in comparison to deionised leachate results. Unfortunately, element mobility in coastal legacy waste is multifaceted, with additional pollution pathways including anoxic environmental conditions, and a combination of coastal erosion of legacy waste and aeolian transportation

of subsequent landfill particulates (Nicholls *et al,* 2021). Under reducing conditions, anaerobic organisms can alter the bonding mechanisms of oxide-based minerals, enabling the distribution of previously bound elements (Lynch *et al,* 2014). Percolation of leachant into sub-surface sediments can temporarily mobilise bound elements, proceeded by re-attenuation within the leachate plume boundary (Brand *et al,* 2018). Seafloor erosion can expose the leachate plume and enable the release of bound contaminants, acting as a considerable source of diffuse pollution. Additionally, direct coastal erosion of legacy waste sites can have a severely detrimental impact on the surrounding environment, exacerbated if there is a catastrophic failure of the landfill structure. Further transferred by aeolian mechanisms, large quantities of highly contaminated sediments transported into ecologically sensitive environments can have negative consequences for the aforementioned 420 coastal legacy waste sites within a 100m proximity to ecologically protected sites (Brand and Spencer, 2019). It is paramount that management of our coastal legacy landfills is carried out, as the increasing impacts of climate change through sea-level-rise and increasing weather events and intensities progressively act as a destructive force, able to mobilise bound contaminants and redistribute directly onto sensitive environmental receptors, causing irreparable damage.

A surprising finding observed in this study regards how current leaching methods are performed under oxidising conditions. The findings in this study reflect the considerable differences in element leaching potential based on the leachant, with deionised water exhibiting a greater leaching potential than ASW and ARW. Presently, the current British standard leaching method (BS EN 12457-2-2002) still uses deionised water as a standard leachant to determine the leaching potential of soils and sediments, as seen throughout the literature (see Kang *et al,* 2020; Gitari *et al,* 2018; Silva *et al,* 2011; Donatello *et al,* 2012). It is imperative that adaptations are made to the standard leaching method such as artificially producing rainwater and seawater in a laboratory setting or collecting aqueous samples at the sample site to further represent real-world saline conditions, further reflected by steel slag-based leachate values for pH and EC post leaching, with decreased values post leaching, therefore highlighting that leaching behaviours cannot be accurately predicted using standard methods. Current leaching results imply that deionised water leachant considerably overestimates the real-world problem of hazardous element mobility in leachates. Changes made to the British standard method could have direct management implications, potentially changing perceptions on the hazard risk rating of coastal legacy waste hazards, allowing for a more targeted approach to landfill management and risk mitigation.

5. Conclusions

This study looked to examine two key research questions that address the aim of *establishing the environmental risk of potentially toxic elements situated within coastal legacy landfills.*

1. *What is the geochemical composition of coastal legacy waste sediments?*
2. *What is the leaching potential of potentially toxic elements from coastal legacy waste under various oxidised aqueous environmental matrixes?*

The composition of coastal legacy waste sites across the North West of England and North Wales are very complex, with diverse array of pollutants attributed to the region's historical industrial practices, mainly colliery and steel-based in this study. Nevertheless, ICP analysis of the two waste type sediments classified in this study, namely colliery-based and steel slag-based, determined significantly hazardous element concentrations pertaining to both waste sediments. More specifically, across colliery waste sediments, V, Cr, Se, Ni, Tl, As, Cu, and Pb trace element concentrations exceed Canadian SGVs at the majority of colliery sediments, whereas across steel slag-based sediments V, Cr, Ni, Se, As, Sb, and Cu concentrations exceed Canadian SGVs. This study recommends mineralogical analysis to determine the species of elements within the sediment, to further understand the mechanisms enabling/hindering the mobility of elements.

Under oxidising leachate conditions, the leaching potential of coastal legacy waste sediments differs. For instance, deionised water leachate presented considerably elevated leached element concentrations in contrast to ARW and ASW leachants. Moreover, under deionised water conditions, the majority of total leachate samples presented elevated concentrations of Al, As, Pb, and Mn, that exceeded WHO drinking water quality guideline values, with Cu, Cr, V, and Ni exceeding WHO drinking water guideline values in a minority of samples. ARW leaching was substantially less than deionised, as seen by only leached Mg concentrations in a majority of colliery-based sediments exceeding WHO drinking water quality guideline values. Furthermore, no leaching was under ASW conditions. However, instrumental issues did impede the analysis of K and Mg concentrations in ASW conditions. Nevertheless, oxidising leachate conditions under real world conditions present minimal leaching of elements, thus not a concern. However, oxidising leachate conditions are only one transport pathway. Other pathways likely present a greater cause for concern. It is recommended that further studies investigating different transport pathways is conducted to broaden the scope of understanding the risks of inorganic element mobilisation and the subsequent risk on the surrounding environmental receptors. Additionally, significant differences in deionised

leachate results in comparison to artificial leachates. Therefore, it is recommended that BS EN 12457-2-2002 is updated to reflect the differences in aqueous matrixes that appear to have a significant influence on the mobilisation of elements in waste sediments.

The findings in this report reinforces the previous statement regarding coastal legacy waste sites as 'ticking time-bombs' (Riley *et al,* 2022). The leaching potential of these inorganic contaminants are highly determined by the leachant under oxidised conditions. Leaching potential is minimal under environmentally representative conditions, although is considerably higher under deionised water conditions.

Reference list

Abbas, G., Murtaza, B., Bibi, I., Shahid, M., Niazi, N.K., Khan, M.I., Amjad, M., Hussain, M. and Natasha (2018) Arsenic uptake, toxicity, detoxification, and speciation in plants: physiological, biochemical, and molecular aspects. *International journal of environmental research and public health*, *15*(1), p.59.

Abdulla, M. (2020) Lead. In: Prasad, A. and Brewer, G. (eds.) *Essential and Toxic Trace Elements and Vitamins in Human Health.* Amsterdam: Elsevier

Acosta, J.A., Jansen, B., Kalbitz, K., Faz, A. and Martínez-Martínez, S. (2011) Salinity increases mobility of heavy metals in soils. *Chemosphere*, *85*(8), pp.1318-1324.

Aftabtalab, A., Rinklebe, J., Shaheen, S.M., Niazi, N.K., Moreno-Jiménez, E., Schaller, J. and Knorr, K.H. (2022) Review on the interactions of arsenic, iron (oxy)(hydr) oxides, and dissolved organic matter in soils, sediments, and groundwater in a ternary system. *Chemosphere*, *286*, p.131790.

Agilent (2014) *Guidelines for Trouble Shooting and Maintenance of ICP-MS Systems* [Online] Available at: https://www.agilent.com/cs/library/slidepresentation/Public/ASTS_2015_AtomicTour_Tips-and-Tricks.pdf
[Accessed: 19/01/2022]

Agnew, U.M. and Slesinger, T.L. (2020) *Zinc toxicity* [Online]
Available at: https://www.ncbi.nlm.nih.gov/books/NBK554548/
[Accessed: 02/02/2024]

Agnieszka, J. and Barbara, G. (2012) Chromium, nickel and vanadium mobility in soils derived from fluvioglacial sands. *Journal of hazardous materials*, *237*, pp.315-322.

Ahmad, Z. (2006) Introduction to corrosion. In: *Principles of corrosion engineering and corrosion control.* 1st ed. Oxford: Butterworth-Heinemann pp. 1-8

Aihemaiti, A., Gao, Y., Meng, Y., Chen, X., Liu, J., Xiang, H., Xu, Y. and Jiang, J. (2020) Review

of plant-vanadium physiological interactions, bioaccumulation, and bioremediation of vanadium-contaminated sites. *Science of the Total Environment*, *712*, p.135637.

Ali, A., Chiang, Y.W. and Santos, R.M. (2022) X-ray diffraction techniques for mineral characterization: A review for engineers of the fundamentals, applications, and research directions. *Minerals*, *12*(2), p.205.

Al Obaidy, A.H.M.J. and Joshi, H. (2006) Chemical composition of rainwater in a tropical urban area of northern India. *Atmospheric Environment*, *40*(35), pp.6886-6891.

Anderson, L.G. (2013). *Carbonate Dissolution. In: Harff, J., Meschede, M., Petersen, S., Thiede, J.* (eds) Encyclopedia of Marine Geosciences. Springer, Dordrecht.

ATSDR (2020) *ToxFAQsTM for Lead* [Online]
Available at: https://wwwn.cdc.gov/TSP/ToxFAQs/ToxFAQsDetails.aspx?faqid=93&toxid=22
[Accessed: 02/02/2024]

ATSDR (2012) *TOXICOLOGICAL PROFILE FOR MANGANESE* [Online]
Available at: https://www.atsdr.cdc.gov/toxprofiles/tp151.pdf
[Accessed: 02/02/2024]

ATSDR (2008) *TOXICOLOGICAL PROFILE FOR ALUMINUM* [Online]
Available at: https://www.atsdr.cdc.gov/toxprofiles/tp22.pdf
[Accessed: 02/02/2024]

Aubert, H. and Pinta, M. (1977) *Trace Elements in Soils.* 7th ed. Amsterdam: Elsevier.

Aumann, H.H., Ruzmaikin, A. and Teixeira, J. (2008) Frequency of severe storms and global warming. *Geophysical Research Letters*, *35*(19).

Australian and New Zealand Guidelines for Fresh and Marine Water Quality (2000) *Lead in freshwater and marine water* [Online]
Available at: https://www.waterquality.gov.au/anz-guidelines/guideline-values/default/water-quality-toxicants/toxicants/lead-2000

[Accessed: 04/02/2024]

Barceloux, D.G. and Barceloux, D. (1999) Vanadium. *Journal of Toxicology: Clinical Toxicology*, *37*(2), pp.265-278.

Bartlett, R.J. and James, B.R. (1988) Mobility and bioavailability of chromium in soils. In: *Chromium in the natural and human environments* (eds.), *20*, p.571. New York: John Wiley & Sons Inc.

Baumgartner, J. and Faivre, D. (2015) Iron solubility, colloids and their impact on iron (oxyhydr) oxide formation from solution. *Earth-Science Reviews*, *150*, pp.520-530.

BBC (2017) *Is it safe to live on a former landfill site?* [Online] 20 June
Available at: https://www.bbc.co.uk/news/uk-40308598
[Accessed: 04/09/2023]

Beaven, R.P., Stringfellow, A.M., Nicholls, R.J., Haigh, I.D., Kebede, A.S. and Watts, J. (2020) Future challenges of coastal landfills exacerbated by sea level rise. *Waste Management*, *105*, pp.92-101.

Begum, W., Rai, S., Banerjee, S., Bhattacharjee, S., Mondal, M.H., Bhattarai, A. and Saha, B. (2022) A comprehensive review on the sources, essentiality and toxicological profile of nickel. RSC Adv 12: 9139–9153.

Belzile, N. and Chen, Y.W. (2017) Thallium in the environment: a critical review focused on natural waters, soils, sediments and airborne particles. *Applied Geochemistry*, *84*, pp.218-243.

Bhatt, A., Priyadarshini, S., Mohanakrishnan, A.A., Abri, A., Sattler, M. and Techapaphawit, S. (2019) Physical, chemical, and geotechnical properties of coal fly ash: A global review. *Case Studies in Construction Materials*, *11*, p.e00263.

Bolan, S., Wijesekara, H., Tanveer, M., Boschi, V., Padhye, L.P., Wijesooriya, M., Wang, L., Jasemizad, T., Wang, C., Zhang, T. and Rinklebe, J. (2023) Beryllium contamination and its

risk management in terrestrial and aquatic environmental settings. *Environmental Pollution*, *320*, p.121077.

Bolan, N., Kumar, M., Singh, E., Kumar, A., Singh, L., Kumar, S., Keerthanan, S., Hoang, S.A., El-Naggar, A., Vithanage, M. and Sarkar, B. (2022) Antimony contamination and its risk management in complex environmental settings: a review. *Environment International*, *158*, p.106908.

Brand, J.H. and Spencer, K.L. (2020) Will flooding or erosion of historic landfills result in a significant release of soluble contaminants to the coastal zone?. *Science of The Total Environment*, *724*, p.138150.

Brand, J.H. and Spencer, K.L. (2019) Potential contamination of the coastal zone by eroding historic landfills. *Marine pollution bulletin*, *146*, pp.282-291.

Brand, J.H. and Spencer, K.L. (2018) Risk screening assessment for ranking historic coastal landfills by pollution risk. *Anthropocene Coasts*, *1*(1), pp.44-61.

Brand, J.H., Spencer, K.L., O'shea, F.T. and Lindsay, J.E. (2018) Potential pollution risks of historic landfills on low-lying coasts and estuaries. *Wiley Interdisciplinary Reviews: Water*, *5*(1), p.e1264.

Brand, J.H. (2017) *Assessing the risk of pollution from historic coastal landfills*. Ph.D. thesis, Queen Mary University of London

Breshears, D.D., Kirchner, T.B., Whicker, J.J., Field, J.P. and Allen, C.D. (2012) Modeling aeolian transport in response to succession, disturbance and future climate: Dynamic long-term risk assessment for contaminant redistribution. *Aeolian Research*, *3*(4), pp.445-457.

BRITISH GEOLOGICAL SURVEY (2012) *The advanced soil geochemical at las of England and Wales* [Online]
Available at:
https://nora.nerc.ac.uk/id/eprint/18016/1/Advanced_Soil_Geochemical_Atlas_of_England_and_Wales.pdf

[Accessed: 28/12/2023]

Buchman, M. (2008) *Screening Quick Reference Tables (SQuiRTs)* [Online]
Available at: https://repository.library.noaa.gov/view/noaa/9327
[Accessed: 1/11/2024]

Byrne, P., Taylor, K.G., Hudson-Edwards, K.A. and Barrett, J.E. (2016) Speciation and potential long-term behaviour of chromium in urban sediment particulates. *Journal of soils and sediments*, *17*, pp.2666-2676.

Canadian council of ministers of the environment (2007) *Canadian Soil Quality Guidelines for the Protection of Environmental and Human Health* [Online]
Available at:
https://support.esdat.net/Environmental%20Standards/canada/soil/rev_soil_summary_tbl_7.0_e.pdf
[Accessed: 04/02/2024]

Canadian council of ministers of the environment (no date) *Conductivity* [Online]
Available at: https://www.gov.nt.ca/sites/ecc/files/conductivity.pdf
[Accessed: 02/01/2024]

Chen, Z. and Ye, H. (2023) Understanding the impact of main seawater ions and leaching on the chloride transport in alkali-activated slag and Portland cement. *Cement and Concrete Research*, *164*, p.107063.

Chen, G., Li, J., Han, H., Du, R. and Wang, X. (2022) Physiological and molecular mechanisms of plant responses to copper stress. *International Journal of Molecular Sciences*, *23*(21), p.12950.

Chen, L., Liu, J.R., Hu, W.F., Gao, J. and Yang, J.Y. (2021) Vanadium in soil-plant system: Source, fate, toxicity, and bioremediation. *Journal of hazardous materials*, *405*, p.124200.

Choi, Y.J., Ahn, D., Nguyen, T.H. and Ahn, J. (2018). Assessment of field compaction of aggregate base materials for permeable pavements based on plate load tests. *Sustainability*,

10(10), p.3817.

Chou, Y.C., Lo, S.L., Kuo, J. and Yeh, C.J. (2013) Derivative mechanisms of organic acids in microwave oxidation of landfill leachate. *Journal of hazardous materials*, *254*, pp.293-300.

Chriswell, B. and Huang, S. H. D. (2006) Chapter 10- Manganese removal. In: Newcombe, G. and Dixon, D. (2006) (eds.) *Interface Science in Drinking Water Treatment: Theory and Application.* 10th ed. Amsterdam: Elsevier pp. 179-192

Control of Pollution Act 1974 [Online]
Available at: https://www.legislation.gov.uk/ukpga/1974/40
[Accessed: 04/09/2023]

Cooper, R.G. and Harrison, A.P. (2009) The exposure to and health effects of antimony. *Indian journal of occupational and environmental medicine*, *13*(1), pp.3-10.

Cornu, S., Lucas, Y., Lebon, E., Ambrosi, J.P., Luizão, F., Rouiller, J., Bonnay, M. and Neal, C. (1999) Evidence of titanium mobility in soil profiles, Manaus, central Amazonia. *Geoderma*, *91*(3-4), pp.281-295.

Costis, S., Coudert, L., Mueller, K., Neculita, C.M. and Blais, J.F. (2021) Behaviour of flotation tailings from a rare earth element deposit at high salinity. *Journal of Environmental Management*, *300*, p.113773.

Cseh, L., Ingerman, L., Keith, S. and Taylor, J. (2012) *Toxicological profile for vanadium* [Online]
Available at: https://www.ncbi.nlm.nih.gov/books/NBK592340/
[Accessed: 02/02/2024]

Cui, W., Meng, Q., Feng, Q., Zhou, L., Cui, Y. and Li, W. (2019) Occurrence and release of cadmium, chromium, and lead from stone coal combustion. *International Journal of Coal Science & Technology*, *6*, pp.586-594.

Cumbria County Council (no date) *11e1 St. Bees Head to Whitehaven* [Online]
Available at:
https://www.cumbria.gov.uk/elibrary/Content/Internet/544/17312/17380/43413151411.pdf?timestamp=434528596
[Accessed: 01/02/2024]

Dai, S., Hower, J.C., Finkelman, R.B., Graham, I.T., French, D., Ward, C.R., Eskenazy, G., Wei, Q. and Zhao, L. (2020) Organic associations of non-mineral elements in coal: A review. *International Journal of Coal Geology*, *218*, p.103347.

Das, K.K., Reddy, R.C., Bagoji, I.B., Das, S., Bagali, S., Mullur, L., Khodnapur, J.P. and Biradar, M.S. (2019) Primary concept of nickel toxicity–an overview. *Journal of basic and clinical physiology and pharmacology*, *30*(2), pp.141-152.

Department for Environment Food & Rural Affairs (2023a) *Sites of Special Scientific Interest (England)* [Online]
Available at: https://naturalengland-defra.opendata.arcgis.com/datasets/Defra::sites-of-special-scientific-interest-england/explore?location=54.421774%2C-3.393594%2C10.00
[Accessed: 03/02/2024]

Department for Environment Food & Rural Affairs (2023b) *Swimfo: Find a bathing water* [Online]
Available at: https://environment.data.gov.uk/bwq/profiles/
[Accessed: 03/04/2024]

Dianyi, Yu. (no date) *What Are the Physiologic Effects of Chromium Exposure?* [Online]
Available at:
https://www.atsdr.cdc.gov/csem/chromium/physiologic_effects_of_chromium_exposure.html
[Accessed: 02/02/2024]

de Souza-Silva, T.G., Oliveira, I.A., da Silva, G.G., Giusti, F.C.V., Novaes, R.D. and de Almeida Paula, H.A. (2022) Impact of microplastics on the intestinal microbiota: A systematic review of preclinical evidence. *Life Sciences*, *294*, p.120366.

Dias, M. and Viegas, C. (2021) Fungal prevalence on waste industry: literature review. *Encyclopedia of mycology*, pp.99-106.

Diquattro, S., Garau, G., Mangia, N.P., Drigo, B., Lombi, E., Vasileiadis, S. and Castaldi, P. (2020) Mobility and potential bioavailability of antimony in contaminated soils: Short-term impact on microbial community and soil biochemical functioning. *Ecotoxicology and environmental safety*, *196*, p.110576.

Donatello, S., Fernández-Jiménez, A. and Palomo, A. (2012) Alkaline Activation as a Procedure for the Transformation of Fly Ash into New Materials Part II: An Assessment of Mercury Immobilization. *World of Coal Ash (WOCA) Conference* [Online], Denver, CO, USA, 9th-12th May 2011
Available at: https://uknowledge.uky.edu/cgi/viewcontent.cgi?article=2001&context=woca
[Accessed: 03/02/2024]

Du Laing, G., De Vos, R., Vandecasteele, B., Lesage, E., Tack, F.M. and Verloo, M.G. (2008) Effect of salinity on heavy metal mobility and availability in intertidal sediments of the Scheldt estuary. *Estuarine, Coastal and Shelf Science*, *77*(4), pp.589-602.

Echlin, P. (2011) *Handbook of sample preparation for scanning electron microscopy and X-ray microanalysis*. New York: Springer

Edwards, T. (2017) *Future of the Sea: Current and Future Impacts of Sea Level Rise on the UK* [Online]
Available at:
https://assets.publishing.service.gov.uk/government/uploads/system/uploads/attachment_data/file/663885/Future_of_the_sea_-_sea_level_rise.pdf
[Accessed: 01/09/2023]

Environment Agency (2024) *Shoreline Management Plans* [Online]
Available at: https://environment.data.gov.uk/shoreline-planning
[Accessed: 22/11/2024]

Environment Agency (2023a) *Historic Landfill Sites* [Online]
Available at: https://www.data.gov.uk/dataset/17edf94f-6de3-4034-b66b-004ebd0dd010/historic-landfill-sites#:~:text=An%20historic%20landfill%20is%20a,existed%20before%20landfills%20were%20regulated
[Accessed: 04/09/2023]

Environment Agency (2023b) *National Coastal Erosion Risk Mapping* [Online]
Available at:
https://environment.maps.arcgis.com/apps/webappviewer/index.html?id=9cef4a084bbb4954b970cd35b099d94c
[Accessed: 04/03/2024]

Environment Agency (2021) *Flood map for planning* [Online]
Available at: https://flood-map-for-planning.service.gov.uk/
[Accessed: 01/02/2024]

Environment Agency (2009) *Soil guideline values* [Online]
Available at: https://www.claire.co.uk/home/news/44-risk-assessment/178-soil-guideline-values?start=1
[Accessed: 04/02/2024]

Environmental Protection Act 1990 (United Kingdom) [Online]
Available at: https://www.legislation.gov.uk/ukpga/1990/43/contents
[Accessed: 04/09/2023]

EPA (2003a) *Ecological Soil Screening Level for Aluminum* [Online]
Available at: https://www.nexi.go.jp/environment/info/pdf/eia_17-042_02.pdf
[Accessed: 08/02/2024]

EPA (2003b) *Ecological Soil Screening Level for Iron* [Online]
Available at: https://rais.ornl.gov/documents/eco-ssl_iron.pdf
[Accessed: 08/02/2024]

EPA (2000a) *Beryllium Compounds* [Online]
Available at: https://www.epa.gov/sites/default/files/2016-09/documents/beryllium-compounds.pdf
[Accessed: 02/02/2024]

EPA (2000b) *Chromium Compounds* [Online]
Available at: https://www.epa.gov/sites/default/files/2016-09/documents/chromium-compounds.pdf
[Accessed: 02/02/2024]

Erdoğan, S.T., Garboczi, E.J. and Fowler, D.W. (2007). Shape and size of microfine aggregates: X-ray microcomputed tomography vs. laser diffraction. *Powder Technology*, *177*(2), pp.53-63.

ESDAT (2000) *Dutch Target and Intervention Values* [Online]
Available at:
https://support.esdat.net/Environmental%20Standards/dutch/annexs_i2000dutch%20environmental%20standards.pdf
[Accessed: 02/02/2024]

Fox-Kemper, B., H.T. Hewitt, C. Xiao, G. Aðalgeirsdóttir, S.S. Drijfhout, T.L. Edwards, N.R. Golledge, M. Hemer, R.E. Kopp, G. Krinner, A. Mix, D. Notz, S. Nowicki, I.S. Nurhati, L. Ruiz, J.-B. Sallée, A.B.A. Slangen, and Y, Yu. (2021) Ocean, Cryosphere and Sea Level Change. In: Masson-Delmotte, V., P. Zhai, A. Pirani, S.L. Connors, C. Péan, S. Berger, N. Caud, Y. Chen, L. Goldfarb, M.I. Gomis, M. Huang, K. Leitzell, E. Lonnoy, J.B.R. Matthews, T.K. Maycock, T. Waterfield, O. Yelekçi, R. Yu, and B. Zhou (eds.) *Climate Change 2021: The Physical Science Basis. Contribution of Working Group I to the Sixth Assessment Report of the Intergovernmental Panel on Climate Change*. Cambridge University Press, Cambridge, United Kingdom and New York, NY, USA, pp. 1211–1362

Farahat, R., Eissa, M., Megahed, G., Fathy, A., Abdel-Gawad, S. and El-Deab, M.S. (2019) Effect of EAF slag temperature and composition on its electrical conductivity. *ISIJ International*, *59*(2), pp.216-220.

Frazer, L. (2005) Metal attraction: an ironclad solution to arsenic contamination?.

Environmental Health Perspectives, 113(6).

Funatsuki, A., Takaoka, M., Oshita, K. and Takeda, N. (2012) Methods of determining lead speciation in fly ash by X-ray absorption fine-structure spectroscopy and a sequential extraction procedure. *Analytical Sciences*, *28*(5), pp.481-490.

Garrabrants, A.C., Sanchez, F. and Kosson, D.S. (2004) Changes in constituent equilibrium leaching and pore water characteristics of a Portland cement mortar as a result of carbonation. *Waste Management*, *24*(1), pp.19-36.

Gates, A., Jakubowski, J., and Regina, A. (2023) Nickel Toxicology. In: *StatPearls [Internet]* [online chapter]. Treasure Island (FL): StatPearls Publishing.
Available at: https://www.ncbi.nlm.nih.gov/books/NBK592400/
[Accessed: 03/03/2024]

Gehle, K. (2011) *Beryllium Toxicity* [Online]
Available at: https://www.atsdr.cdc.gov/csem/beryllium/cover-page.html#acknowledgments
[Accessed: 02/02/2024]

Genchi, G., Carocci, A., Lauria, G., Sinicropi, M.S. and Catalano, A. (2020) Nickel: Human health and environmental toxicology. *International journal of environmental research and public health*, *17*(3), p.679.

Ghisman, V., Muresan, A.C., Buruiana, D.L. and Axente, E.R. (2022) Waste slag benefits for correction of soil acidity. *Scientific Reports*, *12*(1), p.16042.

Gitari, W.M., Thobakgale, R. and Akinyemi, S.A. (2018) Mobility and attenuation dynamics of potentially toxic chemical species at an abandoned copper mine tailings dump. *Minerals*, *8*(2), p.64.

Goldstein, J.I., Newbury, D.E., Michael, J.R., Ritchie, N.W., Scott, J.H.J. and Joy, D.C. (2017). *Scanning electron microscopy and X-ray microanalysis*. 4th ed. New York: Springer.

Gomes, H.I., Mayes, W.M., Rogerson, M., Stewart, D.I. and Burke, I.T. (2016) Alkaline residues

and the environment: a review of impacts, management practices and opportunities. *Journal of Cleaner Production*, *112*, pp.3571-3582.

Goulding, K., Murrell, T.S., Mikkelsen, R.L., Rosolem, C., Johnston, J., Wang, H. and Alfaro, M.A. (2021) Outputs: potassium losses from agricultural systems. *Improving potassium recommendations for agricultural crops*, *75*.

Guagliardi, I. (2022) Editorial for the special issue "potentially toxic elements pollution in urban and suburban environments". *Toxics*, *10*(12), p.775.

Gupta, R. (2019) Solid waste management: an action plan of the Rajasthan government. *International Journal of Humanities and Social Science Invention, 8*(1), pp.100-103

Gupta, M. and Gupta, S. (2017) An overview of selenium uptake, metabolism, and toxicity in plants. *Frontiers in plant science*, *7*, p.234638.

Gustafsson, S. (2011) Corrosion properties of aluminium alloys and surface treated alloys in tap water [online], Independent thesis Advanced level, Uppsala University.
Available at: https://www.diva-portal.org/smash/record.jsf?pid=diva2%3A436113&dswid=-8540
[Accessed: 20/11/2023]

Hao, L., Zheng, F., Chen, X., Li, J., Wang, S. and Fan, Y. (2020) Erosion corrosion behavior of aluminum in flowing deionized water at various temperatures. *Materials*, *13*(3), p.779.

Hartuti, S., Kambara, S., Takeyama, A., Hanum, F.F. and Desfitri, E.R. (2018) Chemical Stabilization of Coal Fly Ash for Simultaneous Suppressing of As, B, and Se Leaching. *Coal Fly Ash Beneficiation: Treatment of Acid Mine Drainage with Coal Fly Ash*, p.29.

Hassan, M.U., Chattha, M.U., Khan, I., Chattha, M.B., Aamer, M., Nawaz, M., Ali, A., Khan, M.A.U. and Khan, T.A. (2019) Nickel toxicity in plants: reasons, toxic effects, tolerance mechanisms, and remediation possibilities—a review. *Environmental Science and Pollution Research*, *26*, pp.12673-12688.

Health Canada (2020) *Draft screening assessment - Thallium and its compounds* [Online] Available at: https://www.canada.ca/en/environment-climate-change/services/evaluating-existing-substances/draft-screening-assessment-thallium-compounds.html [Accessed: 02/02/2024]

Hobson, A.J., Stewart, D.I., Mortimer, R.J., Mayes, W.M., Rogerson, M. and Burke, I.T. (2018) Leaching behaviour of co-disposed steel making wastes: Effects of aeration on leachate chemistry and vanadium mobilisation. *Waste Management*, *81*, pp.1-10.

Hodorowicz, M., Szklarzewicz, J. and Jurowska, A. (2022) The Role of Prussian Blue-Thallium and Potassium Similarities and Differences in Crystal Structures of Selected Cyanido Complexes of W, Fe and Mo. *Materials*, *15*(13), p.4586.

Hong, J., Chen, Y., Wang, M., Ye, L., Qi, C., Yuan, H., Zheng, T. and Li, X. (2017) Intensification of municipal solid waste disposal in China. *Renewable and sustainable energy reviews*, *69*, pp.168-176.

Huggins, F.E., Rezaee, M., Honaker, R.Q. and Hower, J.C. (2016) On the removal of hexavalent chromium from a Class F fly ash. *Waste management*, *51*, pp.105-110.

Huggins, F.E. (2011) *Estimating Cr(VI) in Coal-Derived Fly-Ash* [Online] Available at: https://www-ssrl.slac.stanford.edu/content/sites/default/files/documents/science-highlights/pdf/cr_vi_inflyash-201106.pdf [Accessed: 04/02/2024]

Hughes, P. and Seely, A. (1996) *Landfill Research Paper* (96/103) [Online] Available at: https://researchbriefings.files.parliament.uk/documents/RP96-103/RP96-103.pdf [Accessed: 04/09/2023]

Huliselan, E.K., Bijaksana, S., Srigutomo, W. and Kardena, E. (2010) Scanning electron microscopy and magnetic characterization of iron oxides in solid waste landfill leachate. *Journal of Hazardous Materials*, *179*(1-3), pp.701-708.

Humbal, C., Gautam, S. and Trivedi, U. (2018) A review on recent progress in observations, and health effects of bioaerosols. *Environment International*, *118*, pp.189-193.

Hunter, H.A., Ling, F.T. and Peters, C.A. (2020) Coprecipitation of heavy metals in calcium carbonate from coal fly ash leachate. *Acs Es&T Water*, *1*(2), pp.339-345.

IARC (2012) *CHROMIUM (VI) COMPOUNDS* [Online]
Available at: https://www.ncbi.nlm.nih.gov/books/NBK304377/#rl6
[Accessed: 05/02/2024]

Igbokwe, I.O., Igwenagu, E. and Igbokwe, N.A. (2019) Aluminium toxicosis: a review of toxic actions and effects. *Interdisciplinary toxicology*, *12*(2), p.45.

Irfan, M., Houdayer, B., Shah, H., Koj, A. and Thomas, H. (2019) GIS-based investigation of historic landfill sites in the coastal zones of Wales (UK). *Euro-Mediterranean Journal for Environmental Integration*, *4*, pp.1-10.

Iyaka, Y.A. (2011) Nickel in soils: A review of its distribution and impacts. *Scientific Research and Essays*, *6*(33), pp.6774-6777.

Izquierdo, M. and Querol, X. (2012) Leaching behaviour of elements from coal combustion fly ash: An overview. *International Journal of Coal Geology*, *94*, pp.54-66.

Jabasingh, S.A., Lalith, D. and Garre, P. (2015) Sorption of chromium (VI) from electroplating effluent onto chitin immobilized Mucor racemosus sorbent (CIMRS) impregnated in rotating disk contactor blades. *Journal of Industrial and Engineering Chemistry*, *23*, pp.79-92.

Jalali, M. and Jalali, M. (2022) Investigation of Potassium Leaching Risk with Relation to Different Extractants in Calcareous Soils. *Journal of Soil Science and Plant Nutrition*, pp.1-15.

Jewett, E., Arnott, G., Connolly, L., Vasudevan, N. and Kevei, E. (2022) Microplastics and their impact on reproduction—can we learn from the C. elegans model?. *Frontiers in toxicology*, *4*, p.748912.

Ji, R., Liu, T.J., Kang, L.L., Wang, Y.T., Li, J.G., Wang, F.P., Yu, Q., Wang, X.M., Liu, H., Guo, H.W. and Xu, W.L. (2022) A review of metallurgical slag for efficient wastewater treatment: pretreatment, performance and mechanism. *Journal of Cleaner Production*, *380*, p.135076.

Jones, E.M. and Tansey, E.M. (2015) 'The Development of Waste Management in the UK c.1960–c.2000' (eds.) In: *Wellcome Witnesses to Contemporary Medicine* (56) London: Queen Mary University of London.

Jonsson, H.H. and Vonnegut, B. (1991) Apparatus for measurements of the electrical conductivity of rainwater with high resolution in space and time. *Journal of Applied Meteorology and Climatology*, *30*(8), pp.1220-1227.

Kaiser, D. (2018) *Potassium for crop production* [Online]
Available at: https://extension.umn.edu/phosphorus-and-potassium/potassium-crop-production
[Accessed: 02/02/2024]

Kang, D., Son, J., Yoo, Y., Park, S., Huh, I.S. and Park, J. (2020) Heavy-metal reduction and solidification in municipal solid waste incineration (MSWI) fly ash using water, NaOH, KOH, and NH4OH in combination with CO2 uptake procedure. *Chemical Engineering Journal*, *380*, p.122534.

Karato, S.I. and Wang, D. (2013) Electrical conductivity of minerals and rocks. *Physics and chemistry of the deep Earth*, pp.145-182.

Karbowska, B. (2016) Presence of thallium in the environment: sources of contaminations, distribution and monitoring methods. *Environmental monitoring and assessment*, *188*, pp.1-19.

Kassamba-Diaby, M.L., Galy-Lacaux, C., Yoboué, V., Hickman, J.E., Jaars, K., Gnamien, S., Konan, R., Gardrat, E. and Silué, S. (2022) The chemical characteristics of rainwater and wet atmospheric deposition fluxes at two urban sites and one rural site in Côte d'Ivoire. *EGUsphere*, *2022*, pp.1-52.

Katz, L.E., Criscenti, L.J., Chen, C.C., Larentzos, J.P. and Liljestrand, H.M. (2013) Temperature effects on alkaline earth metal ions adsorption on gibbsite: Approaches from macroscopic sorption experiments and molecular dynamics simulations. *Journal of colloid and interface science*, *399*, pp.68-76.

Kaur, H. and Garg, N. (2021) Zinc toxicity in plants: a review. *Planta*, *253*(6), p.129.

Khan, A.M., Bakar, N.K.A., Bakar, A.F.A. and Ashraf, M.A. (2017) Chemical speciation and bioavailability of rare earth elements (REEs) in the ecosystem: a review. *Environmental Science and Pollution Research, 24*(29), pp.22764-22789.

Kim, J.G. and Dixon, J.B. (2002) Oxidation and fate of chromium in soils. *Soil Science and Plant Nutrition*, *48*(4), pp.483-490.

Komonweeraket, K., Cetin, B., Aydilek, A.H., Benson, C.H. and Edil, T.B. (2015) Effects of pH on the leaching mechanisms of elements from fly ash mixed soils. *Fuel*, *140*, pp.788-802.

Król, A., Mizerna, K. and Bożym, M. (2020) An assessment of pH-dependent release and mobility of heavy metals from metallurgical slag. *Journal of hazardous materials*, *384*, p.121502.

Kryzevicius, Z., Janusiene, L., Karcauskiene, D., Slepetiene, A., Vilkiene, M. and Zukauskaite, A. (2019) Aluminium leaching response to acid precipitation in a lime-affected soil. *Žemdirbystė*, *106*(4), pp.315-320.

Lamble, K.J. and Hill, S.J. (1998). Microwave digestion procedures for environmental matrices. Critical Review. *Analyst*, *123*(7), pp.103-133.

Lee, K., Prezzi, M. and Kim, N. (2007). Subgrade design parameters from samples prepared with different compaction methods. *Journal of Transportation Engineering, 133*(2), pp.82-89.

Lenntech (no date) *Lead (Pb) and water* [Online]
Available at: https://www.lenntech.com/periodic/water/lead/lead-and-water.htm

[Accessed: 26/02/2024]

Leslie, S.A. and Mitchell, J.C. (2007). Removing gold coating from SEM samples. *Palaeontology, 50*(6), pp.1459-1461.

Lévesque, Y., Walter, J., Chesnaux, R., Dugas, S. and Noel, D. (2023) Electrical resistivity of saturated and unsaturated sediments in northeastern Canada. *Environmental Earth Sciences*, *82*(12), p.303.

Lin, L., Yang, H. and Xu, X. (2022) Effects of water pollution on human health and disease heterogeneity: a review. *Frontiers in environmental science*, *10*, p.880246.

Linh, H.N., Tamura, H., Komiya, T., Saffarzadeh, A. and Shimaoka, T. (2020) Simulating the impact of heavy rain on leaching behavior of municipal solid waste incineration bottom ash (MSWI BA) in semi-aerobic landfill. *Waste Management*, *113*, pp.280-293.

Little, M.R., Adell, V., Boccaccini, A.R. and Cheeseman, C.R. (2008). Production of novel ceramic materials from coal fly ash and metal finishing wastes. *Resources, Conservation and Recycling*, *52*(11), pp.1329-1335.

Liu, Y., Zhou, Q., Wang, Y., Cheng, S. and Hao, W. (2021) Deriving soil quality criteria of chromium based on species sensitivity distribution methodology. *Toxics*, *9*(3), p.58.

Liu, J., Yin, M., Luo, X., Xiao, T., Wu, Z., Li, N., Wang, J., Zhang, W., Lippold, H., Belshaw, N.S. and Feng, Y. (2019) The mobility of thallium in sediments and source apportionment by lead isotopes. *Chemosphere*, *219*, pp.864-874.

Liu, R., Xu, W., He, Z., Lan, H., Liu, H., Qu, J. and Prasai, T. (2015) Adsorption of antimony (V) onto Mn (II)-enriched surfaces of manganese-oxide and FeMn binary oxide. *Chemosphere*, *138*, pp.616-624.

Liu, X. and Millero, F.J. (2002) The solubility of iron in seawater. *Marine Chemistry*, *77*(1), pp.43-54.

Wagner, T.P. and Raymond, T. (2015) Landfill mining: Case study of a successful metals recovery project. *Waste Management*, *45*, pp.448-457.

Liu, R., Xu, W., He, Z., Lan, H., Liu, H., Qu, J. and Prasai, T. (2015) Adsorption of antimony (V) onto Mn (II)-enriched surfaces of manganese-oxide and FeMn binary oxide. *Chemosphere*, *138*, pp.616-624.

Liu, Q., Li, H. and Zhou, L. (2008) Galvanic interactions between metal sulfide minerals in a flowing system: Implications for mines environmental restoration. *Applied geochemistry, 23*(8), pp.2316-2323.

Louis, G.E. (2004) A historical context of municipal solid waste management in the United States. *Waste management & research*, *22*(4), pp.306-322.

Lu, J.H., Gu, Z.Q., Qian, W.F., Zhang, H.Y., Huang, C.X., Li, Y.J., He, P. and HUANG, B. (2007). Determination of heavy metals in soils by digestion of reverse aqua regia. *Bull Mineral Petrol Geochem*, *26*, pp.70-73.

Lum, T.S. and Leung, K.S.Y. (2016) Strategies to overcome spectral interference in ICP-MS detection. *Journal of Analytical Atomic Spectrometry, 31*(5), pp.1078-1088.

Lynch, S.F.L. (2015). *Establishing the environmental risk of metal contaminated river bank sediment*. Doctoral dissertation, University of Birmingham.

Lynch, S.F., Batty, L.C. and Byrne, P. (2014) Environmental risk of metal mining contaminated river bank sediment at redox-transitional zones. *Minerals*, *4*(1), pp.52-73.

Ma, A., Zheng, X., Li, S., Wang, Y. and Zhu, S. (2018) Zinc recovery from metallurgical slag and dust by coordination leaching in NH3–CH3COONH4–H2O system. *Royal Society open science*, *5*(7), p.180660.

Magnano, G.C., Marussi, G., Pavoni, E., Adami, G., Filon, F.L. and Crosera, M. (2022) Percutaneous metals absorption following exposure to road dust powder. *Environmental Pollution*, *292*, p.118353.

Mahedi, M., Cetin, B. and Dayioglu, A.Y. (2019) Leaching behavior of aluminum, copper, iron and zinc from cement activated fly ash and slag stabilized soils. *Waste Management*, *95*, pp.334-355.

Makowska, D., Strugała, A., Wierońska, F. and Bacior, M. (2019) Assessment of the content, occurrence, and leachability of arsenic, lead, and thallium in wastes from coal cleaning processes. *Environmental Science and Pollution Research*, *26*, pp.8418-8428.

Mazur, R., Sadowska, M., Kowalewska, Ł., Abratowska, A., Kalaji, H.M., Mostowska, A., Garstka, M. and Krasnodębska-Ostręga, B. (2016) Overlapping toxic effect of long term thallium exposure on white mustard (Sinapis alba L.) photosynthetic activity. *BMC Plant Biology*, *16*, pp.1-17.

Mavakala, B.K., Le Faucheur, S., Mulaji, C.K., Laffite, A., Devarajan, N., Biey, E.M., Giuliani, G., Otamonga, J.P., Kabatusuila, P., Mpiana, P.T. and Poté, J. (2016) Leachates draining from controlled municipal solid waste landfill: detailed geochemical characterization and toxicity tests. *Waste management*, *55*, pp.238-248.

Mehdi, Y., Hornick, J.L., Istasse, L. and Dufrasne, I. (2013) Selenium in the environment, metabolism and involvement in body functions. *Molecules*, *18*(3), pp.3292-3311.

Mengel, K., Kirkby, E.A., Kosegarten, H. and Appel, T. (2001) Soil copper. In: *Principles of plant nutrition* (pp. 599-611). Dordrecht: Springer Netherlands.

Merck (no date) *Solubility Table of Compounds in Water at Temperature* [Online]
Available at: https://www.sigmaaldrich.com/GB/en/support/calculators-and-apps/solubility-table-compounds-water-temperature
[Accessed: 04/02/2024]

Met Office (2023) *UKCP18 Factsheet: Sea-level rise and storm surge - supplementary data* [Online]
Available at:
https://www.metoffice.gov.uk/binaries/content/assets/metofficegovuk/pdf/research/ukcp/u

kcp18_factsheet_sea_level_rise_storm_surge_supp_data_mar23.pdf
[Accessed: 04/09/2023]

Met Office (2022) *UK Climate Projections: Headline Findings* [Online]
Available at:
https://www.metoffice.gov.uk/binaries/content/assets/metofficegovuk/pdf/research/ukcp/ukcp18_headline_findings_v4_aug22.pdf
[Accessed: 04/09/2023]

Morrissey, J. and Guerinot, M.L. (2009) Iron uptake and transport in plants: the good, the bad, and the ionome. *Chemical reviews*, *109*(10), pp.4553-4567.

Muzaffar, S., Khan, J., Srivastava, R., Gorbatyuk, M.S. and Athar, M. (2023) Mechanistic understanding of the toxic effects of arsenic and warfare arsenicals on human health and environment. *Cell Biology and Toxicology*, *39*(1), pp.85-110.

Myron L Company (no date) *Deionized water* [Online]
Available at: https://www.myronl.com/product-applications/deionized-water/
[Accessed: 04/02/2024]

Nail, A.N., Cardoso, A.P.F., Montero, L.K. and States, J.C. (2023) miRNAs and arsenic-induced carcinogenesis. *Advances in Pharmacology*, *96*, pp.203-240.

NASA (2021) *Sea Level Projection Tool* [Online]
Available at: https://sealevel.nasa.gov/ipcc-ar6-sea-level-projection-tool
[Accessed: 03/10/2024]

NASA (no date) *Forms of corrosion* [Online]
Available at: https://public.ksc.nasa.gov/corrosion/forms-of-corrosion/
[Accessed: 04/02/2024]

National Institute of Health (2021) *Potassium* [Online]
Available at: https://ods.od.nih.gov/factsheets/Potassium-Consumer/
[Accessed: 29/12/2023]

Natural Resources Wales (2023) *Flood and Coastal Erosion Risk Maps* [Online]
Available at: https://flood-risk-maps.naturalresources.wales/?locale=en
[Accessed: 15/10/2023]

Neal, C., Reynolds, B., Neal, M., Pugh, B., Hill, L. and Wickham, H. (2001). Long-term changes in the water quality of rainfall, cloud water and stream water for moorland, forested and clear-felled catchments at Plynlimon, mid-Wales. *Hydrology and Earth System Sciences*, *5*(3), pp.459-476.

New Jersey Department of Health and Senior Services (2007) *Hazardous substance fact sheet: Zinc Oxide* [Online]
Available at: https://nj.gov/health/eoh/rtkweb/documents/fs/2037.pdf
[Accessed: 02/02/2024]

Ngatia, L.W., De Oliveira, L.M., Betiku, O.C., Fu, R., Moriasi, D.N., Steiner, J.L., Verser, J.A. and Taylor, R.W. (2021) Relationship of arsenic and chromium availability with carbon functional groups, aluminum and iron in Little Washita River Experimental Watershed Reservoirs, Oklahoma, USA. *Ecotoxicology and Environmental Safety*, *207*, p.111468.

Nicholls, R.J., Beaven, R.P., Stringfellow, A., Monfort, D., Le Cozannet, G., Wahl, T., Gebert, J., Wadey, M., Arns, A., Spencer, K.L. and Reinhart, D. (2021) Coastal landfills and rising sea levels: A challenge for the 21st century. *Frontiers in Marine Science*, *8*, p.710342.

Nieder, R. and Benbi, D.K. (2023) Potentially toxic elements in the environment–a review of sources, sinks, pathways and mitigation measures. *Reviews on Environmental Health*. DOI: https://doi.org/10.1515/reveh-2022-0161
[Accessed: 02/02/2024]

Njoku, P.O., Edokpayi, J.N. and Odiyo, J.O. (2019) Health and environmental risks of residents living close to a landfill: A case study of Thohoyandou Landfill, Limpopo Province, South Africa. *International journal of environmental research and public health*, *16*(12), p.2125.

Njue, C.N., Cundy, A.B., Smith, M., Green, I.D. and Tomlinson, N. (2012) Assessing the impact of historical coastal landfill sites on sensitive ecosystems: a case study from Dorset, Southern England. *Estuarine, Coastal and Shelf Science*, *114*, pp.166-174.

Nriagu, J.O., Bhattacharya, P., Mukherjee, A.B., Bundschuh, J., Zevenhoven, R. and Loeppert, R.H. (2007) Arsenic in soil and groundwater: an overview. *Trace Metals and other Contaminants in the Environment*, *9*, pp.3-60.

O'Connor, T.P. (2004) The sediment quality guideline, ERL, is not a chemical concentration at the threshold of sediment toxicity. *Marine Pollution Bulletin*, *49*(5-6), pp.383-385.

Oppenheimer, M., B.C. Glavovic , J. Hinkel, R. van de Wal, A.K. Magnan, A. Abd-Elgawad, R. Cai, M. Cifuentes-Jara, R.M. DeConto, T. Ghosh, J. Hay, F. Isla, B. Marzeion, B. Meyssignac, and Z. Sebesvari, (2019) Sea Level Rise and Implications for Low-Lying Islands, Coasts and Communities. In: *IPCC Special Report on the Ocean and Cryosphere in a Changing Climate.* H.-O. Pörtner, D.C. Roberts, V. Masson-Delmotte, P. Zhai, M. Tignor, E. Poloczanska, K. Mintenbeck, A. Alegría, M. Nicolai, A. Okem, J. Petzold, B. Rama, N.M. Weyer (eds.). Cambridge University Press, Cambridge

OriginLab (2012) *OriginPro 9* [computer software]
Available at: https://www.originlab.com/
[Accessed: 13/08/2022]

Östürk, Ö. and Sevimoğlu, O. (2021) Trace elements microanalysis of metal oxides in deposit formed on combustion chamber surface of landfill gas engine using focused ion beam/scanning electron microscopy technique. *Engineering Failure Analysis*, *123*, p.105297.

Pahlevaninezhad, M., Pahlevani, M. and Roberts, E.P. (2022) Effects of aluminum, iron, and manganese sulfate impurities on the vanadium redox flow battery. *Journal of Power Sources*, *529*, p.231271.

Pan, D.A., Li, L., Tian, X., Wu, Y., Cheng, N. and Yu, H. (2019) A review on lead slag generation, characteristics, and utilization. *Resources, Conservation and Recycling*, *146*, pp.140-155.

Papp, C.S. and Fischer, L.B. (1987). Application of microwave digestion to the analysis of peat. *Analyst*, *112*(3), pp.337-338.

Park, J.E., Shin, J.H., Oh, W., Choi, S.J., Kim, J., Kim, C. and Jeon, J. (2022) Removal of hexavalent chromium (VI) from wastewater using chitosan-coated iron oxide nanocomposite membranes. *Toxics*, *10*(2), p.98.

Patočka, J. and Černý, K. (2003) Inorganic lead toxicology. *Acta Medica (Hradec Kralove)*, *46*(2), pp.65-72.

Peel, H.R., Balogun, F.O., Bowers, C.A., Miller, C.T., Obeidy, C.S., Polizzotto, M.L., Tashnia, S.U., Vinson, D.S. and Duckworth, O.W. (2022) Towards understanding factors affecting arsenic, chromium, and vanadium mobility in the subsurface. *Water*, *14*(22), p.3687.

Piatak, N.M., Seal, R.R., Hoppe, D.A., Green, C.J. and Buszka, P.M. (2019) Geochemical characterization of iron and steel slag and its potential to remove phosphate and neutralize acid. *Minerals*, *9*(8), p.468.

Pina, A.A., Villaseñor, G.T., Fernández, M.M., Kudra, A.L. and Ramos, R.L. (2000) Scanning electron microscope and statistical analysis of suspended heavy metal particles in San Luis Potosi, Mexico. *Atmospheric environment*, *34*(24), pp.4103-4112.

Plum, L.M., Rink, L. and Haase, H. (2010) The essential toxin: impact of zinc on human health. *International journal of environmental research and public health*, *7*(4), pp.1342-1365.

Podlasek, A., Vaverková, M.D., Jakimiuk, A. and Koda, E. (2024) Potentially toxic elements (PTEs) and ecological risk at waste disposal sites: An analysis of sanitary landfills. *Plos one*, *19*(5), p.e0303272.

Prata, J.C., da Costa, J.P., Lopes, I., Andrady, A.L., Duarte, A.C. and Rocha-Santos, T. (2021) A One Health perspective of the impacts of microplastics on animal, human and environmental health. *Science of the Total Environment*, *777*, p.146094.

Prichard, L. and Barwick, V. (2003) *Preparation of Calibration Curves A Guide to Best Practice* [Online]
Available at: https://biosearch-cdn.azureedge.net/assetsv6/Calibration-curve-guide.pdf
[Accessed: 04/01/2022].

Propp, V.R., De Silva, A.O., Spencer, C., Brown, S.J., Catingan, S.D., Smith, J.E. and Roy, J.W. (2021) Organic contaminants of emerging concern in leachate of historic municipal landfills. *Environmental Pollution*, 276, p.116474.

Public Health England (2015) *Manganese Incident Management* [Online]
Available at:
https://assets.publishing.service.gov.uk/media/5a7f7a6de5274a2e87db618b/Manganese_incident_management.pdf
[Accessed: 02/02/2024]

Puhakka, E., Li, X., Ikonen, J. and Siitari-Kauppi, M. (2019) Sorption of selenium species onto phlogopite and calcite surfaces: DFT studies. *Journal of contaminant hydrology*, *227*, p.103553.

Rahimzadeh, M.R., Rahimzadeh, M.R., Kazemi, S., Amiri, R.J., Pirzadeh, M. and Moghadamnia, A.A. (2022) Aluminum poisoning with emphasis on its mechanism and treatment of intoxication. *Emergency medicine international*, *2022*.

Rai, D., Sass, B.M. and Moore, D.A. (1987) Chromium (III) hydrolysis constants and solubility of chromium (III) hydroxide. *Inorganic chemistry*, *26*(3), pp.345-349.

Rajmohan, K.V.S., Ramya, C., Viswanathan, M.R. and Varjani, S. (2019) Plastic pollutants: effective waste management for pollution control and abatement. *Current Opinion in Environmental Science & Health*, *12*, pp.72-84.

Ravipati, E.S., Mahajan, N.N., Sharma, S., Hatware, K.V. and Patil, K. (2021) The toxicological effects of lead and its analytical trends: an update from 2000 to 2018. *Critical reviews in analytical chemistry*, *51*(1), pp.87-102.

Reed, S.T. and Martens, D.C. (1996) Copper and zinc. *Methods of Soil Analysis: Part 3 Chemical Methods*, *5*, pp.703-722.

Riley, A.L., Cameron, J., Burke, I.T., Onnis, P., MacDonald, J.M., Gandy, C.J., Crane, R.A., Byrne, P., Comber, S., Jarvis, A.P. and Hudson-Edwards, K.A. (2024) Environmental behaviour of iron and steel slags in coastal settings. *Environmental Science and Pollution Research*, pp.1-17.

Riley, A.L., Amezaga, J., Burke, I.T., Byrne, P., Cooper, N., Crane, R.A., Comber, S.D., Gandy, C.J., Hudson-Edwards, K.A., Jennings, E. and Lewis, E. (2022) Incorporating conceptual site models into national-scale environmental risk assessments for legacy waste in the coastal zone. *Frontiers in Environmental Science*, p.2141.

Riley, A.L., Onnis, P., Jennings, E., Crane, R.A., Hudson-Edwards, K.A., Comber, S.D., Burke, I.T., Byrne, P., Gandy, C.J., Jarvis, A.P. and Mayes, W.M. (2021) A GIS-based prioritisation of coastal legacy mine spoil deposits in England and Wales for effective future management. In *Newport, Wales: International Mine Water Association Conference*.

Riley, A.L., MacDonald, J.M., Burke, I.T., Renforth, P., Jarvis, A.P., Hudson-Edwards, K.A., McKie, J. and Mayes, W.M. (2020) Legacy iron and steel wastes in the UK: Extent, resource potential, and management futures. *Journal of Geochemical Exploration*, *219*, p.106630.

Robbins, K., Bernard, B., Brooks, B. and Frost, N. (2023) *Investigating the impact of landfill sites at the coast on Marine Protected Area features in Wales* [Online] Available at: https://cdn.cyfoethnaturiol.cymru/media/696908/nrw-evidence-report-673-investigating-the-impact-of-landfill-sites-at-the-coast-on-marine-protected-area-features-in-wales.pdf [Accessed: 04/09/2023]

Romera-Castillo, C., Lucas, A., Mallenco-Fornies, R., Briones-Rizo, M., Calvo, E. and Pelejero, C. (2023) Abiotic plastic leaching contributes to ocean acidification. *Science of The Total Environment*, *854*, p.158683.

Roy, W.R. and Berger, P.M. (2011) Geochemical controls of coal fly ash leachate pH. *Coal*

Combustion and Gasification Products, *3*(4), pp.63-66.

Royer, A. and Sharman, T. (2023) *Copper Toxicity* [Online]
Available at: https://www.ncbi.nlm.nih.gov/books/NBK557456/
[Accessed: 02/02/2024]

Saddique, A. and Peterson, C.D. (1983) Thalium poisoning: A review. *Veterinary and Human Toxicology*, *25*(1), pp.16-22.

Sankar, A.R. and Das, S. (2013) Experimental analysis of galvanic corrosion of a thin metal film in a multilayer stack for MEMS application. *Materials Science in Semiconductor Processing*, *16*(2), pp.449-453.

Sanusi, A., Wortham, H., Millet, M. and Mirabel, P. (1996) Chemical composition of rainwater in eastern France. *Atmospheric environment*, *30*(1), pp.59-71.

Sauvé, S., McBride, M.B. and Hendershot, W.H. (1997) Speciation of lead in contaminated soils. *Environmental Pollution*, *98*(2), pp.149-155.

Sayadi, M.H., Rezaei, M.R. and Rezaei, A. (2015) Sediment toxicity and ecological risk of trace metals from streams surrounding a municipal solid waste landfill. *Bulletin of environmental contamination and toxicology*, *94*, pp.559-563.

Schlieker, M., Schüring, J., Hencke, J. and Schulz, H.D. (2001) The influence of redox processes on trace element mobility in a sandy aquifer—an experimental approach. *Journal of Geochemical Exploration*, *73*(3), pp.167-179.

Schulte, E.E. and Kelling, K.A. (2004) *Soil and Applied Manganese* [Online]
Available at: http://corn.agronomy.wisc.edu/Management/pdfs/a2526.pdf
[Accessed: 28/12/2023]

Ścibior, A., Wnuk, E. and Gołębiowska, D. (2021) Wild animals in studies on vanadium bioaccumulation-Potential animal models of environmental vanadium contamination: A comprehensive overview with a Polish accent. *Science of the Total Environment*, *785*,

p.147205.

Selwyn, L. (2021) *Understanding galvanic corrosion* [Online]
Available at: https://www.canada.ca/en/conservation-institute/services/training-learning/in-person-workshops/galvanic-corrosion.html
[Accessed: 03/02/2024]

Semwal, A.D., Padmashree, A., Khan, M.A., Sharma, G.K. and Bawa, A.S. (2006) Leaching of aluminium from utensils during cooking of food. *Journal of the Science of Food and Agriculture*, *86*(14), pp.2425-2430.

Setiawati, T.C. and Mutmainnah, L. (2016) Solubilization of potassium containing mineral by microorganisms from sugarcane rhizosphere. *Agriculture and Agricultural Science Procedia*, *9*, pp.108-117.

Shaver, T. (2014) Nutrient Management for Agronomic Crops in Nebraska. Lincoln, Nebraska: The University of Nebraska Press

Siaka, M., Owens, C.M. and Birch, G.F. (1998). Evaluation of some digestion methods for the determination of heavy metals in sediment samples by flame-AAS. *Analytical letters*, *31*(4), pp.703-718.

Sidana, N., Kaur, H. and Devi, P. (2020) Organic linkers for colorimetric detection of inorganic water pollutants. In: *Inorganic Pollutants in Water.* Elsevier, Amsterdam, pp. 135-152.

Siddiqua, A., Hahladakis, J.N. and Al-Attiya, W.A.K. (2022) An overview of the environmental pollution and health effects associated with waste landfilling and open dumping. *Environmental Science and Pollution Research*, *29*(39), pp.58514-58536.

Siddique, R., Kaur, G. and Rajor, A. (2010) Waste foundry sand and its leachate characteristics. *Resources, Conservation and Recycling*, *54*(12), pp.1027-1036.

Silva, L.F., Izquierdo, M., Querol, X., Finkelman, R.B., Oliveira, M.L., Wollenschlager, M., Towler, M., Pérez-López, R. and Macias, F. (2011) Leaching of potential hazardous elements

of coal cleaning rejects. *Environmental monitoring and assessment*, *175*, pp.109-126.

Singh, G., Gupta, S.K., Kumar, R. and Sunderarajan, M. (2007) Dispersion modeling of leachates from thermal power plants. *Journal of Environmental Engineering*, *133*(12), pp.1088-1097.

Smith, L., Hunt, A., Capstick, M., Hughes, T. and Buchman, A. (2021) *A UK-WIDE SOLUTION FOR THE RECOVERY OF ZINC FROM ELECTRIC STEELMAKING WASTE* [Online] Available at: https://www.mpiuk.com/downloads/industry-papers/EESC21-Paper-01-A-UK-wide-solution-for-the-recovery-of-zinc-from-electric-steelmaking-waste.pdf [Accessed: 02/02/2024]

Smrzka, D., Zwicker, J., Bach, W., Feng, D., Himmler, T., Chen, D. and Peckmann, J. (2019) The behavior of trace elements in seawater, sedimentary pore water, and their incorporation into carbonate minerals: a review. *Facies*, *65*, pp.1-47.

Sparks, D.L. (2001) Dynamics of K in soils and their role in management of K nutrition. *International Potash Institute PR II K in nutrient management for sustainable crop production in India, New Delhi, India*, *305*, pp.79-101.

Spex Certiprep (2023). Inorganic Standards/ICP-MS/Multi-Element [Online] Available at: https://www.spex.com/Product/Detail/Multi-Element/500791dc-5bf4-4324-9a87-9f64f4eff621/ICP-MS-Multi-Element-Solution-2-with-Mercury%2c-10-%C2%B5 [Accessed: 14/08/2023]

Srivastava, P., Bolan, N., Casagrande, V., Benjamin, J., Adejumo, S.A. and Sabir, M. (2022) Cobalt in soils: sources, fate, bioavailability, plant uptake, remediation, and management. In: *Appraisal of Metal (loids) in the Ecosystem* (pp. 81-104). Amsterdam: Elsevier.

Stahnke, C.A. and Poor, C.J. (2017) Implications of using different water sources when hydrologically compacting bioretention columns. *Water Environment Research*, *89*(5), pp.451-455.

Stearney, ER., Jakubowski, JA. and Regina, AC. (2023) *Beryllium Toxicity* [Online]

Available at: https://www.ncbi.nlm.nih.gov/books/NBK585042/
[Accessed: 02/02/2024]

Struis, R.P., Ludwig, C., Lutz, H. and Scheidegger, A.M. (2004) Speciation of zinc in municipal solid waste incineration fly ash after heat treatment: an X-ray absorption spectroscopy study. *Environmental science & technology*, *38*(13), pp.3760-3767.

Sun, H.J., Rathinasabapathi, B., Wu, B., Luo, J., Pu, L.P. and Ma, L.Q. (2014) Arsenic and selenium toxicity and their interactive effects in humans. *Environment international*, *69*, pp.148-158.

Sundar, S. and Chakravarty, J. (2010) Antimony toxicity. *International journal of environmental research and public health*, *7*(12), pp.4267-4277.

Takahashi, F. and Shimaoka, T. (2012) The weathering of municipal solid waste incineration bottom ash evaluated by some weathering indices for natural rock. *Waste management*, *32*(12), pp.2294-2305.

Tang, H., Meng, G., Xiang, J. and Liu, Y. (2022) Toxic effects of antimony in plants: Reasons and remediation possibilities—A review and future prospects. *Frontiers in Plant Science*, *13*, p.1011945.

Tanveer, M. and Wang, L. (2019) Potential targets to reduce beryllium toxicity in plants: A review. *Plant physiology and biochemistry*, *139*, pp.691-696.

Tarpada, S.P., Loloi, J. and Schwechter, E.M. (2020) A case of titanium pseudotumor and systemic toxicity after total hip arthroplasty polyethylene failure. *Arthroplasty Today*, *6*(4), pp.710-715.

ThermoFisher (2023) *Spot size in scanning electron microscopy (SEM): why it matters!* [Online]
Available at: https://www.thermofisher.com/uk/en/home/global/forms/industrial/spot-size-sem.html
[Accessed: 27/07/2023]

Tian, G., Fan, S.B., Huang, Y.H., Nie, L. and Li, G. (2008) Relationship between wind velocity and PM10 concentration & emission flux of fugitive dust source. *Huan Jing ke Xue= Huanjing Kexue*, *29*(10), pp.2983-2986.

Tolu, J., Bouchet, S., Helfenstein, J., Hausheer, O., Chékifi, S., Frossard, E., Tamburini, F., Chadwick, O.A. and Winkel, L.H. (2022) Understanding soil selenium accumulation and bioavailability through size resolved and elemental characterization of soil extracts. *Nature Communications*, *13*(1), p.6974.

Tyler, R.H., Boyer, T.P., Minami, T., Zweng, M.M. and Reagan, J.R. (2017) Electrical conductivity of the global ocean. *Earth, Planets and Space*, *69*, pp.1-10.

Ullah, S., Liu, Q., Wang, S., Jan, A.U., Sharif, H.M.A., Ditta, A., Wang, G. and Cheng, H. (2023) Sources, impacts, factors affecting Cr uptake in plants, and mechanisms behind phytoremediation of Cr-contaminated soils. *Science of the Total Environment*, p.165726.

USGS (2015) *Trace elements in coal ash* [Online]
Available at: https://pubs.usgs.gov/fs/2015/3037/pdf/fs2015-3037.pdf
[Accessed: 02/02/2024]

Vaverková, M.D. (2019) Landfill impacts on the environment. *Geosciences*, *9*(10), p.431.

Vedolin, M.C., Teophilo, C.Y.S., Turra, A. and Figueira, R.C.L. (2018) Spatial variability in the concentrations of metals in beached microplastics. *Marine pollution bulletin*, *129*(2), pp.487-493.

Velling, A. (2020) *Aluminium Corrosion & Its Different Types* [Online]
Available at: https://fractory.com/aluminium-corrosion/
[Accessed: 04/02/2024]

Verma, C. and Verma, R. (2019) Leaching behaviour of fly ash: A review. *Nature Environment and Pollution Technology*, *18*(2), pp.403-412.

Verma, K.C. and Kushwaha, A.S. (2014) Demineralization of drinking water: Is it prudent?. *medical journal armed forces india*, *70*(4), pp.377-379.

Vidya, C.S.N., Shetty, R., Vaculíková, M. and Vaculík, M. (2022) Antimony toxicity in soils and plants, and mechanisms of its alleviation. *Environmental and Experimental Botany*, *202*, p.104996.

Vítková, M., Hyks, J., Ettler, V. and Astrup, T. (2013) Stability and leaching of cobalt smelter fly ash. *Applied geochemistry*, *29*, pp.117-125.

Vodyanitskii, Y.N. (2010) Zinc forms in soils (Review of publications). *Eurasian Soil Science*, *43*, pp.269-277.

Vojteková, V., Nováková, J. and Mackových, D. (2010) Simple assessment of the reactive aluminium in sediments. *Environmental Chemistry Letters*, *8*, pp.45-51.

Wadey, M., Kermode, T., Cope, S. and Neill, S. (2019) *SCOPAC Coastal Landfills Study: Coastal Flooding, Erosion and Funding Assessment* [Online]
Available at: https://southerncoastalgroup-scopac.org.uk/wp-content/uploads/2019/06/2019-06-19_SCOPAC-LANDFILLS-REPORT-FINAL.pdf
[Accessed: 04/09/2023]

Wang, R., Zhang, J., Liu, Z., Liu, X., Xu, C. and Li, Y. (2020) Interaction between iron ore and magnesium additives during induration process of pellets. *Powder technology*, *361*, pp.894-902.

Wang, G., Jensen, P.A., Wu, H., Frandsen, F.J., Laxminarayan, Y., Sander, B. and Glarborg, P. (2019a) Potassium capture by coal fly ash: K_2CO_3, KCl and K_2SO_4. *Fuel processing technology*, *194*, p.106115.

Wang, X., Bayon, G., Kim, J.H., Lee, D.H., Kim, D., Guéguen, B., Rouget, M.L., Barrat, J.A., Toffin, L. and Feng, D. (2019b) Trace element systematics in cold seep carbonates and associated lipid compounds. *Chemical Geology*, *528*, p.119277.

Wang, G.C. (2016) 9—Usability criteria for slag use as a granular material. In: *The utilization of slag in civil infrastructure construction*, pp.185-199. Amsterdam: Elsevier.

Wdowczyk, A. and Szymańska-Pulikowska, A. (2020) Differences in the composition of leachate from active and non-operational municipal waste landfills in Poland. *Water*, *12*(11), p.3129.

Wei, C., Ge, Z., Chu, W. and Feng, R. (2015) Speciation of antimony and arsenic in the soils and plants in an old antimony mine. *Environmental and experimental botany*, *109*, pp.31-39.

Wei, G.Y., Qu, J.K., Zheng, Y.D., Tao, Q.I., Qiang, G.U.O., Han, B.B. and Zhao, H.X. (2014) Crystallization behaviors of bayerite from sodium chromate alkali solutions. *Transactions of Nonferrous Metals Society of China*, *24*(10), pp.3356-3365.

Wierzba, S., Makuchowska-Fryc, J., Kłos, A., Ziembik, Z. and Ochędzan-Siodłak, W. (2022) Role of calcium carbonate in the process of heavy metal biosorption from solutions: synergy of metal removal mechanisms. *Scientific Reports*, *12*(1), p.17668.

Wilkie, J.A. and Hering, J.G. (1996) Adsorption of arsenic onto hydrous ferric oxide: effects of adsorbate/adsorbent ratios and co-occurring solutes. *Colloids and Surfaces A: Physicochemical and Engineering Aspects*, *107*, pp.97-110.

Williams, A.T., Rangel-Buitrago, N., Pranzini, E. and Anfuso, G. (2018) The management of coastal erosion. *Ocean & coastal management*, *156*, pp.4-20.

Wille, E. (2018) Flooding risks at old landfill sites: linear economy meets climate change. *Proceedings of the 4th International Symposium on Enhanced Landfill Mining* [Online] Echelon, Belgium, 5-6 February, pp. 361-365
Available at: Proceedings of the 4th International Symposium on Enhanced Landfill Mining (ELFM IV) (diva-portal.org)
[Accessed: 04/09/2023]

Wise, A. and Gilburt, D.J. (1981) Binding of cadmium and lead to the calcium-phytate complex in vitro. *Toxicology letters*, *9*(1), pp.45-50.

Witkowska, D., Słowik, J. and Chilicka, K. (2021) Heavy metals and human health: Possible exposure pathways and the competition for protein binding sites. *Molecules*, *26*(19), p.6060.

Wnuk, E. (2023) Mobility, bioavailability, and toxicity of vanadium regulated by physicochemical and biological properties of the soil. *Journal of Soil Science and Plant Nutrition*, *23*(1), pp.1386-1396.

World Health Organisation (2022) *Guidelines for drinking-water quality: Fourth edition incorporating the first and second addenda* [Online]
Available at: https://www.who.int/publications/i/item/9789240045064
[Accessed: 05/01/2024]

World Health Organisation (2020) *Manganese in drinking-water* [Online]
Available at: https://www.who.int/docs/default-source/wash-documents/wash-chemicals/gdwq-manganese-background-document-for-public-review.pdf?sfvrsn=9296741f_5
[Accessed: 04/03/2024]

Xie, W., Li, Y., Bai, W., Hou, J., Ma, T., Zeng, X., Zhang, L. and An, T. (2021) The source and transport of bioaerosols in the air: A review. *Frontiers of Environmental Science & Engineering*, *15*, pp.1-19.

Xu, B. and Yi, Y. (2022) Immobilization of lead (Pb) using ladle furnace slag and carbon dioxide. *Chemosphere*, *308*, p.136387.

Yamada, M., Takahashi, S., Sato, H., Kondo, T., Kikuchi, T., Furuya, K. and Tanaka, I. (1993) Solubility of nickel oxide particles in various solutions and rat alveolar macrophages. *Biological trace element research*, *36*, pp.89-98.

Yan, G., Gao, Y., Xue, K., Qi, Y., Fan, Y., Tian, X., Wang, J., Zhao, R., Zhang, P., Liu, Y. and Liu, J. (2023) Toxicity mechanisms and remediation strategies for chromium exposure in the environment. *Frontiers in Environmental Science*, *11*, p.1131204.

Yan, B. and Hou, Y. (2018). Effect of soil magnesium on plants: a review. In: *IOP Conference Series: Earth and Environmental Science*, *170,* pp. 022168. IOP Publishing.

Yang, W., Liu, Z. and Huang, H. (2021) Galvanic corrosion behavior between AZ91D magnesium alloy and copper in distilled water. *Corrosion Science*, *188*, p.109562.

Yang, J., Wang, M., Jia, Y., Gou, M. and Zeyer, J. (2017) Toxicity of vanadium in soil on soybean at different growth stages. *Environmental Pollution*, *231*, pp.48-58.

Yarmolenko, M. and Mogilei, S. (2023) Iron, copper, and aluminium electrochemical corrosion in motionless and moving electrolytes investigation during electrolysis. *Results in Materials*, *20*, p.100479.

Yildirim, I.Z. and Prezzi, M. (2011) Chemical, mineralogical, and morphological properties of steel slag. *Advances in civil engineering*, *2011*.

Youcai, Z. (2018) *Pollution control technology for leachate from municipal solid waste: landfills, incineration plants, and transfer stations*. Oxford: Butterworth-Heinemann

Zdeb, M., Papciak, D. and Zamorska, J. (2018) An assessment of the quality and use of rainwater as the basis for sustainable water management in suburban areas. In *E3S Web of conferences* (Vol. 45, p. 00111). EDP Sciences.

Zha, F., Liu, C., Kang, B., Xu, L., Yang, C., Chu, C., Yu, C., Zhang, W., Zhang, J. and Liu, Z. (2021) Effect of carbonation on the leachability of solidified/stabilized lead-contaminated expansive soil. *Advances in Civil Engineering*, *2021*, pp.1-13.

Zhang, T., Chen, Y., Cai, Y., Yu, Y., Liu, J., Shen, X., Li, G. and An, T. (2023) Abundance and cultivable bioaerosol transport from a municipal solid waste landfill area and its risks. *Environmental Pollution*, *320*, p.121038.

Zhang, B., Wang, S., Diao, M., Fu, J., Xie, M., Shi, J., Liu, Z., Jiang, Y., Cao, X. and Borthwick, A.G. (2019) Microbial community responses to vanadium distributions in mining geological environments and bioremediation assessment. *Journal of Geophysical Research:*

Biogeosciences, *124*(3), pp.601-615.

Zhang, Y., Cetin, B., Likos, W.J. and Edil, T.B. (2016) Impacts of pH on leaching potential of elements from MSW incineration fly ash. *Fuel*, *184*, pp.815-825.

Zheng ShunAn, Z.S., Zheng XiangQun, Z.X. and Chen Chun, C.C. (2012) Leaching behavior of heavy metals and transformation of their speciation in polluted soil receiving simulated acid rain.